Physiological Basis of Variation in Mesophyll Conductance of Black Cottonwood (*Populus trichocarpa* Torr. & Gray)

by

Mina Momayyezi

B.Sc., The Ferdowsi University of Mashhad, 2008

M.Sc., The University of British Columbia, 2012

A DISSERTATION SUBMITTED IN PARTIAL FULFILLMENT OF
THE REQUIREMENTS FOR THE DEGREE OF

DOCTOR OF PHILOSOPHY

in

THE FACULTY OF GRADUATE AND POSTDOCTORAL STUDIES

(Forestry)

THE UNIVERSITY OF BRITISH COLUMBIA

(Vancouver)

April 2017

Abstract

There is dramatic provenance level variation in tree species with geographically wide ranges. For example, in *Populus trichocarpa* Torr. & Gray, net photosynthesis (A_n) and stomatal conductance (g_s) both increase with latitude of origin. This thesis reports a parallel cline in mesophyll conductance (g_m) and explores its physiological basis. In addition to anatomical constraints, variation in g_m should depend on chloroplast positioning, transmembrane CO_2 diffusion through aquaporins (AQPs), and biochemical facilitation of the $CO_2 \leftrightarrow HCO_3^-$ equilibrium by carbonic anhydrase (CA), but evidence for the former has been lacking. I found that g_m increases with latitude across 12 genotypes, as measured by chlorophyll fluorescence, and confirmed this pattern by the isotope discrimination method in six representative genotypes. Northern genotypes had greater CA activity. An inhibitor of CA, acetazolamide, reduced CA activity, g_m, g_s, chloroplast CO_2 concentration and A_n at normal CO_2 (400 μmol mol^{-1}), the latter being reversible at saturating CO_2. The relationship between CA activity and g_m was similar whether the variation was inherent or inhibitor-induced. I then explored the role of chloroplast positioning in relation to g_m, driven by the ratio of blue (BL) to red light supplied to leaves. Repositioning was manifested by a reversible decrease in chlorophyll content index (CCI), while actual chlorophyll content remained unchanged. Although g_m was found to decrease as BL increased, and more so in northern genotypes, cytochalasin D, an inhibitor of chloroplast motility, blocked the effect of BL on CCI but not g_m, suggesting that BL can mediate g_m independently of repositioning. High BL reduced CA activity, consistent with a possible reduction in protein-facilitated diffusion, which might also involve AQPs. I found that the AQP inhibitor mercuric chloride reduces g_m more in northern genotypes than in southern genotypes, both absolutely and proportionally, but also reduces CA activity. Although greater g_m in high-latitude genotypes likely reflects contributions from several

components of the liquid-phase diffusion pathway, this thesis draws particular attention to a major role for CA. Because g_m is an equal or greater limitation on photosynthesis than g_s, these findings may help direct crop improvement efforts to promote resource use efficiencies and yield.

Preface

Research chapters of this thesis are written as separate manuscripts for publishing in peer-review journals. My contribution to Chapters 2, 3 and 4 involves experimental design, data collection, data analyses and preparation of full written draft including figures and table. Dr. Robert Guy, my supervisor, provided help with developing my research proposal and assisted with experimental design, data interpretation and editorial revisions of my thesis.

Chapter 2 is based on a published paper in *Plant, Cell and Environment* as "Momayyezi M. & Guy R.D. (2017) Substantial role for carbonic anhydrase in latitudinal variation in mesophyll conductance of *Populus trichocarpa* Torr. & Gray."

A version of Chapter 3 is accepted pending minor revision in *Journal of Plant Physiology* as "Momayyezi M. & Guy R.D. (2017) Blue light differentially represses mesophyll conductance in high vs low latitude genotypes of *Populus trichocarpa* Torr. & Gray."

A version of Chapter 4 will be submitted for publication as "Momayyezi M. & Guy R.D. Effect of mercuric chloride on mesophyll conductance in diverse *Populus trichocarpa* Torr. & Gray genotypes."

Table of contents

List of tables

List of figures

List of symbols and abbreviations

α	leaf absorptance
β	the fraction of absorbed quanta reaching photosystem II
Φ_{PSII}	quantum yield of photosystem II
$\delta^{13}C$	$^{13}C/^{12}C$ isotope ratio (‰)
Γ^*	chloroplast CO_2 photocompensation point (μmol mol^{-1})
Δ_o	observed carbon isotope discrimination (‰)
Δ_i	predicted carbon isotope discrimination (‰)
Δ_e	respiratory associated carbon isotope discrimination (‰)
Δ_f	photorespiratory associated carbon isotope discrimination (‰)
Δ_{gm}	discrimination associated with the diffusion of CO_2 from intercellular airspace to sites of carboxylation (‰)
$\delta^{13}C_e$	isotopic ratio of reference CO_2 (‰)
$\delta^{13}C_a$	isotopic ratio of unconsumed sample CO_2 (‰)
$\delta^{13}C_{atm}$	isotopic composition for atmospheric CO_2 (‰)
ζ	ratio of the reference CO_2 concentration entering the cuvette and the net amount consumed in photosynthesis
a'	combined factor for diffusional fractionation through stomata and the boundary layer
a	fractionations occurring during diffusion across the stomata (‰)

a_i	fractionation factor associated with hydration and diffusion in water (‰)
a_b	fractionations occurring through the boundary layer (‰)
A_n	net assimilation rate (µmol CO_2 m^{-2} s^{-1})
ACC	actual chlorophyll content (µg/cm^2)
AQP	aquaporin
BL	blue light
CA	carbonic anhydrase
C_a	ambient chamber CO_2 concentration (µmol mol^{-1})
C_c	CO_2 concentration at sites of carboxylation (µmol mol^{-1})
C_e	reference CO_2 concentration (µmol mol^{-1})
C_i	intercellular air space CO_2 (µmol mol^{-1})
C_i*	intercellular CO_2 photocompensation point (µmol mol^{-1})
C_s	CO_2 concentration at the leaf surface (µmol mol^{-1})
CCI	chlorophyll content index
CO_2P	air exiting the LI-COR chamber with leaf present (µmol mol^{-1})
CO_2R	air exiting the LI-COR chamber with leaf absent (µmol mol^{-1})
df	dilution factor
DMSO	dimethyl sulfoxide
e	fractionations associated with respiration (‰)

E	transpiration rate (mmol H_2O m^{-2} s^{-1})
f	fractionations associated with photorespiration (‰)
g_m	mesophyll conductance (mol CO_2 m^{-2} s^{-1})
g_{ac}^{t}	combination of boundary layer and stomatal conductance to CO_2
g_s	stomatal conductance (mol H_2O m^{-2} s^{-1})
g_s/g_m	stomatal conductance to mesophyll conductance ratio
$HgCl_2$	mercuric chloride II
J_{flu}	electron transport rate
J_{max}	maximum electron transport rate
K_i	inhibitory constant
leaf N	leaf nitrogen concentration (µg mm^{-2})
LMA	leaf mass per area (mg mm^{-2})
MIPs	major intrinsic proteins
NUE	nitrogen-use efficiency (μmol CO_2 g^{-1} N s^{-1})
PAR	photosynthetically active radiation (µmol m^{-2} s^{-1})
PIPs	plasma membrane intrinsic proteins
PPFD	photosynthetic photon flux density (µmol m^{-2} s^{-1})
R_d	non-photorespiratory respiration rate in the light (µmol m^{-2} s^{-1})
RL	red light

RNAi	RNA interference
rubisco	ribulose-1,5-bisphosphate carboxylase/oxygenase
RuBP	ribulose-1,5-bisphosphate
t	ternary correction factor
$T_{Control}$	time required for change of the buffer pH in control solution (s)
T_{Enzyme}	time required for change of the buffer pH in enzyme-containing solution (s)
V	volume of enzyme extract (mL)
V_{cmax}	maximum carboxylation rate
VPD	vapour pressure deficit (kPa)
WUE	water-use efficiency (μmol CO_2 $mmol^{-1}$ H_2O)
XIPs	uncharacterized aquaporin subfamily

Acknowledgements

First and foremost, I would like to express my sincere gratitude to my advisor, Dr. Robert Guy for his excellent guidance, and tremendous support. Rob's profound insight into plant physiology and his great patience led me through understanding complex research subjects as mesophyll conductance and helped me to be a better researcher. His precision and time dedication all through scientific editing of this thesis is greatly appreciated.

I would like to thank my supervisory committee, Dr. Arthur Fredeen and Dr. Sue Grayston for their guidance and very constructive feedback. I am very thankful to Dr. Carl Douglas, his memory will be eternal, for all his encouraging advice and guidance through my PhD study.

I like to thank Dr. Athena McKown for all inspiring and fruitful discussions. I offer my thanks to Dr. Raju Soolanayakanahally for supplying plant materials used in a part of my research. I am grateful to all Tree Physiology lab members, Estefania, Shofi, Shalom, and Yi for their help and encouragement.

I would like to share my gratitude to Dr. Valerie Lemay and Dr. Anthony Kozak for providing help with choosing and developing statistical models of analysis.

My deep appreciation goes to my parents and my brother who never stopped believing in me. I send my heartfelt thank you to the love of my life, Ali for being beside me with constant love and support all through challenges I faced in this journey.

To my beloved mom

Chapter 1: Introduction

1.1 Climate change and tree population adaptation

Responses of forest tree species to the possibility of rapid climate change, such as increased temperature, CO_2 level, and growing season length (Parmesan 2006; Bronson et al. 2009; Way & Oren 2010; Wertin et al. 2012), may include adaptation, migration or extinction of populations within a local and/or regional context (Aitken et al. 2008). The presence of genetic variations in morphological and physiological traits within and between plant populations, due to natural selection under different geoclimatic conditions, reflects the capacity for local adaption within plant species (Aitken & Whitlock 2013; Benomar et al. 2016). In geographically wide-spread species such as poplars (*Populus* spp.), latitudinal and longitudinal gradients in precipitation, temperature, elevation, and growing season length influence ecophysiological traits (Keller et al. 2011). An understanding of how key features of carbon uptake (photosynthesis-related traits) vary naturally, as a function of climate, would help to predict how populations will/should adapt to changing climatic conditions to maintain fitness and persist into the future (Savolainen et al. 2013; Valladares et al. 2014).

1.2 Latitudinal variation in physiological traits

Net assimilation rate (A_n) has been reported to increase with latitude in several poplar species (Gornall & Guy 2007: Soolanayakanahally et al. 2009, 2015; Kaluthota et al. 2015), including *Populus trichocarpa* Torr. & Gray (black cottonwood), *Populus balsamifera* L. (balsam poplar), *Populus angustifolia* James (narrowleaf cottonwood), and *Populus tremula* L. (European aspen), and in *Alnus rubra* Bong. (red alder) and *Betula papyrifera* Marsh. (paper birch) (Dang et al. 1994; Benowicz, et al. 2000). These higher rates of photosynthesis are supported by higher conductances

for CO_2 from the atmosphere to sites of carboxylation at rubisco (i.e., ribulose-1,5-bisphosphate carboxylase/oxygenase). Concurrent to A_n, stomatal conductance (g_s) increases with latitude in black cottonwood (Gornall & Guy 2007; McKown et al. 2014a), narrowleaf cottonwood (Kaluthota et al. 2015) and European aspen (Soolanayakanahally et al. 2015). In balsam poplar, g_s was reported to increase with latitude in a study utilizing field-grown plants (Soolanayakanahally et al. 2015). However, in an earlier study on greenhouse-grown plants (Soolanayakanahally et al. 2009) there was no relationship between g_s and latitude but, based on A-C_i curve analysis (A: net CO_2 assimilation, C_i: intercellular air space CO_2), balsam poplars from high latitudes were shown to have greater mesophyll conductance (g_m) compared to low-latitude genotypes (Soolanayakanahally et al. 2009). The mesophyll conductance indicates the ease of CO_2 diffusion from the substomatal cavity to rubisco. The positive correlation between latitude and A_n, and by extension, g_s and/or g_m, is presumed to reflect adaptation of northern balsam poplar genotypes to a shorter growing season (Soolanayakanahally et al. 2009).

Net assimilation rate may relate to other variables like leaf nitrogen concentration (leaf N) and leaf mass per area (LMA). They both increase in balsam poplar and narrowleaf cottonwood with latitude (Soolanayakanahally et al. 2009, 2015; Kaluthota et al. 2015). Variation in LMA in balsam poplar is primarily attributable to mesophyll palisade thickness, and not leaf thickness more generally (Milla-Moreno et al. 2016). Thus, LMA in balsam poplar is also correlated with anatomical properties of the palisade that may affect g_m, such as the cell wall area available for CO_2 diffusion. Accordingly, in a balsam poplar family resulting from a cross between geographically widely separated parents, g_m was found to be well correlated with LMA (Ryan 2015). While black cottonwood overlaps and hybridizes with balsam poplar in northeastern British Columbia and in the Canadian Rocky Mountains (Viereck et al. 1974), LMA and leaf N do not

seem to show the same changes with latitude. Likewise, patterns of variation in g_s and g_m may not be the same.

In black cottonwood (Gornall & Guy 2007; McKown 2014a), and also in narrowleaf cottonwood (Kaluthota et al. 2015), g_s has been shown to increase as leaves become more amphistomatous with latitude. The higher g_s in northern black cottonwood genotypes is positively related to higher stomatal adaxial:abaxial ratio and to total stomatal density (Gornall & Guy 2007). Although there is latitudinal variation in g_m in balsam poplar, it is unclear whether the same variation exists in black cottonwood. The absence of any latitudinal trend in LMA in black cottonwood might suggest that g_m would also show no pattern. However, there are many other physiological variables that could affect g_m independently from LMA.

1.3 Mesophyll conductance (g_m)

After ambient CO_2 molecules present in the bulk atmosphere cross the boundary layer and enter leaves through stomata, they face a series of resistances in both gas and liquid phases along the remaining diffusion pathway from the substomatal cavity to the sites of carboxylation inside the mesophyll cells (Flexas et al. 2008). More than half a century ago, Gaastra (1959) suggested that the internal resistance is an important determinant of the photosynthetic activity of plants. Using quantitative data obtained for several crop species, Gaastra attributed considerable variation in photosynthetic rate in response to CO_2 concentration, light intensity and temperature to this resistance. Quantitative computations suggested that the CO_2-limitation effect on photosynthesis is related to the sum of diffusion resistances, including the mesophyll resistance. Later, Jones & Slatyer (1972) confirmed that the mesophyll resistance can significantly constrain the photosynthetic rate. Using data for *Pelargonium hortorum* Bailey leaves, they developed a

more comprehensive model for net CO_2 uptake considering the "intercellular space resistance" to CO_2 diffusion from both upper and lower leaf surfaces and discussed possible errors in the estimation of this resistance. Earlier photosynthetic models were based on physical limitations at the boundary layer and across stomata. About the same time, theoretical models to describe and/or estimate the mesophyll resistance and the role of its various components were evolving, while direct and more accurate measurements of leaf CO_2 and water vapour exchange were also becoming possible.

In 1980, Farquhar et al. introduced a model (the widely used "Farquhar-von Caemmerer-Berry" model) based on known biochemical limitations (e.g., rubisco concentration, kinetics, temperature, CO_2 and O_2 concentrations, electron transport capacity, RuBP, etc.) to predict CO_2 assimilation rate in C_3 plants. Those authors noted that the term "mesophyll conductance" referred to the initial slope of an A-C_i curve (and not an A-C_c curve) and was linearly related to the maximum carboxylation rate (V_{cmax}). Thus, to this point, the concept of mesophyll resistance did not isolate the diffusional resistance from the biochemical "carboxylation resistance". Later, Farquhar and Sharkey (1982) equated the mesophyll resistance to just the liquid phase resistance for CO_2 diffusion through mesophyll cells, as previously suggested by Gasstra (1959), but this resistance was, nonetheless, considered minimal and "could be neglected for most purposes in modeling photosynthesis." During the mid-1980's, however, Evans and co-workers (Evans 1983; Evans et al. 1986; Evans & Terashima 1988) used various approaches to show that there was a substantial draw-down in CO_2 concentration from the substomatal space to the sites of carboxylation, consistent with a significant resistance. Using a three-dimensional model, Parkhurst (1994) described limitations on CO_2 assimilation as affected by diffusion through the intercellular air space (gas phase), noting that this portion of the pathway could reduce A_n by 25% or more in

some leaves. He also discussed the limitation expected from liquid phase diffusion through cell walls and to the chloroplasts based on the distance and physical properties of the pathway, concluding that it should be of similar magnitude to resistance through the gas phase.

Although the concept of resistance is perhaps an easier way to envision how various barriers impact CO_2 diffusion, conductance (the inverse of resistance) is now more commonly used to describe the direct relationship between CO_2 flux and photosynthesis. The mesophyll conductance (g_m) is finite and limits photosynthesis by dropping the CO_2 concentration at sites of carboxylation (C_c) lower than C_i (Pons et al. 2009). Improving photosynthetic capacity by means of increasing g_m could be an effective way to increase resource use efficiency (i.e., both water and nitrogen use efficiencies, simultaneously) in crop plants (Flexas et al. 2008). This realization has driven an exponential growth in the number of studies on g_m within the last decade. For example, during water shortage, an increase in g_m rather than g_s increases the water-use efficiency (WUE) by promoting CO_2 gain without affecting water loss (Flexas et al. 2008; Buckley & Warren 2014). Similarly, in relation to N investments in rubisco and the rest of the photosynthetic apparatus, maintenance of C_c under drought conditions (or a higher C_c under non-drought conditions) should maintain (or increase) the nitrogen-use efficiency (NUE).

Based on both theoretical estimations and experimental examinations, variation in g_m is related to structural, physiological and biochemical properties of mesophyll cells (Flexas et al. 2008; Flexas et al. 2012). As noted above, morphological (i.e., physical) properties of the leaf such as LMA and palisade cell wall area, but also wall thickness, cell packing/density, leaf thickness, etc., constrain diffusion and place upper limits on g_m. These properties can change developmentally but are fixed thereafter. Physiological components such as carbonic anhydrase (CA) activity, chloroplast

repositioning, and aquaporin function are known to be responsible for more rapid g_m responses to environmental changes (Flexas et al. 2012).

1.4 Physiological components

In the liquid phase, carbonic anhydrase (CA) maintains the equilibrium between CO_2 and HCO_3^- for a steady supply of CO_2 to rubisco (Badger & Price 1994). Multiple isozymes of CA are found free and/or bound to membranes within the cytosol, chloroplasts, and mitochondria (Fabre et al. 2007; Flexas et al. 2008). Tholen and Zhu (2011) developed a reaction-diffusion model to predict the mechanism of limitations to g_m based on the Farquhar-von Caemmerer-Berry model for photosynthesis in C_3 plants, and by using available numeric data. According to their model, removal of stromal CA activity is predicted to reduce g_m by 44% and A_n by 7%. One experimental approach to remove CA activity is through chemical inhibition. Sulfonamide compounds (e.g., acetazolamide, ethoxyzolamide) can inhibit CA activity by binding to the active site of the enzyme (Coleman 1975). They have indeed been shown to reduce photosynthesis by affecting CO_2 diffusion (Jacobson et al. 1975), but may also have direct effects on photosynthetic electron transport (Badger & Price 1994). Alternatively, gene silencing techniques such as RNA interference (RNAi) and RNA antisense can specifically block the function of candidate genes known to be associated with the expression of components of g_m (Hachez et al. 2006). However, and in contrast to the predictions of Tholen and Zhu (2011), an early study by Price et al. (1994) showed that removing stromal CA from chloroplasts using the antisense technique had little or no detectable effect on photosynthesis in tobacco (*Nicotiana tabacum* L.). Williams et al. (1996) performed a similar experiment on transgenic tobacco with CA activity reduced to 8% of normal and also detected no impact on A_n; however, based on isotope discrimination, these authors estimated that C_c was reduced by 13-22 μmol mol^{-1}. The failure of genetic modification to establish

a clear role for CA in CO_2 diffusion may stem from the molecular diversity and possible functional redundancy of CAs. For example, 18 genes for CA have been identified in black cottonwood (v11.0, https://phytozome.jgi.doe.gov/pz/portal.html).

Aquaporins, as another dynamic player for g_m, are abundant in cell membranes and facilitate transport of various molecules such as H_2O, CO_2 and NH_3 (Kaldenhoff & Fischer 2006). The plasma membrane intrinsic proteins (PIPs) are reported to transfer CO_2 selectively compared to other aquaporin subfamilies (Maurel et al. 2008). Terashima & Ono (2002) reported that the application of mercuric chloride II ($HgCl_2$), an inhibitor of aquaporin activity, decreases CO_2 diffusion from the intercellular air space to the chloroplast stroma in *Vicia faba* and, possibly, *Phaseolus vulgaris*. Consistent with the effects observed by Terashima and Ono (2002), a mutant of *Arabidopsis thaliana* lacking an aquaporin gene (AtPIP1;2) had lower photosynthesis compared to wild-type and this was attributable to a reduction in g_m (Heckwolf et al. 2011). Likewise, changes in PIP1 gene expression in transgenic lines of *N. tabacum* were directly reflected in both g_m and A_n (Uehlein et al. 2008). Down regulation of PIP1 inconsistently reduced g_m and A_n in transgenic *P. tremula* × *alba*, depending on the level of water stress (Secchi & Zwieniescki 2013). The role(s) of genes encoding and/or regulating CO_2-conducting aquaporins in *P. trichocarpa,* which has 55 such genes (Gupta & Sankararamakrishnan 2009; Almeida-Rodriguez et al. 2010), have yet to be studied.

Chloroplast movements may also mediate g_m. For example, the re-anchoring of chloroplasts from the periclinal to anticlinal position during the transition from low to high light is associated with a reduction in g_m, presumably by changing the chloroplast surface area exposed to the intercellular air space (Takagi et al. 2009). Blue light perceived by blue light photoreceptors such as phototropin

modulates chloroplast movement by affecting actin and/or myosin filaments (Banaś et al. 2012).

Chloroplast re-arrangement in response to light quality increases the absorption under low light conditions and protects photosystems from exposure to excessive light. A reduction in chloroplast surface area adjacent to intercellular air space under high blue light has been shown to decrease g_m, and consequently A_n, both theoretically (Loreto et al. 2009) and experimentally (Tholen et al. 2008; Weise et al. 2015).

1.5 Black cottonwood (*Populus trichocarpa*)

The genus *Populus* includes cottonwoods and aspens and is one of two genera in the traditional *Salicaceae* family (*sensu stricto*), the other genus being *Salix*. Poplars are deciduous tree species native to boreal, temperate, and subtropical sites in the northern hemisphere (Eckenwalder 1996; Dickmann 2001). They have been used as model trees for several decades, but especially so in recent years. Poplars grow rapidly and regenerate quickly, have high biomass production, and are easily propagated by vegetative means (Ellis et al. 2010). Due to these prominent characteristics, many poplar lines have been bred for plantation purposes, particularly in north-temperate latitudes (Dillen et al. 2010). *Populus* also has a relatively small genome size, and black cottonwood was the first tree to have its genome fully sequenced (Tuskan et al. 2003). *Populus* species have a high ability to deal with various environmental changes of photoperiod, growing season length, temperature and precipitation (Keller et al. 2012). They grow very well in floodplains, moist uplands and bottomlands with nutrient-rich soil and high light intensity (Saarela et al. 2011). Black cottonwood has a wide latitudinal distribution from southern Alaska at 62°N latitude to northern Baja California at 31°N latitude (Figure 1.1). Its native range continues inland through British Columbia to the Rocky Mountains in Alberta, Idaho and Montana (DeBell 1990).

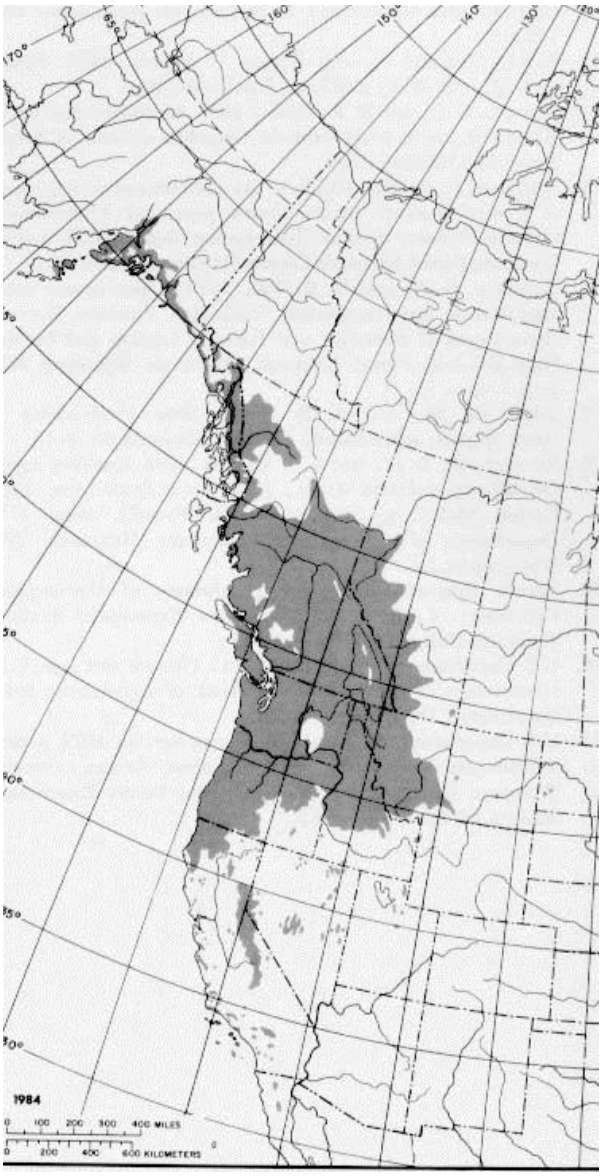

Figure 1.1 Native range of *Populus trichocarpa*

(https://www.na.fs.fed.us/spfo/pubs/silvics_manual/volume_2/populus/trichocarpa.htm).

1.6 Objectives

Theoretical derivations of CO_2 conductance predict that several anatomical and physiological properties of the mesophyll may constrain photosynthetic rate. The overall objective of my research was to evaluate inherent variation in g_m and explore the physiological basis for interspecific differences in g_m in black cottonwood genotypes. It was hypothesized that in *P. trichocarpa*, variation in g_m will correlate with latitude. This variation, assuming it exists, will reflect differences in one or more of CA activity, AQP functioning and/or chloroplast positioning. Specific objectives were to:

1. Investigate the presence or absence of genotypic and clinal variation in g_m in *P. trichocarpa*.
2. Ascertain if there is any latitudinal difference in g_m between northern and southern *P. trichocarpa* genotypes in relation to CA activity under natural and inhibitor-induced conditions.
3. Test whether high blue light affects g_m differently in northern and southern *P. trichocarpa* genotypes.
4. Evaluate the effects of mercuric chloride II on g_m in northern and southern *P. trichocarpa* genotypes.

Chapter 2: Substantial role for carbonic anhydrase in latitudinal variation in mesophyll conductance of *Populus trichocarpa* Torr. & Gray

2.1 Introduction

Populus trichocarpa (black cottonwood), a geographically widespread species distributed from 31° N to 62° N latitude, is the predominant cottonwood poplar in British Columbia, Canada, and in the Pacific Northwest of the United States. The closely related balsam poplar (*P. balsamifera* L.) replaces black cottonwood in the boreal forest of North America. There is clinal variation in A_n in both species, whereby a trend towards higher A_n in genotypes from high latitudes is thought to reflect their adaptation to shorter growing seasons (Gornall & Guy 2007; Soolanayakanahally et al. 2009). In balsam poplar, higher A_n in northern genotypes is supported by higher leaf N and higher LMA, and, at least under some conditions (Soolanayakanahally et al. 2015), higher g_s. Leaf mass per area in balsam poplar reflects both the density and thickness of palisade tissue in leaves (Milla-Moreno et al. 2016), and is positively correlated with structural properties that may affect CO_2 transport, such as the mesophyll cell wall area. In black cottonwood, g_s, stomatal ratio and density, and leaf N are all strongly correlated with the latitudinal cline in A_n; whereas, in contrast to balsam poplar, LMA is not (McKown et al. 2014a, 2014b).

During photosynthesis, water vapour is exchanged for CO_2 entering the leaf by way of stomatal pores. Given set diffusion gradients, g_s describes the ease with which water escapes from the leaf, as well as the ease with which CO_2 enters. After reaching the substomatal cavity, CO_2 molecules must transit intercellular air space, cell walls, membranes, cytosol, etc., to reach sites of carboxylation within chloroplasts. Carbon dioxide diffusion along these parts of the pathway is controlled by the mesophyll conductance (g_m), which has both gas and liquid-phase components

(Flexas et al. 2008). In an experiment comparing three high latitude genotypes of balsam poplar with three low latitude genotypes, the three northern accessions were found to have greater g_m (Soolanayakanahally et al. 2009). It is unknown whether there is any similar relationship between g_m and latitude of origin in black cottonwood.

When CO_2 dissolves in water it exists in chemical equilibrium with carbonic acid (H_2CO_3), which dissociates into bicarbonate ion (HCO_3^-). The reversible conversion of CO_2 to HCO_3^- is catalyzed by CA. Accounting for 0.5-2% of total soluble leaf protein, CA is the second most abundant protein in C_3 plants after rubisco (Badger & Price 1994). In photosynthetic tissues, CA contributes to g_m by maintaining the $CO_2 \leftrightarrow HCO_3^-$ equilibrium in the cytosol and chloroplasts, facilitating access to CO_2 for fixation by rubisco (Evans et al. 2009; Perez-Martin et al. 2014). Carbonic anhydrase consists of a family of four isozymes in eukaryotic, archaeal, and bacterial cells (Brinkman 1933; Bradfield 1947; Hewett-Emmett & Tashian 1996; Dimou et al. 2009). Carbonic anhydrase is abundant in chloroplast stroma and cytoplasm (Tsuzuki et al. 1985; Stemler 1986; Fett & Coleman 1994; Moroney et al. 2001; Rudenko et al. 2007; DiMario et al. 2016), and has been associated with various membrane fractions (Utsunomiya & Muto 1993; Ignatova et al. 2011). In C_3 plants, chloroplast CAs are believed to have a greater effect on mesophyll CO_2 diffusion than cytosolic CAs (Evans et al. 2009; Tholen & Zhu 2011) but other CAs may also be involved. Interrogation of the black cottonwood genome in Phytozome (v11.0, https://phytozome.jgi.doe.gov/pz/portal.html) indicates the presence of 18 genes encoding CA.

Only a few studies have investigated the effect of CA activity on g_m, either theoretically or experimentally (Makino et al. 1992; Price et al. 1994; Gillon & Yakir 2000; Tholen & Zhu 2011). Carbonic anhydrase activity varies in C_3 and C_4 species (Gillon & Yakir 2001), and limitation of

g_m by CA activity is suggested to be species-dependent (Gillon & Yakir 2000). Variation in CA activity may reflect inter- and intraspecific adaptive variation in leaf anatomy in relation to g_m limitations, such as compensating for greater resistance in other parts of the diffusion pathway (Gillon & Yakir 2000; Tosens et al. 2012, Tomás et al. 2013). Diffusion of dissolved CO_2 through the liquid phase is 10,000 times slower than diffusion in the gas phase. Cell wall surface area, chloroplast positioning, protein channels (aquaporins), and CA activity may all act together to reduce diffusion limitations in the liquid phase (Flexas et al. 2008; Evans et al. 2009; Hassiotou et al. 2009; Flexas et al. 2012; Perez-Martin et al. 2014).

To study effects on photosynthesis, CA activity has been manipulated chemically and/or genetically with mixed results. For example, photosynthesis was insufficient to support establishment of young *A. thaliana* seedlings with reduced plastid-localized carbonic anhydrase, but older plants were unaffected (Ferreira et al. 2008). Price et al. (1994) reported no effects on assimilation rate in antisense mutants of *N. tabacum* with just 1-3% residual stromal CA activity. Williams et al. (1996) reported lower carbon isotope discrimination and chloroplast CO_2 concentrations in transgenic *N. tabacum* having only 8% residual chloroplastic CA, but detected no measureable effect on photosynthetic rate. Other authors have reported reductions in photosynthesis by isolated chloroplasts after inhibition of CA with sulfonamides such as acetazolamide and ethoxyzolamide (e.g., Jacobson et al. 1975), but there is some evidence that these agents may affect photosynthesis independently of CA (Badger & Price 1994).

In this chapter, I demonstrate that in black cottonwood, despite little latitudinal variation in LMA, there is still a substantial cline in g_m. I, then examine the potential contribution of differences in CA as a partial basis for genotypic variation in g_m, by assaying CA activity and relating that activity

to the differential effects of acetazolamide on photosynthesis. Acetazolamide penetrates membranes, albeit somewhat slowly, to unselectively inhibit different CA isozymes (Swader & Jacobson 1972; Wu et al. 1998; Scozzafava et al. 2000). It was expected that acetazolamide, by inhibiting CA, would reduce g_m and, consequently, A_n. I hypothesized that effects would be greater in high latitude genotypes because of their intrinsically higher g_m.

2.2 Material and methods

2.2.1 Plant material

To assess latitudinal patterns in g_m and select representative genotypes for acetazolamide experiments, branch cuttings (whips) of twelve *P. trichocarpa* genotypes from 43°98′ to 59º42′ N and 137º83′ to 122º92′ W (Table 2.1) were taken in late January from the Totem Field common garden, University of British Columbia (UBC) (Figure 2.1). Bagged cuttings were kept in a dark cold room at +4°C until they were recut into ~10 cm lengths with two lateral buds for rooting and planting (Pointeau & Guy 2014). Cuttings were grown with supplemental lighting in a greenhouse (minimum photosynthetic photon flux density (PPFD) was 500 µmol m^{-2} s^{-1}) under a 20 hour photoperiod, maximum temperature of 25°C during day and 20°C during night, in 3.78 L pots containing a 70% peat moss and 30% perlite mixture. In subsequent experiments, fresh cuttings of just three northern (SKNP-4, TAKA-2 and TATB-4) and three southern (HALS-2, PITS-3 and LONG-1) genotypes (Table 2.1) were chosen from either end of the latitudinal range. For the initial screening of 12 genotypes, the youngest fully expanded leaf per plant was used to measure A_n, LMA, g_s and g_m (by the fluorescence method), as described below. To determine LMA, five discs of known area were punched from above the middle of the leaf, dried at 70ºC for 72 hours, and weighed. After pulverizing, 3 mg subsamples were analyzed for total nitrogen at the UBC Stable

Table 2.1 Provenance of origin for *Populus trichocarpa* genotypes used in this study. Asterisks (*) indicate genotypes chosen to represent high and low latitudes in carbonic anhydrase experiments.

Genotype	Drainage	Latitude (N)	Longitude (W)	Elevation (m)
JASP-5	Jasper	43.98°	122.92º	150
HALS-2 *	Halsey	44.40°	123.32º	300
PITS-3 *	Pittsburg	45.48°	123.12º	900
LONG-1 *	Longview	46.06°	123.92º	100
MCMN-2	McMillan Island	49.17°	122.57º	15
HARB-1	Lillooet	50.02°	122.52º	213
KLNE-5	Klinaklini	51.73°	125.57º	427
BELC-2	Bella Coola	52.37°	126.58º	135
QLKE-2	Quesnel Lake	53.00°	122.32º	488
SKNP-4 *	Skeena	54.55°	128.52º	61
TAKA-2 *	Taku	58.60°	133.57º	31
TATB-4 *	Alsek	59.42º	137.83º	34

Figure 2.1 *Populus trichocarpa* cuttings were taken from a gene bank in Totem Field at UBC (left image). Cuttings were grown under greenhouse conditions (right image).

Isotope Facility to determine leaf N. Experiments with acetazolamide used three leaves per plant. Measurements began after 6 weeks growth by processing two plants (initial assessment) and one plant (acetazolamide experiments) per day, and lasted in each case for 5-6 weeks. Experiments had a completely randomized design with four biological replicates per genotype.

2.2.2 Treatments and photosynthesis measurements

For the acetazolamide experiments, the three youngest fully expanded leaves per plant were used to measure A_n, g_s and C_i using a LI-COR 6400 XT gas exchange system fitted with a 6400-40 chlorophyll fluorescence chamber. One leaf was treated with acetazolamide to inhibit carbonic anhydrase, while the other two served as controls (see below). All routine measurements were done in triplicate under 10% blue to 90% red light ratio at a total PPFD of 1200 µmol m^{-2} s^{-1}. Leaf temperature was maintained at 25°C and the ambient chamber CO_2 concentration (C_a), supplied from 12 g CO_2 cartridges, was set to 400 µmol mol^{-1}. In order to maximize isotopic differences between the outlet sample CO_2 and inlet reference CO_2, the flow rate was set to 90 µmol air s^{-1} as the lowest rate that also allowed the vapour pressure deficit (VPD) to be kept between 1.4-1.6 kPa. A control leaf was dark adapted for 20 minutes prior to all other measurements to obtain the maximum quantum yield of photosystem II. Later, during gas exchange measurements, the quantum yield of photosystem II (Φ_{PSII}) under actinic light was obtained by application of saturating flashes (>7000 µmol m^{-2} s^{-1}) as per Genty et al. (1989).

2.2.3 Carbonic anhydrase inhibition

Control and acetazolamide treatments, and order of measurement, were randomly assigned to the three leaves processed each day to eliminate effects of any possible age or time dependent errors. Each leaf was cut at the petiole base under distilled water and placed in a 5 mL vial filled with

either distilled water (control 1), 10 mM NH_4OH aqueous solution (control 2, pH = 9.7), or 1 mM acetazolamide (Stemler & Jursinic 1983) in 10 mM NH_4OH (pH = 9.4), to promote dissolution. After 45 minutes, leaves were placed inside the LI-COR 6400 XT cuvette to equilibrate to chamber conditions for 20 minutes prior to gas exchange measurements. In preliminary tests, there was no effect of leaf detachment on A_n, g_s and g_m (see Appendix A, Table A.1).

2.2.4 Carbon isotope discrimination measurements

Seven pre-evacuated 1.5 L gas sampling bags were used to collect air exiting the LI-COR chamber through a tube connected to the cuvette exhaust, either with (CO_2P) or without (CO_2R) leaf material inside the chamber (Figure 2.2). There were four CO_2R samples taken per plant, alternating with three CO_2P samples. After taking the first CO_2R sample, a leaf was placed inside the chamber and light adapted for 20 minutes before taking the first CO_2P sample. The same protocol was followed for a second and then a third leaf, ending with a final CO_2R sample. Gas exchange and chlorophyll fluorescence measurements were recorded three times during each sampling for CO_2P.

On the day of sampling, bags were transferred to the Biometeorology and Soil Physics lab in the Faculty of Land and Food Systems, UBC for measuring carbon isotope discrimination for each air bag sample using a tunable diode laser (TGA 200, Campbell Scientific, Inc, Logan, UT, USA) according to Semmens et al. (2014) (Figure 2.2). The system was referenced against internal standard tanks calibrated against NOAA-ESRL and UoC-INSTAAR isotopic standards at 398.2 $\mu mol\ mol^{-1}$ and 467.6 $\mu mol\ mol^{-1}$, in air. The TGA automatically switches between the gas sampling bag, the low calibration tank, the high calibration tank and ambient outdoor air (to flush). Each sample went through the TGA twice according to the following cycle: Low Tank – Flush –

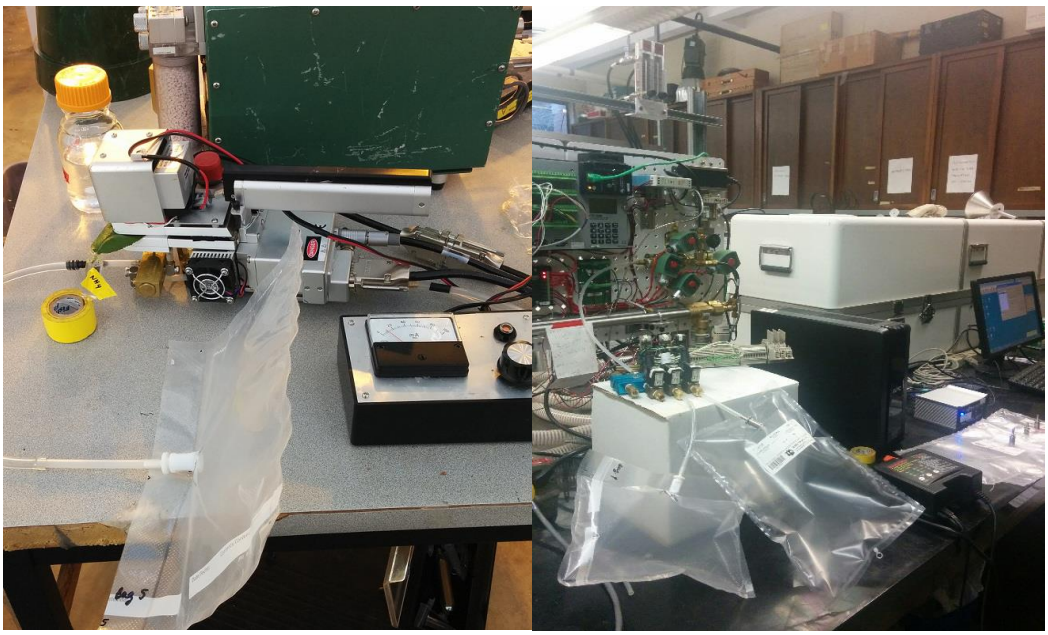

Figure 2.2 Air sample bags were filled from the LI-COR exhaust (left image), and analyzed for $\delta^{13}C$ using a Tunable Diode Laser (right image).

Sample – Flush – High Tank – Flush – Sample – Flush – Low Tank. $^{13}C/^{12}C$ isotope ratios ($\delta^{13}C$ ‰) were expressed relative to Vienna-Pee Dee belemnite (V-PDB). The gas sampling bags were fabricated from commonly available multilayer polyethylene plus nylon heat-sealable freezer bags (FoodSaver, Brampton, ON, Canada) fitted with PTFE valves (Scentroid Inc. ON, Canada). These were rigorously pre-tested for their ability to hold a gas sample without change in CO_2 concentration or isotopic composition. They were slightly better in performance relative to polyvinyl fluoride (Tedlar) gas sampling bags with stainless steel fittings (Scentroid Inc., ON, Canada), and far superior to polytetrafluoroethylene (PTFE) bags with PTFE valves (Scentroid Inc., ON, Canada). Samples in FoodSaver and/or Tedlar bags were stable for at least 3 days but showed some drift in isotopic composition after 7 days. In another test, 15 mL air samples from the gas exchange cuvette were simultaneously collected in Pyrex vacuum flasks for cryogenic purification and analysis (Ribas-Carbo et al. 2002) on an Isoprime (GV Instruments) Isotope Ratio Mass Spectrometer (IRMS) in the Stable Isotope Facility, Faculty of Forestry, UBC. After one day, there were no significant differences between $\delta^{13}C$ values obtained from flask (-31.36 ± 1.50‰) and Tedlar (-31.96 ± 0.13‰) or FoodSaver (-31.87 ± 0.02‰) bag samples, but PTFE bag samples were significantly enriched (-30.88 ± 0.48‰) ($P < 0.0001$). The IRMS analysis confirmed the accuracy of the TGA measurements, but TGA had higher precision, was more convenient and, because bags took longer to fill, was more coincident with the period over which foliar gas exchange measurements were made.

2.2.5 Calculation of g_m by chlorophyll fluorescence method

The "constant *J* method" was used to estimate g_m based on calculation of electron transport rate (J_{flu}) from measurements of chlorophyll fluorescence (Genty et al. 1989):

$$J_{\mathrm{flu}} = \Phi_{\mathrm{PSII}} \times \mathrm{PPFD} \times \alpha \times \beta \quad (1)$$

where β (= 0.5 for C_3 plants) is the fraction of absorbed quanta reaching photosystem II (Bernacchi et al. 2002). The leaf absorptance, α, was taken to be 0.827 based on the average value (± 0.03) of direct measurements of five plants from each of six genotypes using a CI-710 leaf spectrometer (CID BioScience Inc. Camas, WA, USA) (see Appendix A, Table A.2). g_m was given by (Harley et al. 1992):

$$g_{\mathrm{m}} = A_{\mathrm{n}} / \left[C_{\mathrm{i}} - \left(\frac{\Gamma^{*}\left(J_{\mathrm{flu}} + 8(A_{\mathrm{n}} + R_{\mathrm{d}})\right)}{J_{\mathrm{flu}} - 4(A_{\mathrm{n}} + R_{\mathrm{d}})} \right) \right] \quad (2)$$

where R_d is the non-photorespiratory respiration rate in the light (1.12 ± 0.37 µmol m^{-2} s^{-1}), and Γ^* is the chloroplast CO_2 photocompensation point (43.41 ± 1.25 µmol mol^{-1}). These values were estimated, using the Laisk method (Laisk 1977 in Gilbert et al. 2012), as the point of intersection of the linear portion of six sets of A-C_i curves obtained at two irradiances (125 and 500 µmol m^{-2} s^{-1}) and 12 CO_2 concentrations (50, 60, 70, 80, 90, 100, 120, 150, 180, 200, 230, and 250 µmol mol^{-1}) (see Appendix A, Figure A.1). As per Gilbert et al. (2012), Γ^* was assumed to equal the intercellular CO_2 photocompensation point (C_i^*). There was no effect of acetazolamide treatment on C_i^* and R_d (see Appendix A, Figure A.2).

2.2.6 Calculation of g_m from carbon isotope discrimination

Rubisco discriminates against $^{13}CO_2$ relative to $^{12}CO_2$ during carboxylation (Guy et al. 1993). The amount of discrimination expressed *in vivo* depends on the diffusion gradient for CO_2 from the bulk atmosphere. By comparing the observed discrimination (Δ_o) with the predicted discrimination (Δ_i) based only on the diffusion gradient through the stomata (i.e., C_a to C_i), the gradient associated with the remaining portion of the diffusion pathway (i.e., C_i to C_c) can be estimated and used to

calculate g_m (Evans et al. 1986). Smaller contributions to total discrimination associated with respiratory (Δ_e) and photorespiratory carbon flux (Δ_f) must also be accounted for. The effect of g_m on overall isotope discrimination (Δ_{gm}) is then given by:

$$\Delta_{g_m} = \Delta_i - \Delta_o - \Delta_e - \Delta_f \quad (3)$$

Observed discrimination was calculated according to Evans et al. (1986):

$$\Delta_o = \frac{1000\zeta(\delta^{13}C_a - \delta^{13}C_e)}{1000 + \delta^{13}C_a - \zeta\,(\delta^{13}C_a - \delta^{13}C_e)} \quad (4)$$

$$\zeta = \frac{C_e}{(C_e - C_a)} \quad (5)$$

where $\delta^{13}C_e$ and $\delta^{13}C_a$ are the isotopic ratios of reference CO_2 and unconsumed sample CO_2, respectively, which were measured by TGA. ζ is the ratio of the reference CO_2 concentration (C_e) entering the cuvette, as determined by the LI-COR 6400 XT, and the net amount consumed in photosynthesis (i.e., $C_e - C_a$).

Predicted discrimination was calculated from gas exchange data with corrections for ternary effects as per Farquhar & Cernusak (2012):

$$\Delta_i = \frac{1}{(1-t)}a' + \frac{1}{(1-t)}((1+t)b - a')\frac{C_i}{C_a} \quad (6)$$

where b is the fractionation in carboxylation of ribulose bisphosphate catalyzed by rubisco (-29‰; Guy et al. 1993). The ternary correction factor, t, is:

$$t = \frac{(1+a')E}{2g_{ac}^t} \quad (7)$$

where E is the transpiration rate and g_{ac}^t is the combination of boundary layer and stomatal conductance to CO_2. The combined factor for diffusional fractionation through stomata and the

boundary layer, a', is:

$$a' = \frac{a_b(C_a - C_s) + a(C_s - C_i)}{(C_a - C_i)} \quad (8)$$

where a and a_b are the fractionations occurring during diffusion across the stomata (4.4‰) and through the boundary layer (2.9‰), respectively, and C_s is the CO_2 concentration at the leaf surface (Evans et al. 1986).

Discriminations associated with respiration (Δ_e) and with photorespiration (Δ_f) were calculated from equations 9 and 10 (Farquhar & Cernusak 2012):

$$\Delta_e = \frac{1+t}{1-t}\left[\frac{eR_d}{(A_n + R_d)C_a}\right](C_i - \Gamma*) \quad (9)$$

$$\Delta_f = \frac{1+t}{1-t}\left[f\frac{\Gamma*}{C_a}\right] \quad (10)$$

where e and f are the fractionations associated with respiration and photorespiration, respectively. I took f to be -11.6‰ (Lanigan et al. 2008) and assumed that there is no significant fractionation associated with dark respiration during the day (Wingate et al. 2007). However, because respired carbon was likely fixed during prior photosynthesis in the greenhouse, I took e to equal the difference between $\delta^{13}C_e$ (-32 to -37‰) and the isotopic composition for atmospheric CO_2 ($\delta^{13}C_{atm}$) in the greenhouse (assumed to be -8‰; Alonso-Cantabrana & von Caemmerer 2015):

$$e = \delta^{13}C_e - \delta^{13}C_{atm} \quad (11)$$

Discrimination associated with g_m is described by (Farquhar & Cernusak 2012):

$$\Delta_{g_m} = \frac{1+t}{1-t}\left[b - a_i - \frac{eR_d}{A + R_d}\right]\frac{A_n}{g_m C_a} \quad (12)$$

where a_i is the fractionation factor associated with hydration and diffusion in water (1.8‰ at 25°C).

Substitution of equation 3 into equation 12 yields the following for calculation of g_m:

$$g_m = \frac{1+t}{1-t}\left[b - a_i - \frac{eR_d}{(A_n+R_d)}\right]\frac{A_n}{C_a}/(\Delta_i - \Delta_o - \Delta_e - \Delta_f) \quad (13)$$

2.2.7 Calculation of C_c

Having obtained g_m by either method, the CO_2 concentration at sites of carboxylation (C_c) was estimated according to Harley et al. (1992):

$$C_c = C_i - \frac{A_n}{g_m} \quad (14)$$

2.2.8 Carbonic anhydrase activity

Immediately after gas exchange measurements, leaf punches were taken for LMA as described above, and 0.5 g of laminal tissue from the middle of each leaf was weighed, wrapped in aluminum foil and stored on dry ice for determination of CA activity as described by Wilbur & Anderson (1948). The leaf tissue was ground in 1 mL of 40 mM potassium phosphate buffer (pH= 8.3) at 0ºC using a mortar and pestle (Figure 2.3). All further steps were at 4ºC. The homogenate was centrifuged for 15 minutes at 4500×g and 20 µL of the supernatant was added to 1 mL of the buffer solution containing 20 ppm bromothymol blue as a pH indicator. The time required for the pH of the buffer solution to change from 8.3 to 6.3 for control ($T_{Control}$) and enzyme-containing (T_{Enzyme}) solutions was recorded visually upon the further addition of 1 mL of CO_2-saturated water. The CO_2-saturated water was prepared by bubbling CO_2 through distilled water for two hours (also at 4ºC) (Figure 2.3). As a control, 20 µL of buffer solution was used in place of the supernatant. There were five technical replicates per assay. Enzyme activity was calculated as follows:

$$\text{Units CA / mL of supernatant} = \frac{(T_{Control} - T_{Enzyme}) \times df}{(T_{Enzyme}) \times V} \quad (15)$$

Figure 2.3 Thawed leaf samples were ground in buffer solution in preparation for the CA activity measurement assay (left image). The right image shows CO_2-saturated water in preparation.

where *df* is the dilution factor and *V* is the volume of enzyme extract used. Activities were expressed on a leaf area and fresh mass basis.

2.2.9 *A*-C_i curves

In order to test whether feeding through petioles with acetazolamide has any effect on photosynthesis other than a direct inhibitory effect on facilitated CO_2 diffusion, A_n was measured in the LONG-1 genotype in five replications over a range of 15 CO_2 concentrations from 50 to 1400 µmol mol^{-1}, at 1200 µmol m^{-2} s^{-1} PPFD (10% blue light) under distilled water (control) and 1 mM acetazolamide treatments. Data were fitted to version 2.0 of curve-fitting model described by Sharkey (2016) to estimate (V_{cmax}), maximum electron transport rate (J_{max}), and g_m.

2.2.10 Statistics

Pearson correlation coefficients and, where warranted, linear regression lines were used to illustrate relationships between latitude and A_n, g_s, g_m and LMA for the initial twelve genotypes, and between A_n, LMA, g_s, g_m, WUE, C_c and CA activity for representative genotypes, using GraphPad prism 6 software (GraphPad Software, Inc. CA, USA). Paired *t*-tests were run in GraphPad prism 6 to check for systematic differences between the isotope discrimination and chlorophyll fluorescence methods for estimating g_m and C_c.

Mixed linear models with contrast statements were used to compare A_n, g_m, g_s, C_c and CA activity for northern versus southern genotypes under control 1, control 2, and acetazolamide treatments using SAS 9.4 (SAS Institute Inc. NC, USA 2013). Both factors were fixed and genotypes were nested in latitude. The *P* value required for significance (0.016) was adjusted by dividing α (0.05) by the number of contrasts per test (three). Because controls did not differ, mixed linear models were used to compare within-plant absolute and percentage reductions in A_n, g_m, g_s, C_c and CA

activity under acetazolamide relative to the two controls (adjusted P value for two contrasts = 0.025). Mixed linear models without latitude as a factor were used to compare treatment effects on A_n, g_m, g_s, C_c and CA activity for the six genotypes independently (adjusted P value = 0.002). Logarithm or squared transformations were performed to meet normality and equal variance assumptions where needed.

2.3 Results

2.3.1 Initial assessment of latitudinal pattern

There was a positive correlation between latitude of origin and A_n (0.587, P = 0.044), g_s (r = 0.558, P = 0.049) and, notably, g_m (r = 0.671, P = 0.017) (Figure 2.4A-C). Leaf N (Figure 2.5), but not LMA (Figure 2.4D), also varied with latitude (r = 0.589, P = 0.043).

2.3.2 Comparison of two methods

Estimated values of g_m obtained from measurements of stable isotope discrimination versus chlorophyll fluorescence were well correlated (r = 0.772, P < 0.0001) (Figure 2.6). Estimates of C_c were also correlated but not as strongly so (r = 0.372, P = 0.0013) (Figure 2.7). There was a tendency for the isotope discrimination method to yield slightly (5%) higher estimates of g_m (P = 0.008), but not for C_c (P = 0.148). Unless otherwise noted, g_m and C_c data from the isotope discrimination method are presented, the former ranging from 0.03-0.34 mol CO_2 m^{-2} s^{-1} and the latter from 85-252 µmol mol^{-1}.

2.3.3 Treatment effects

Northern genotypes had significantly greater A_n (1.5 fold; P = 0.0011) and g_m (2.32 fold; P = 0.002) than southern ones under all three treatments (Figure 2.8 & 2.9). There was no consistent,

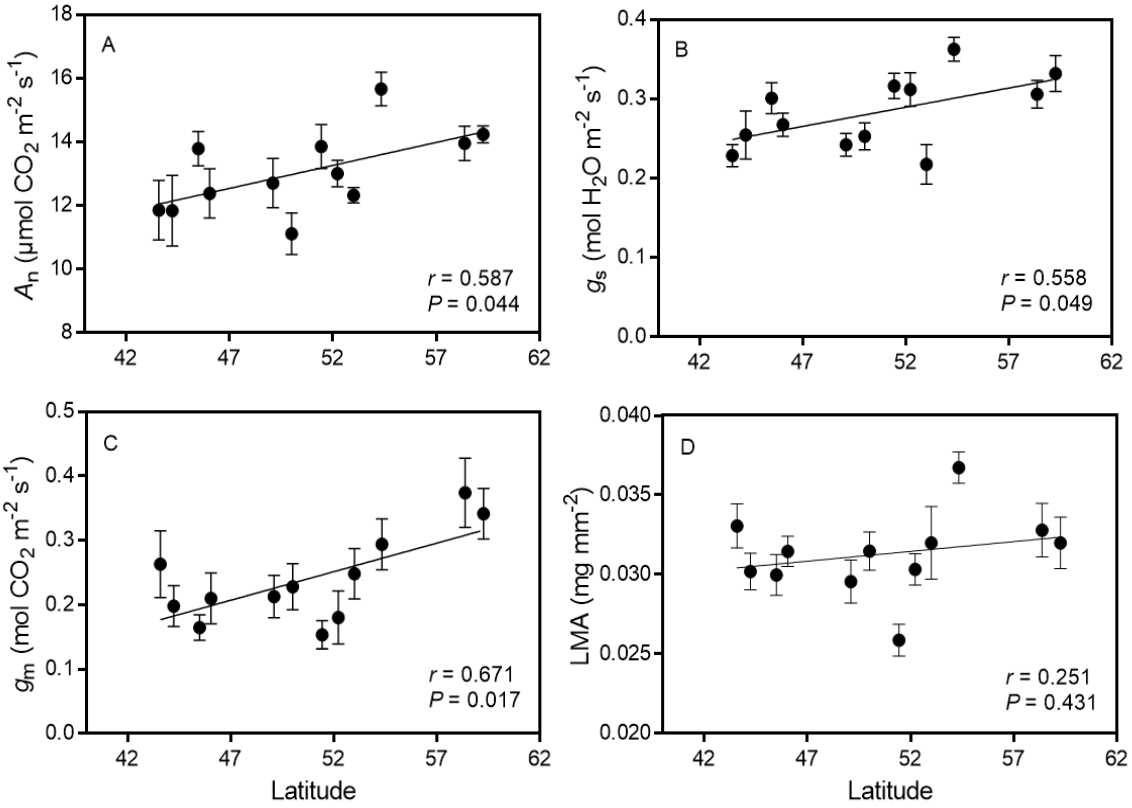

Figure 2.4 Photosynthetic traits across latitude of origin for 12 genotypes (clones) of *Populus trichocarpa*. A, net assimilation rate (A_n, µmol CO_2 m^{-2} s^{-1}); B, stomatal conductance (g_s, mol H_2O m^{-2} s^{-1}); C, mesophyll conductance (g_m, mol CO_2 m^{-2} s^{-1}); D, leaf mass per area (LMA, mg mm^{-2}). Data points are means of four biological replicates (ramets) per clone (± SE).

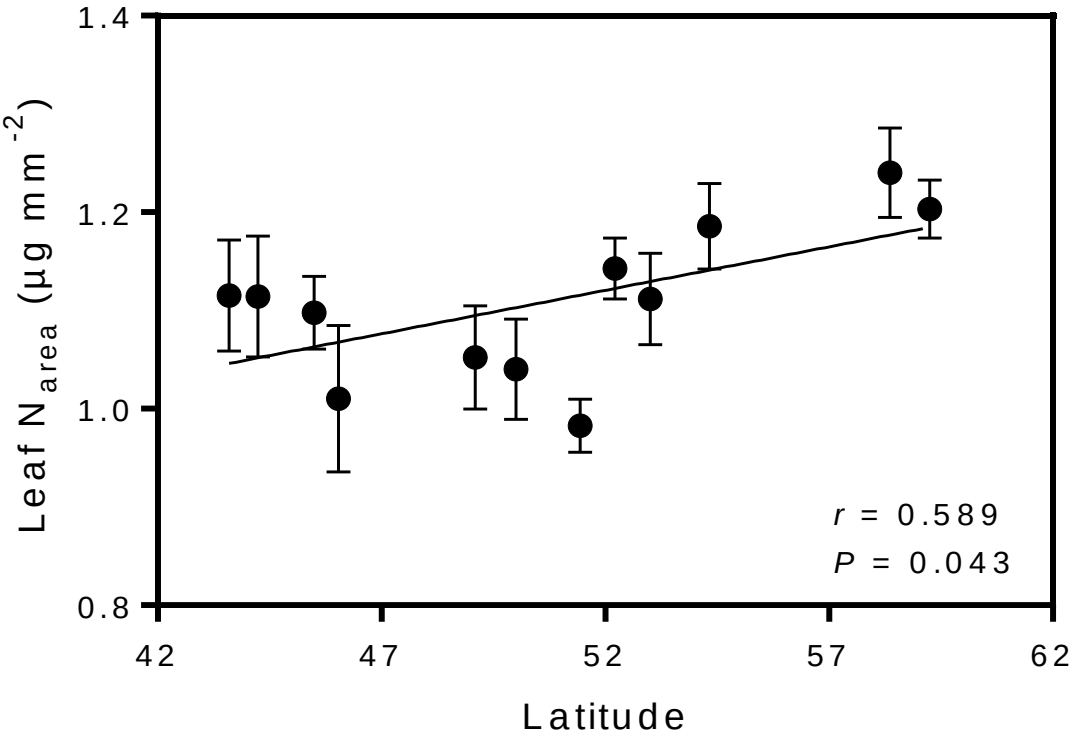

Figure 2.5 Leaf nitrogen concentration (leaf N, µg mm^{-2}) across latitude of origin for 12 genotypes (clones) of *Populus trichocarpa*. Data points are means of four biological replicates (ramets) per clone (± SE).

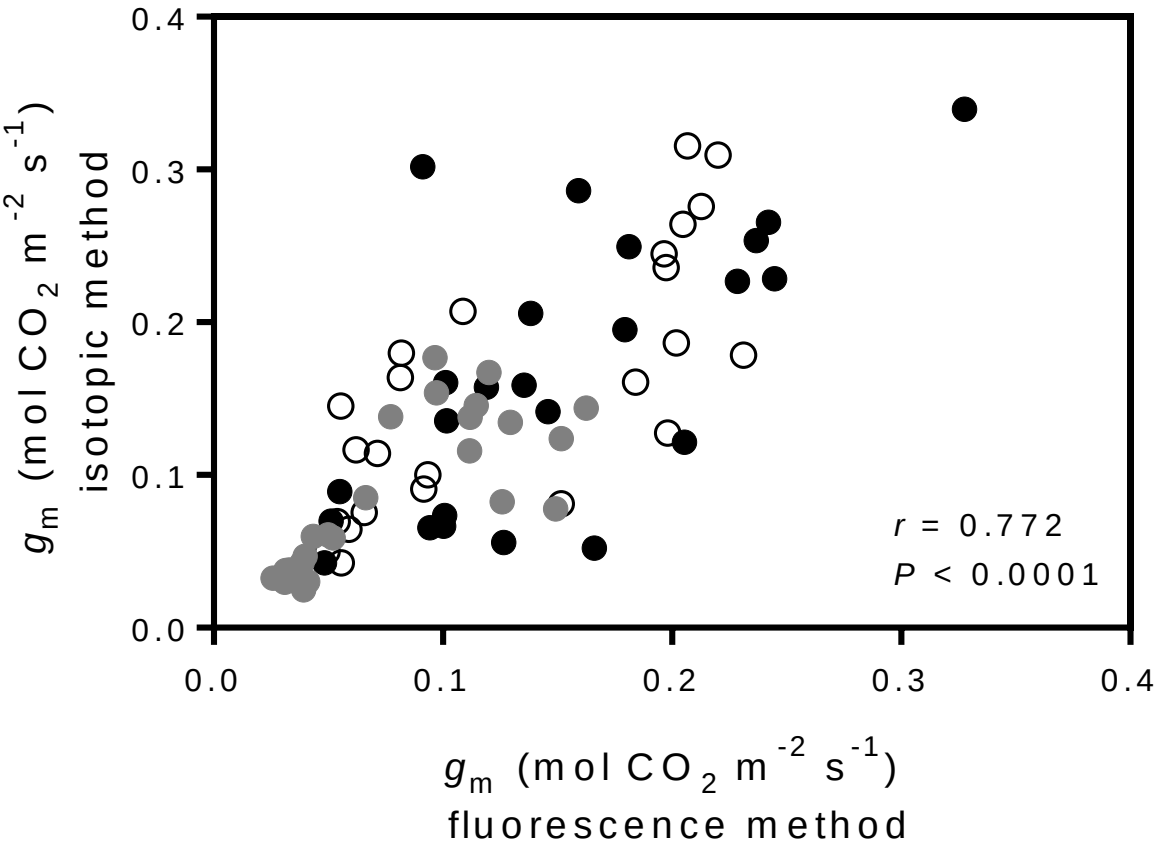

Figure 2.6 Correlation between mesophyll conductances (g_m, mol CO_2 m^{-2} s^{-1}) obtained from stable carbon isotope and chlorophyll fluorescence methods (n = 72) under three treatments; distilled water control (●), aqueous NH_4OH control (○), and acetazolamide (●).

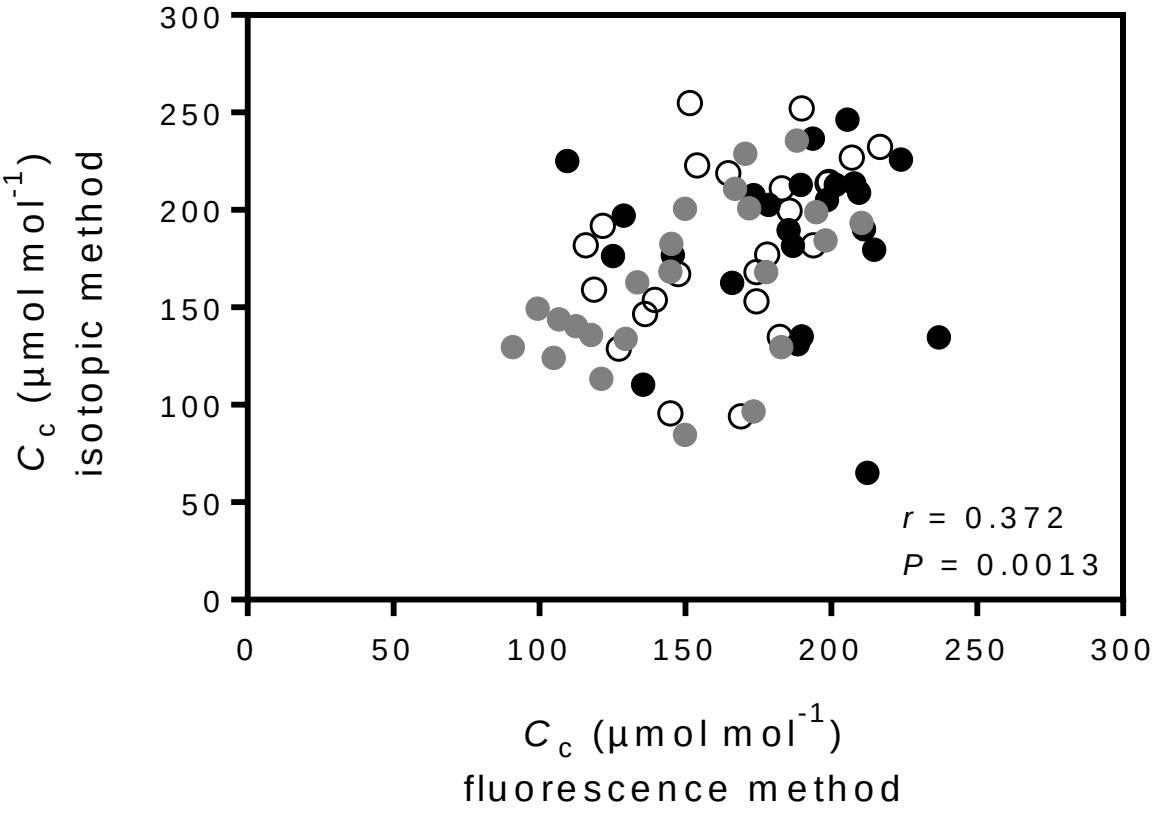

Figure 2.7 Correlation between chloroplast CO_2 concentrations (C_c, µmol mol^{-1}) obtained from stable carbon isotope and chlorophyll fluorescence methods (n = 72) under three treatments; distilled water (●), aqueous NH_4OH (○), and acetazolamide (●).

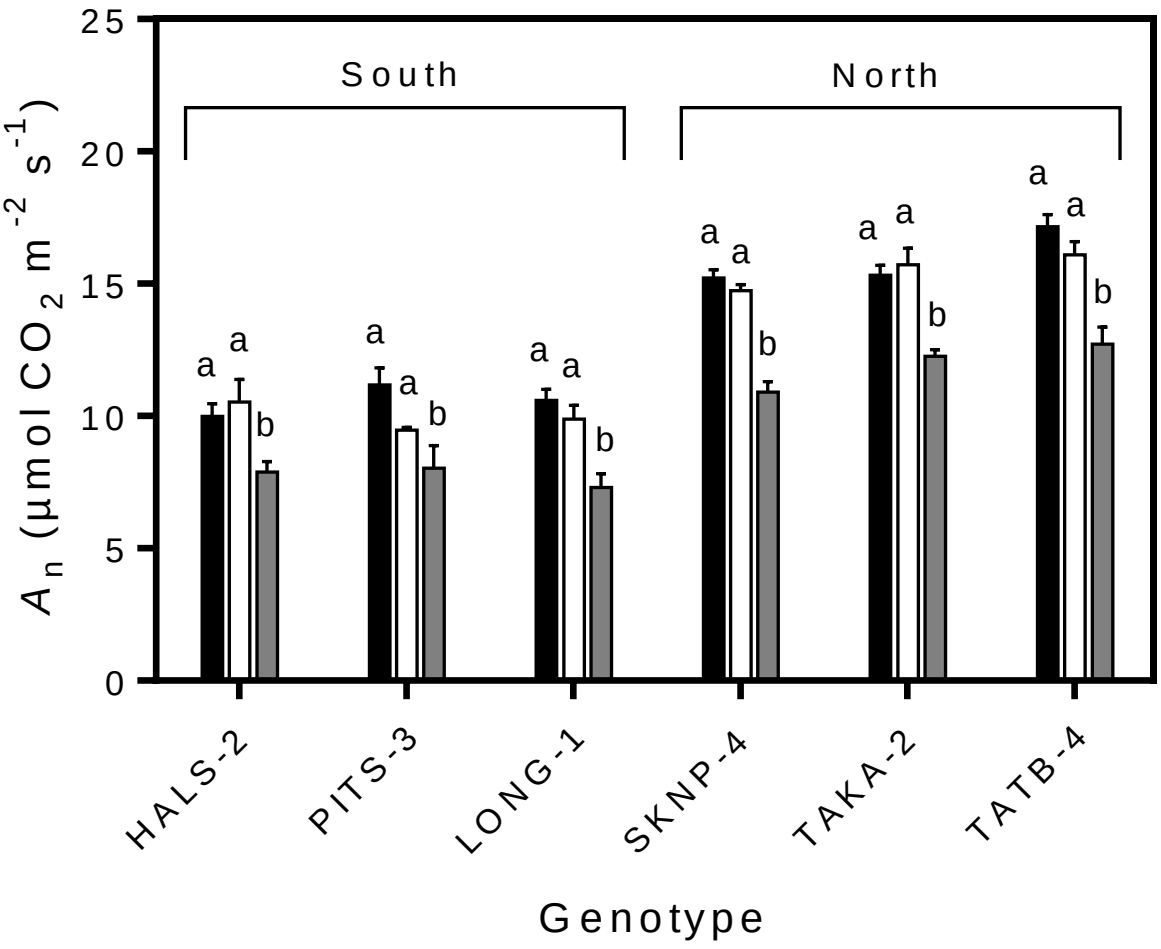

Figure 2.8 Mean values (± SE; $n = 4$) for net assimilation rate (A_n, µmol CO_2 m^{-2} s^{-1}) of six *Populus trichocarpa* genotypes under three treatments (distilled water in black, aqueous NH_4OH in white, and acetazolamide in grey). Different letters show significant differences between distilled water (control 1), aqueous NH_4OH (control 2) and acetazolamide treatments for each genotype at $P < 0.002$.

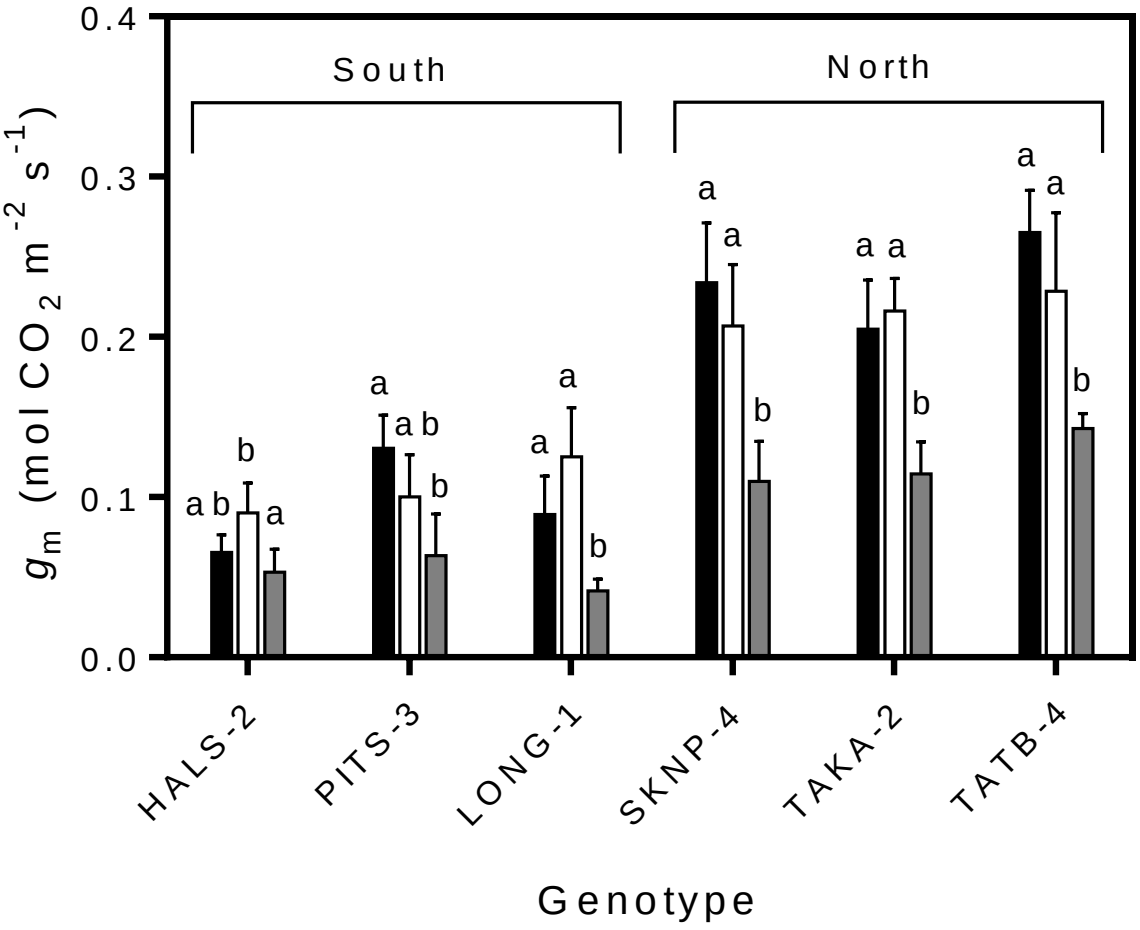

Figure 2.9 Mean values (± SE; n = 4) for mesophyll conductance (g_m, mol CO_2 m^{-2} s^{-1}) of six *Populus trichocarpa* genotypes under three treatments (distilled water in black, aqueous NH_4OH in white, and acetazolamide in grey). Different letters show significant differences between distilled water (control 1), aqueous NH_4OH (control 2) and acetazolamide treatments for each genotype at $P < 0.002$.

statistically significant difference between the distilled water and aqueous NH_4OH controls in any trait (Table 2.2). In contrast, most traits in most genotypes were strongly affected by treatment with acetazolamide. Net assimilation rate and mesophyll conductance were significantly lower for leaves treated with acetazolamide compared to controls at both latitudes (Figure 2.8 & 2.9, Table 2.2). In northern genotypes, g_s decreased significantly (by ~20%) under acetazolamide treatment compared to distilled water, but not in comparison to the NH_4OH control (Figure 2.10, Table 2.2). There was no significant effect of acetazolamide on g_s relative to either control in southern genotypes. Acetazolamide treatment significantly reduced C_c compared to distilled water and aqueous NH_4OH controls in the northern genotypes (by 19% and 14% respectively) but had comparatively larger effects in the southern genotypes, where C_c was reduced by 31% relative to either control (Figure 2.11, Table 2.2). Only under acetazolamide treatment did northern genotypes show a significantly different C_c from southern genotypes (Figure 2.11).

Results from A-C_i curve analysis were consistent with chlorophyll fluorescence and stable isotope discrimination methods for determining g_m. Average g_m over the range of CO_2 concentrations used was 58% lower in leaves fed with acetazolamide, in comparison to distilled water controls (Table 2.3). Both V_{cmax} and J_{max} were unaffected by treatment with acetazolamide (Table 2.3). Consequently, photosynthesis at a CO_2 concentration (i.e., C_a) of 400 µmol mol^{-1} was reduced by 22%, but there was no significant effect of acetazolamide on A_n at saturating CO_2 (Figure 2.12).

Control leaves from northern genotypes had just over twice as much CA activity as southern genotypes on a leaf area basis (Figure 2.13, Table 2.2). This difference, though smaller (1.8 fold), persisted when activity was expressed relative to leaf mass (Figure 2.14). On average, the northern

Table 2.2 A_n, g_s, CA activity, g_m and C_c in northern vs. southern genotypes under control 1 (distilled water), control 2 (aqueous NH_4OH), and acetazolamide treatments. Different letters show significant differences for mean values (± SE; $n = 4$) of controls 1 and 2 compared to the acetazolamide treatment within each latitudinal group at $P < 0.016$.

		north			south		
		control 1	control 2	acetazolamide	control 1	control 2	acetazolamide
A_n		15.90 ± 0.34 [a]	15.51 ± 0.31 [a]	11.97 ± 0.33 [b]	10.59 ± 0.31 [a]	9.96 ± 0.33 [a]	7.75 ± 0.34 [b]
g_s		0.218 ± 0.006 [a]	0.205 ± 0.006 [ab]	0.175 ± 0.008 [b]	0.196 ± 0.008 [a]	0.174 ± 0.007 [a]	0.175 ± 0.012 [a]
CA activity		1.81 ± 0.12 [a]	1.84 ± 0.19 [a]	1.06 ± 0.10 [b]	0.90 ± 0.07 [a]	0.84 ± 0.10 [a]	0.51 ± 0.06 [b]
g_m	isotopic method	0.234 ± 0.018 [a]	0.217 ± 0.020 [a]	0.122 ± 0.011 [b]	0.095 ± 0.013 [a]	0.099 ± 0.012 [a]	0.053 ± 0.009 [b]
	fluorescence method	0.198 ± 0.018 [a]	0.188 ± 0.012 [a]	0.114 ± 0.010 [b]	0.100 ± 0.010 [a]	0.073 ± 0.008 [a]	0.048 ± 0.007 [b]
C_c	isotopic method	200.4 ± 8.4 [a]	193.6 ± 9.3 [ab]	167.1 ± 12.3 [b]	184.8 ± 10.4 [a]	180.7 ± 14.0 [a]	143.9 ± 10.6 [b]
	fluorescence method	193.2 ± 4.8 [a]	188.3 ± 4.9 [a]	165.6 ± 8.8 [b]	182.1 ± 11.1 [a]	166.9 ± 4.0 [a]	132.3 ± 6.3 [b]

A_n, net assimilation rate (μmol CO_2 m^{-2} s^{-1}); g_s, stomatal conductance (mol H_2O m^{-2} s^{-1}); CA activity, carbonic anhydrase activity (units cm^{-2}); g_m, mesophyll conductance (mol CO_2 m^{-2} s^{-1}); C_c, CO_2 concentration at sites of carboxylation (μmol mol^{-1}).

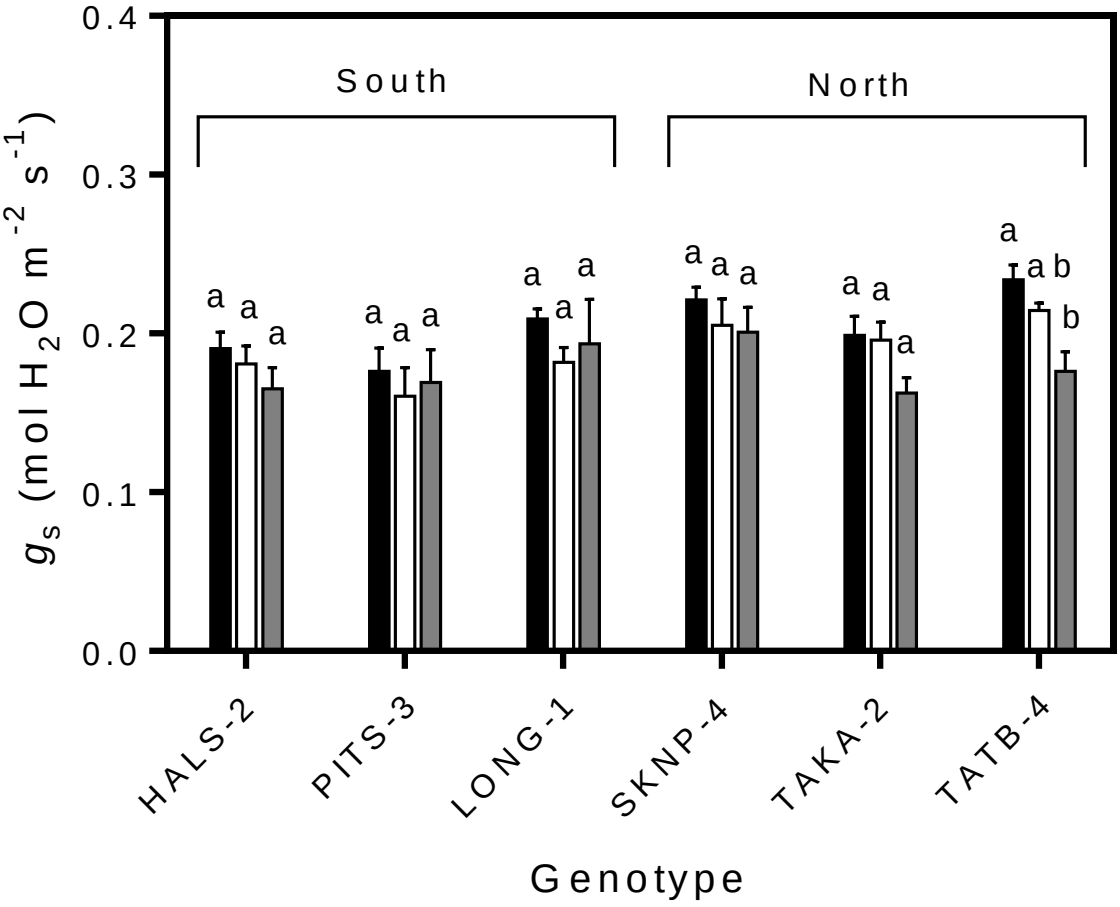

Figure 2.10 Mean values (± SE; n = 4) for stomatal conductance (g_s, mol H_2O m^{-2} s^{-1}) of six *Populus trichocarpa* genotypes under three treatments (distilled water in black, aqueous NH_4OH in white, and acetazolamide in grey). Different letters show significant differences between distilled water (control 1), aqueous NH_4OH (control 2) and acetazolamide treatments for each genotype at $P < 0.002$.

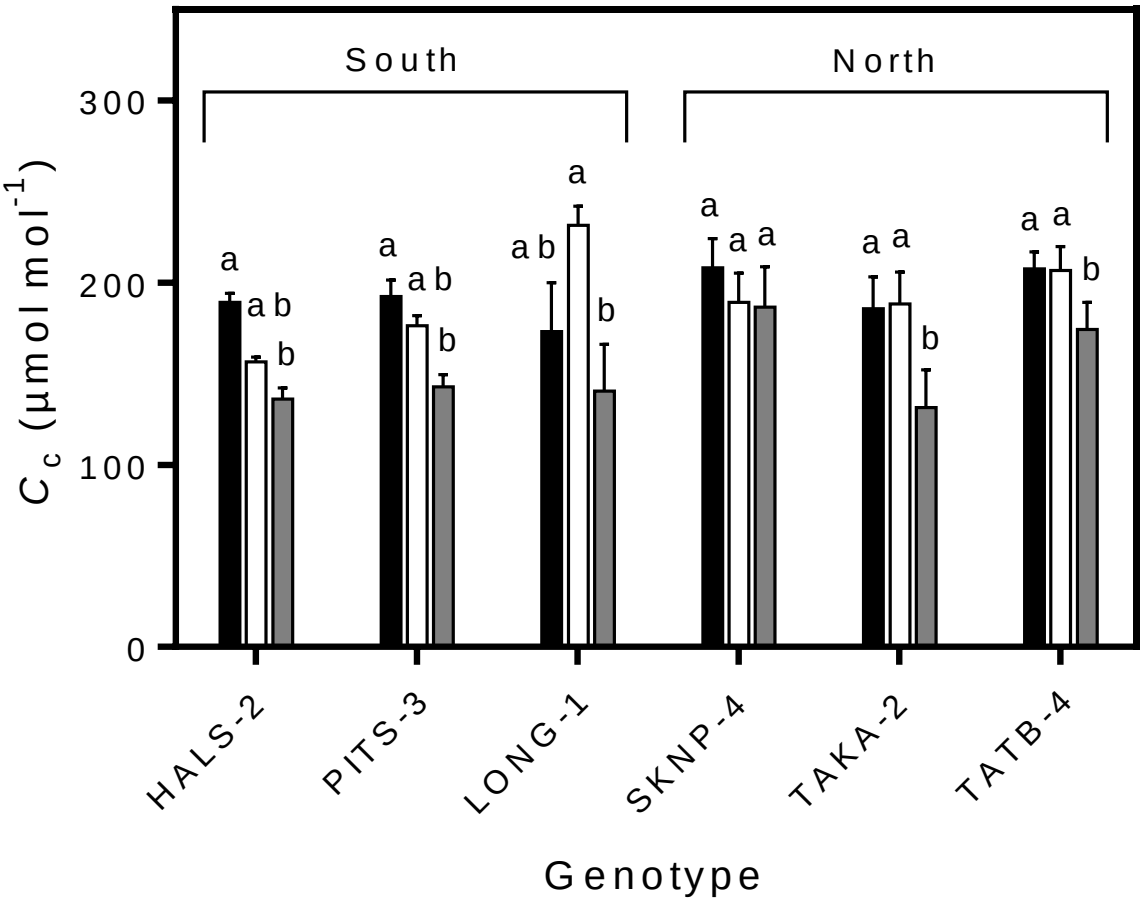

Figure 2.11 Mean values (± SE; n = 4) for CO_2 concentration at sites of carboxylation (C_c, µmol mol^{-1}) of six *Populus trichocarpa* genotypes under three treatments (distilled water in black, aqueous NH_4OH in white, and acetazolamide in grey). Different letters show significant differences between distilled water (control 1), aqueous NH_4OH (control 2) and acetazolamide treatments for each genotype at $P < 0.002$.

Table 2.3 A_n, g_m, V_{cmax} and J_{max} mean values (± SE) over five replications estimated for leaves under control (distilled water) and acetazolamide treatments using the A-C_i curve method. Data were introduced to PROC GLM in SAS 9.4 for analysis of variances. Significant differences between control and acetazolamide treatments are shown with different letters at $P < 0.05$.

	control	acetazolamide
^1A_n	13.33 ± 0.26 [a]	10.34 ± 0.23 [b]
^2A_n	15.89 ± 0.29 [a]	15.50 ± 0.15 [a]
g_m	0.216 ± 0.012 [a]	0.090 ± 0.008 [b]
V_{cmax}	75.00 ± 4.77 [a]	78.60 ± 5.94 [a]
J_{max}	89.18 ± 1.97 [a]	81.22 ± 3.59 [a]

^1A_n, and ^2A_n net assimilation rates (µmol CO_2 m^{-2} s^{-1}) at the ambient and saturating CO_2 concentrations, respectively; g_m, mesophyll conductance (mol CO_2 m^{-2} s^{-1}); V_{cmax}, maximum carboxylation rate allowed by rubisco (µmol m^{-2} s^{-1}); J_{max}, maximum rate of photosynthetic electron transport rate (based on NADPH requirement) (µmol m^{-2} s^{-1}).

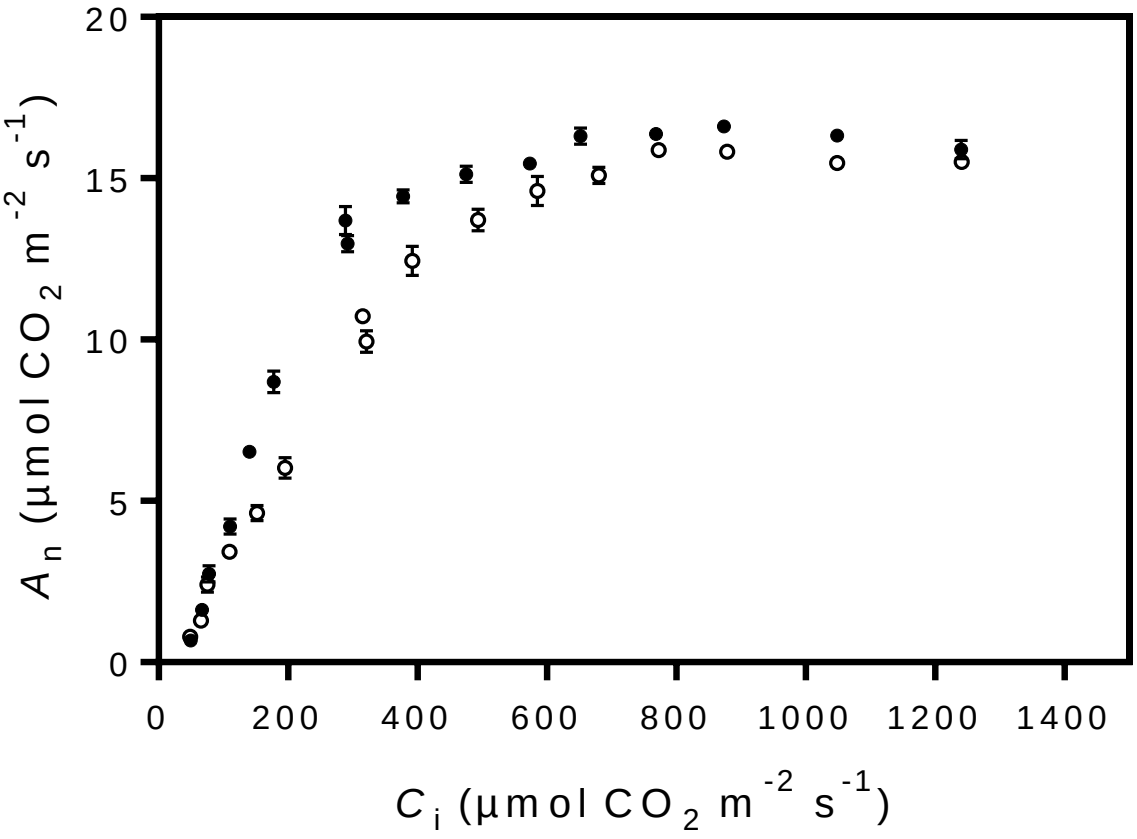

Figure 2.12 Relationship between mean A_n (net assimilation rate) and C_i (intercellular air space CO_2 concentration) (± SE; n = 5) averaged over five replications under control (distilled water) and acetazolamide treatments at 1200 µmol m^{-2} s^{-1} PPFD. The LONG-1 genotype was chosen arbitrarily for this experiment. There was no NH_4OH control treatment.

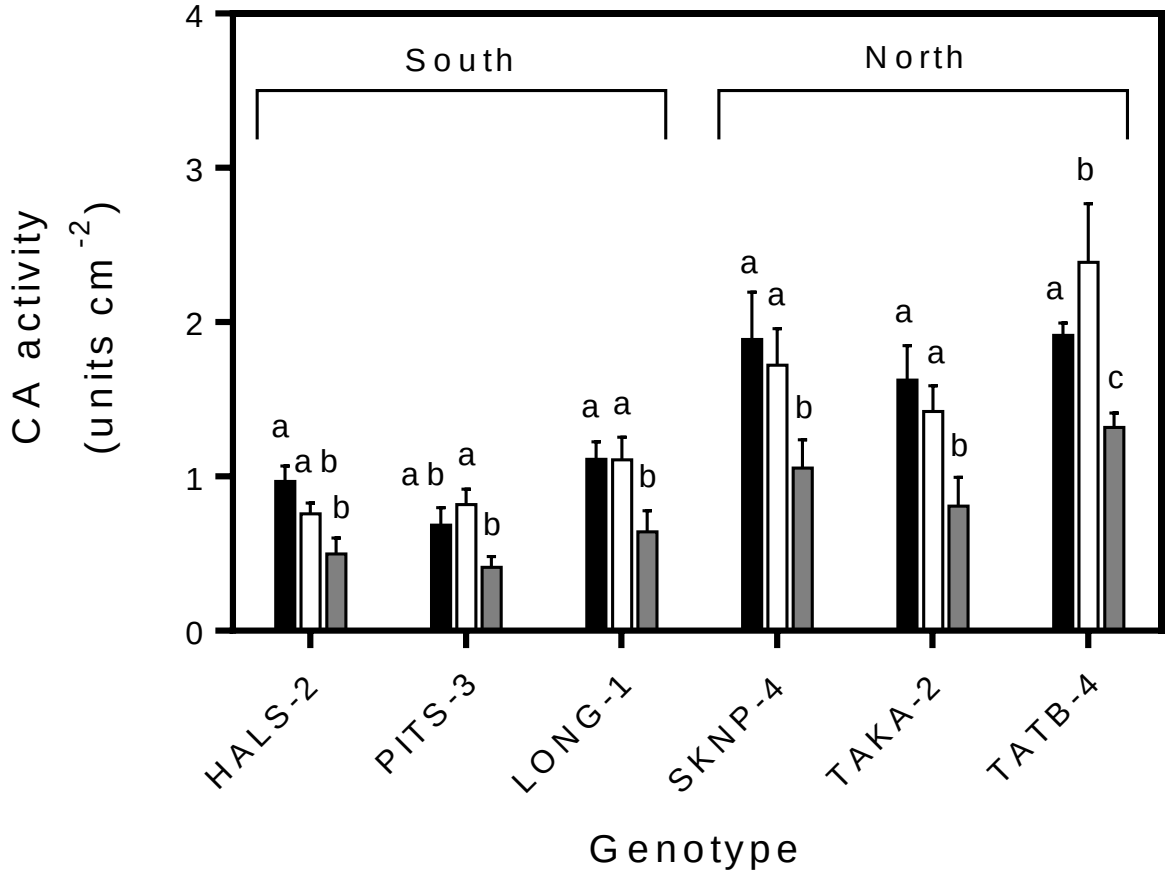

Figure 2.13 Mean values (± SE; *n* = 4) for carbonic anhydrase activity, CA activity (units cm^{-2}) of six *Populus trichocarpa* genotypes under three treatments (distilled water in black, aqueous NH_4OH in white, and acetazolamide in grey). Different letters show significant differences between distilled water (control 1), aqueous NH_4OH (control 2) and acetazolamide treatments for each genotype at $P < 0.002$.

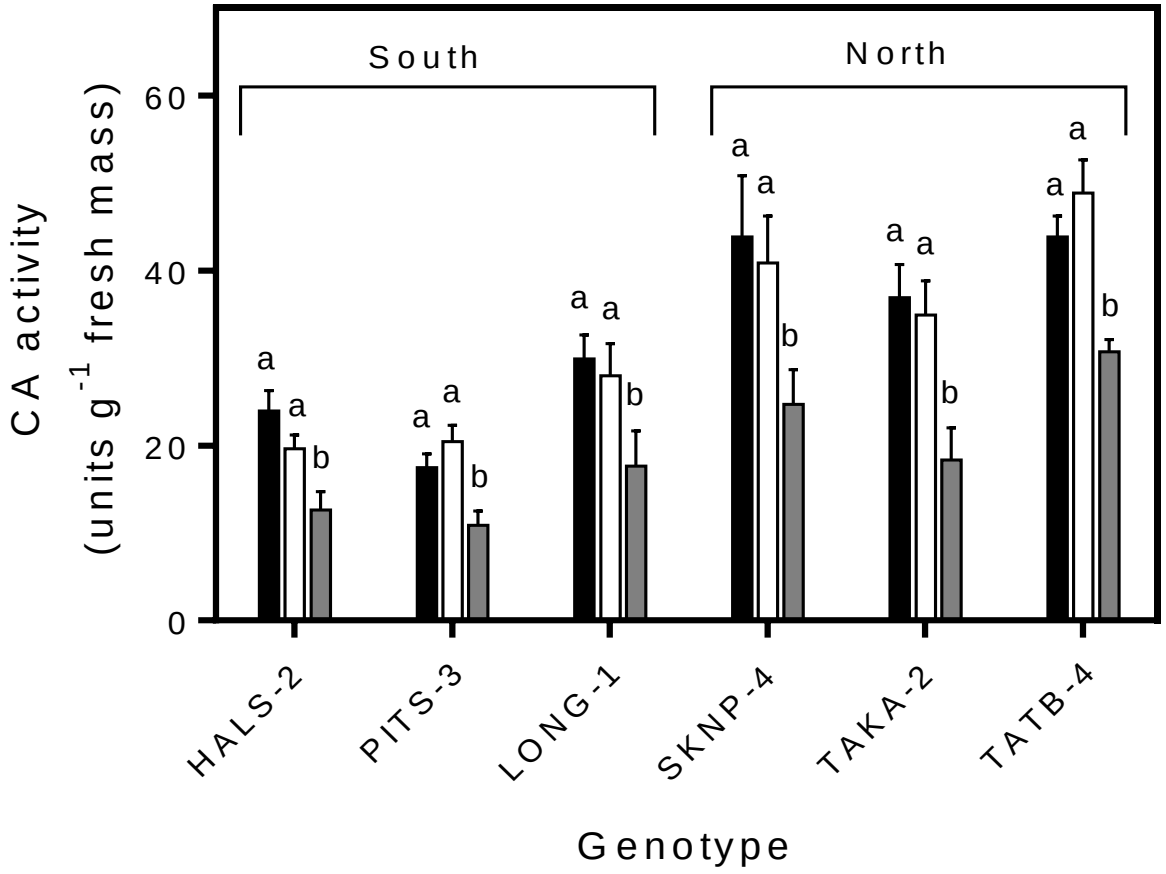

Figure 2.14 Mean values (± SE; $n = 4$) for carbonic anhydrase activity, CA activity (units g^{-1} fresh mass) of six *Populus trichocarpa* genotypes under three treatments (distilled water in black, aqueous NH_4OH in white, and acetazolamide in grey). Different letters show significant differences between distilled water (control 1), aqueous NH_4OH (control 2) and acetazolamide treatments for each genotype at $P < 0.002$.

genotypes had just 11% greater LMA than the southern genotypes (Figure 2.15, $P < 0.0001$). Inhibitory effects of acetazolamide treatment on CA activity paralleled effects on A_n and g_m ($P < 0.016$). Under acetazolamide, northern genotypes still had a significantly higher CA activity (2.4 fold) than southern ones (Figure 2.13).

Commensurate with their higher control values, northern genotypes had greater absolute reductions in A_n, g_m, and CA activity under acetazolamide compared to southern ones (Table 2.4). These differences disappeared when reductions in A_n, g_m, g_s, and CA activity were expressed as percentages relative to either the distilled water or the aqueous NH_4OH controls (Table 2.4). In contrast, percent reduction in C_c was greater for southern genotypes compared to northern genotypes (Table 2.4).

2.3.4 Trait correlations

There was a strong correlation between g_m and CA activity whether treatments were combined ($r = 0.752$, $P < 0.0001$) or considered separately (Figure 2.16). Thus, g_m and CA activity were related to each other, whether the variation was inherent or induced (i.e., by acetazolamide).

Inhibitor affects aside, several traits were correlated with each other when assayed under either the distilled water (Table 2.5) or, similarly, the aqueous NH_4OH control (not shown). Net assimilation rate was positively correlated with g_s ($r = 0.497$, $P = 0.013$), but more so with g_m ($r = 0.794$, $P < 0.0001$) and, consequently, also with WUE ($r = 0.685$, $P < 0.0001$). In fact, A_n, g_m, WUE and CA were all positively intercorrelated with each other, and with LMA. Although CA activity was correlated with LMA ($r = 0.641$, $P < 0.001$) across all genotypes, it had a much larger coefficient of variation (28% vs. 9%), reflecting higher activities in northern genotypes on both a mass and area basis.

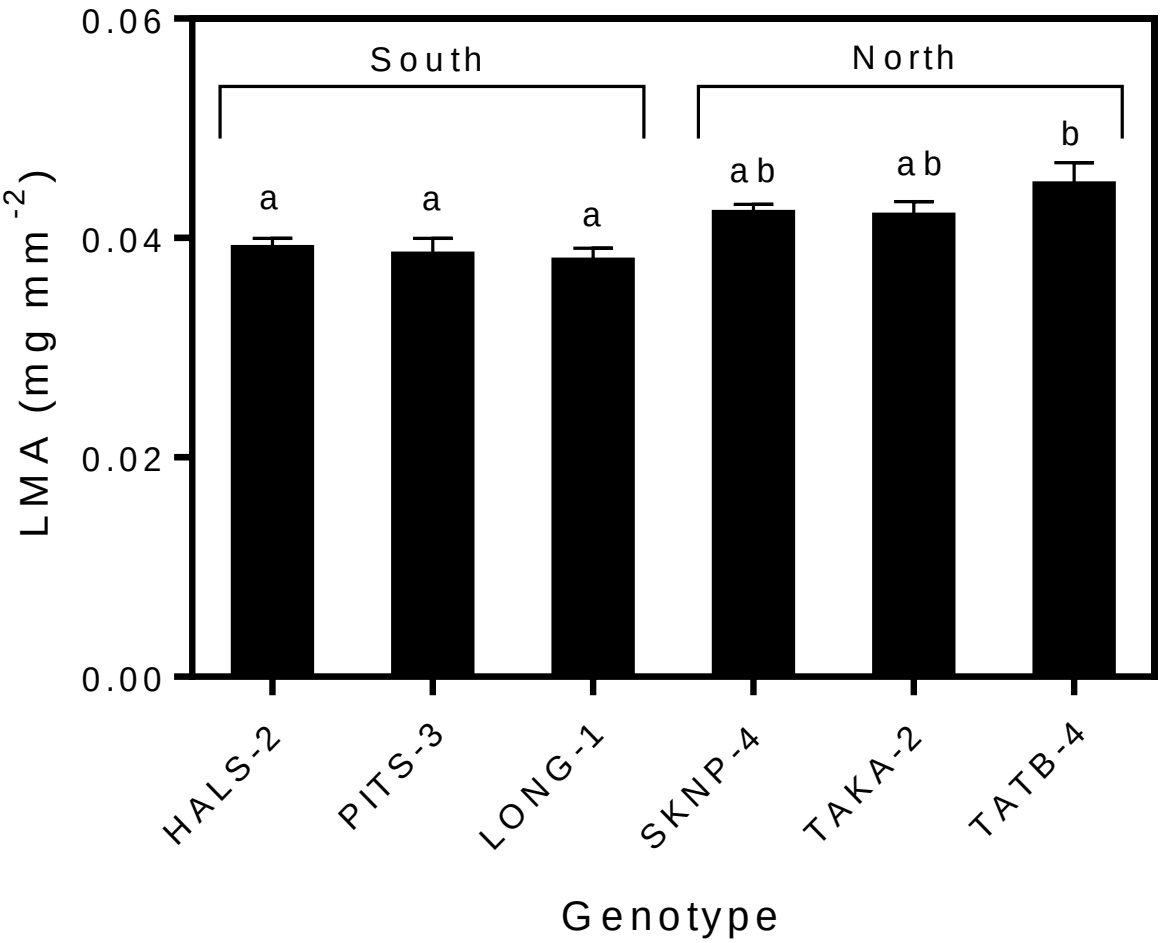

Figure 2.15 Leaf mass per area (LMA, mg mm^{-2}) of six *Populus trichocarpa* genotypes. Shown are mean values (± SE) determined on 12 leaves per genotype. Different letters show significant differences between genotypes.

Table 2.4 Absolute and percentage reductions in A_n, g_s, CA activity, g_m and C_c under acetazolamide treatment from controls 1 and 2 (distilled water and aqueous NH_4OH) for the northern vs. the southern genotypes. Data pairing was on a plant per plant basis. Different letters show significant differences for mean values (± SE; $n = 4$) of control 1 and 2 compared to the acetazolamide treatment for northern vs. southern genotypes at $P < 0.025$.

		north		south	
		control 1	control 2	control 1	control 2
A_n	absolute	3.94 ± 0.29 ^{a}	3.55 ± 0.20 ^{a}	2.84 ± 0.45 ^{b}	2.22 ± 0.25 ^{b}
	percentage	24.7 ± 1.7 ^{a}	22.9 ± 1.3 ^{a}	26.7 ± 3.7 ^{a}	22.3 ± 3.3 ^{a}
g_s	absolute	0.044 ± 0.007 ^{a}	0.030 ± 0.006 ^{ac}	0.021 ± 0.010 ^{bc}	-0.001 ± 0.009 ^{b}
	percentage	19.8 ± 2.9 ^{a}	14.2 ± 2.7 ^{a}	11.0 ± 5.8 ^{ab}	-0.068 ± 5.46 ^{b}
CA activity	absolute	0.75 ± 0.05 ^{a}	0.78± 0.11 ^{a}	0.40 ± 0.06 ^{b}	0.33 ± 0.04 ^{b}
	percentage	42.0 ± 3.6 ^{a}	42.5 ± 3.7 ^{a}	43.3 ± 5.6 ^{a}	40.0 ± 5.1 ^{a}
g_m	absolute	0.112 ± 0.019 ^{a}	0.100 ± 0.015 ^{a}	0.042 ± 0.011 ^{b}	0.047 ± 0.016 ^{b}
	percentage	47.8 ± 5.4 ^{a}	43.8 ± 5.2 ^{a}	44.2 ± 7.3 ^{a}	46.5 ± 8.1 ^{a}
C_c	absolute	33.3 ± 7.0 ^{a}	26.6 ± 8.6 ^{a}	56.5 ± 7.3 ^{b}	62.4 ± 13.9 ^{b}
	percentage	16.3 ± 4.1 ^{ac}	13.8 ± 4.8 ^{a}	30.9 ± 3.9 ^{bc}	30.7 ± 5.4 ^{bc}

A_n, net assimilation rate (μmol CO_2 m^{-2} s^{-1}); g_s, stomatal conductance (mol H_2O m^{-2} s^{-1}); CA activity, carbonic anhydrase activity (units cm^{-2}); g_m, mesophyll conductance (mol CO_2 m^{-2} s^{-1}); C_c, CO_2 concentration at sites of carboxylation (μmol mol^{-1}).

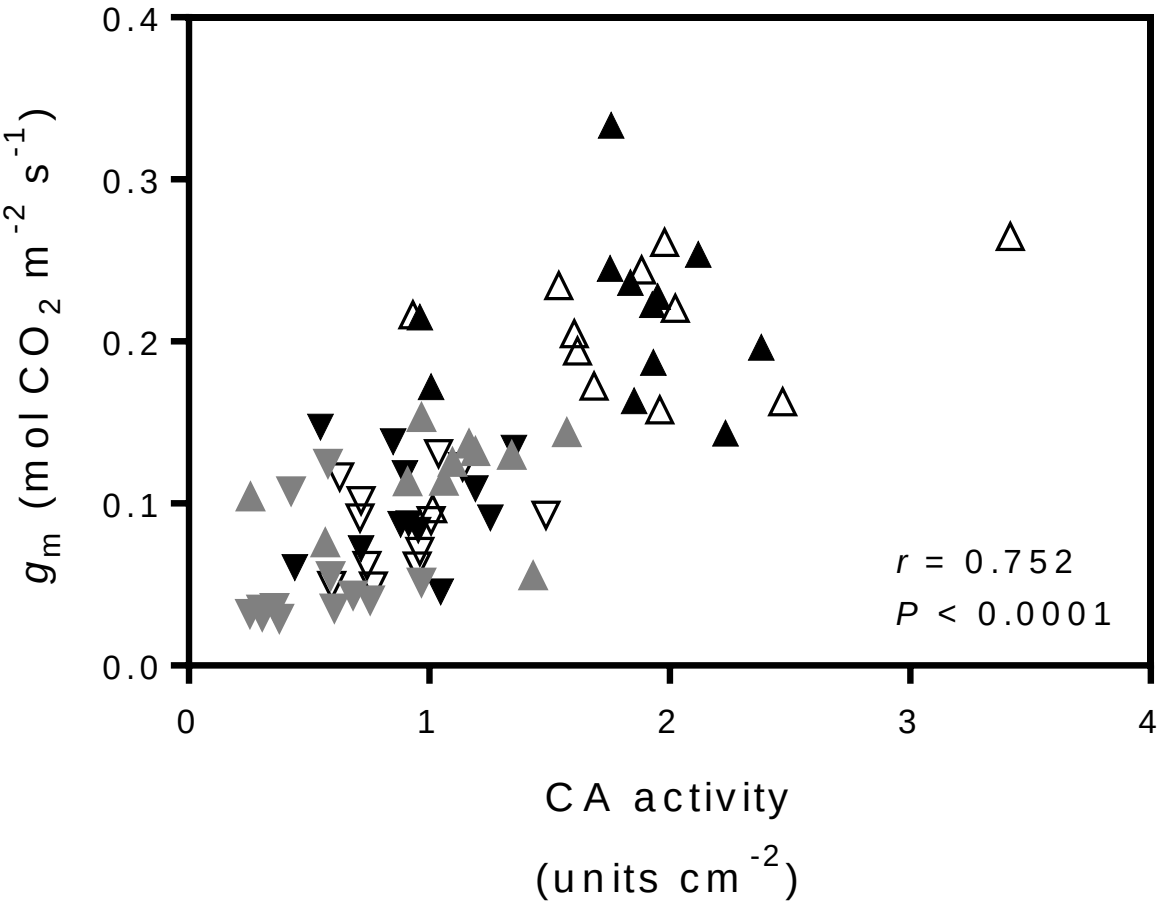

Figure 2.16 Correlation between CA activity (units cm^{-2}) and mesophyll conductance (g_m, mol CO_2 m^{-2} s^{-1}) under three treatments; control 1 (northern genotypes ▲, southern genotypes ▼), control 2 (northern genotypes △, southern genotypes ▽), and acetazolamide (northern genotypes ▲, southern genotypes ▼). The correlation coefficient and associated *P*-value shown are for all treatments combined. For the individual treatments considered separately, the correlation coefficients were 0.623 ($P = 0.0011$) for control 1, 0.713 ($P < 0.0001$) for control 2, and 0.675 ($P = 0.0003$) for acetazolamide.

Table 2.5 Pearson correlation coefficients (*r*) between traits measured across all leaves (4 per genotype) in the distilled water treatment ($n = 24$). Significant correlations are in bold ($P < 0.05$) and bold* are significant after Bonferroni correction ($P < 0.003$).

	A_n	LMA	g_s	g_m	WUE	C_c
LMA	**0.565**					
g_s	**0.497**	0.131				
g_m	**0.794***	**0.492**	0.327			
WUE	**0.685***	**0.659***	0.076	**0.544**		
C_c	0.348	0.100	0.244	**0.714***	0.114	
CA activity	**0.784***	**0.641***	**0.514**	**0.623***	**0.613***	0.200

A_n, net assimilation rate (μmol CO_2 m^{-2} s^{-1}); LMA, leaf mass per area (mg mm^{-2}); g_s, stomatal conductance (mol H_2O m^{-2} s^{-1}); g_m, mesophyll conductance (mol CO_2 m^{-2} s^{-1}); WUE, water-use efficiency (μmol CO_2 $mmol^{-1}$ H_2O); C_c, CO_2 concentration at sites of carboxylation (μmol mol^{-1}); CA activity, carbonic anhydrase activity (units cm^{-2}).

2.4 Discussion

The availability of CO_2 to rubisco, and therefore the rate of carboxylation, depends not only on stomatal conductance but also on mesophyll conductance, in varying, but often similar, proportion. As recommended by Pons et al. (2009), I used two methods to estimate g_m (isotope discrimination and fluorescence-based methods) and obtained comparable results by either method. Because of the technical constraints inherent to the measurement of g_m by these methods, the present study made detailed use of a small number of *Populus trichocarpa* genotypes chosen to be representative of either low (southern) or high (northern) latitudes. Our initial assessment of 12 genotypes covering 16 degrees latitude was consistent with and within the range of previous studies on field-grown material (Gornall & Guy 2007; McKown et al. 2014a), whereby there is a cline in A_n and g_s (Figure 2.4A, B), and leaf N (Figure 2.5), but not LMA (Figure 2.4D). Likewise, in completely separate analyses, the three representative northern genotypes had greater A_n (Figure 2.8) and marginally higher g_s (Figure 2.10) than the three representative southern genotypes. Going beyond previous studies, I show here, reproducibly (Figure 2.4C & Figure 2.9), that there is also a strong latitudinal cline in g_m. Across a wide variety of species, g_m and g_s often co-vary both statically and dynamically (Flexas et al. 2012). It is not surprising, then, that g_m in black cottonwood increases with latitude just as g_s does, though they were not significantly intercorrelated in this study. Intrinsically higher rates of photosynthesis in short-growing season plants are likely to be achieved by a variety of mechanisms working together, in different proportion in different species, populations or individuals.

As per our expectations, variation in g_m across control treatments was well correlated with CA activity (Figure 2.16). Furthermore, when leaves were pre-treated with acetazolamide through the

petiole, g_m and CA activity were inhibited in parallel (Figure 2.9 & 2.13), while g_s was significantly reduced only in the northern genotypes (Table 2.2) and only in the TATB-4 genotype (Figure 2.10), relative to the distilled water control. Northern and southern genotypes had similar C_c under control conditions, but the southern genotypes were significantly more susceptible to acetazolamide (Figure 2.11). Although treatment with acetazolamide resulted in similar reductions in A_n across all genotypes, C_c was perhaps more strongly affected in southern genotypes because of their lower levels of residual CA activity (Table 2.4). In fact, in the presence of acetazolamide, northern genotypes had residual CA activity that was still more-or-less equivalent to controls of the southern genotypes. Higher absolute reductions in g_m and CA activity in northern genotypes reflect their much higher control values relative to southern genotypes, but percent reductions were similar (Table 2.4). Although inhibition was in all cases incomplete, the differential "titration" of activity *in vivo* revealed the relationship shown in Figure 2.16. Taken together, the data strongly implicate a role for CA as one factor determining genotypic and induced variation in g_m.

A crucially important feature of the observed differences in CA activity is that they are largely, though not wholly, independent of differences in LMA. Although in previous work (Gornall & Guy 2007; McKown et al. 2014a) and in my initial assessment of 12 genotypes I did not find a significant latitudinal pattern in LMA in *P. trichocarpa*, the representative northern genotypes had 11% greater LMA than the southern genotypes (Figure 2.15). Most of this difference, however, is attributable to a single accession (TATB-4), and is nowhere near sufficient to account for the more than two times greater CA activity in the northern genotypes. Soolanayakanahally et al. (2009) also reported higher A_n and g_m in northern genotypes of *P. balsamifera*. In *P. balsamifera*, however, these tendencies seem to be more clearly related to LMA, with no consistent pattern in

g_s (Soolanayakanahally et al. 2015). Patterns in CA activity have not been studied in *P. balsamifera*.

Within the liquid phase, the cell wall and chloroplast envelope are thought to have the largest shares in total diffusive resistance (Tholen & Zhu 2011). Carbonic anhydrase activity has been found in the cytosol, chloroplast envelope, stroma, and mitochondria (Fabre et al. 2007; Evans et al. 2009) and in thylakoids (Ignatova et al. 2011; Fedorchuk et al. 2014). Because of the pH difference, the HCO_3^- concentration of the stromal space is up to five times greater than in the cytosol (Werdan & Heldt 1972). According to the model of Tholen & Zhu (2011), reductions in stromal CA activity or leakage of HCO_3^- from stroma to cytosol are predicted to reduce g_m. These authors estimated that removal of all CA activity from the stroma would reduce g_m by around 44%, and A_n by only 7%, relative to their arbitrary default conditions. Therefore it is surprising that in *P. trichocarpa* (Table 2.4), a 40-43% inhibition of total CA activity reduced g_m by 44-48% and decreased A_n by 22-26%.

Experiments utilizing genetically modified plants with reduced levels of CA have logically focused on the stromal isozyme, but substantially reduced expression of this CA has had little impact on g_m or A_n (e.g., Price et al. 1994). However, other CAs may also be important in facilitating CO_2 diffusion. For example, Shingles et al. (1997) reported that unless CA was provided externally, CO_2 diffusion across chloroplast inner envelope membranes was limited by the dehydration rate of bicarbonate. The various known CAs are differentially susceptible to acetazolamide (Huang et al. 2011); αCAs are very sensitive, whereas βCAs, which include the predominant stromal CA, can be quite resistant to acetazolamide in archaeal, bacterial, yeast and (particularly) mammalian cells, but are more sensitive in plants and green algae. The K_i value of

acetazolamide binding to pea βCA is 28 μM (Huang et al. 2011) – well below our feeding concentration (1 mM). In addition, the effect of CA inhibition could be species dependent and reflect differences in leaf microanatomy, photosynthetic capacity, etc. Species with low g_m, as is typical of woody species (Flexas et al. 2008), are expected to be more dependent on CA-facilitated CO_2 diffusion (Gillon & Yakir 2000).

Although acetazolamide, supplied through the petiole, clearly resulted in reduced CA activity, its impact on photosynthesis may be partially attributable to other effects. Both acetazolamide and ethoxyzolamide can directly impact photosynthetic electron transport (Swader & Jacobson 1972; Lonergan & Sargent 1978). I emphasize, however, that direct inhibition of photosynthesis would result in a reduced diffusion gradient for CO_2 and thus an increase in C_c, whereas I observe the opposite (Figure 2.11). Furthermore, comparison of A-C_i curves for control and acetazolamide treatments showed that increasing CO_2 to the saturation point overcomes limitations to photosynthesis caused by acetazolamide, consistent with an effect on g_m and not on the capacity for electron transport (Figure 2.12).

Another explanation for the efficacy of our acetazolamide treatments are possible additional effects on aquaporins. Acetazolamide reversibly blocks water movement across aquaporin-4 (AQP4) in mammalian cells (Tanimura et al. 2009; Kamegawa et al. 2016). In turn, mercuric ion, a widely used aquaporin blocker, inhibits CA (Blundell & Jenkins 1977). In fact, there are recent reports that aquaporins and CAs may be functionally related and CA near or associated with membranes may be working in conjunction with aquaporins to facilitate diffusion. Physical interaction between the two proteins facilitates water transport in mammalian cells (Vilas et al. 2015), and Borisova et al. (2012) suggested that CA binds to aquaporins in chloroplast envelopes.

In the CO_2-signaling pathway of Arabidopsis guard cells, the CO_2-permeable aquaporin PIP2;1 interacts with a CA located at the intercellular side of the plasma membrane (βCA4) to regulate stomata opening (Wang et al. 2016).

2.5 Conclusion

As shown here, the tendency towards greater A_n in black cottonwood accessions originating from higher latitude is mirrored not only by higher foliar nitrogen and g_s, but also by higher g_m. The linear relationship between g_m and CA activity across genotypes and inhibitor treatments, either in combination or considered separately (Figure 2.16), suggests that CA activity plays a significant role in mediating the mesophyll resistance to CO_2 diffusion in this species. Inherent clonal and latitudinal variation in g_m is strongly linked to this trait. Nonetheless, variation in other physiological and/or morphological components, such as differences in cell wall area and thickness, or chloroplast positioning and aquaporin channels, may contribute, in parallel, to these genotypic differences.

Chapter 3: Blue light differentially represses mesophyll conductance in high vs low latitude genotypes of *Populus trichocarpa* Torr. & Gray

3.1 Introduction

In widely distributed species, variations in ecophysiological traits mirror genetic adaptation to gradient (spatial) climatic conditions (Marchin et al. 2008; Hoffmann & Sgró 2011). *Populus trichocarpa* ranges from Kodiak Island in Alaska (62º N lat.) to northern Baja California (31º N lat.), and inland in the Pacific Northwest and in southern British Columbia to southern Alberta (Maini & Cayford 1968; Niemiec et al. 1995). In *P. trichocarpa*, net assimilation rate, leaf nitrogen concentration, and stomatal conductance co-vary with latitude (Gornall & Guy 2007; McKown et al. 2014a). Stomatal conductance in *P. trichocarpa* is positively correlated with adaxial stomatal density and the adaxial/abaxial stomatal ratio that are, on average, greater for high latitude genotypes (McKown et al. 2014b). In addition, greater A_n in northern *P. trichocarpa* is supported by higher mesophyll conductance (Momayyezi & Guy 2017), which defines the ease of CO_2 diffusion from the substomatal cavity to the site of fixation by rubisco.

The mesophyll conductance is mediated by anatomical and biochemical features of the mesophyll (Peguero-Pina et al. 2012; Flexas et al. 2013). Mesophyll conductance is affected by palisade cell wall area, wall thickness, aquaporin channels and carbonic anhydrase activity. Like photosynthetic capacity, all of these may at least partly scale with leaf mass per area (Flexas et al. 2008; Milla-Moreno et al. 2016). However, as reported by Momayyezi & Guy (2017), northern *P. trichocarpa* genotypes have an almost two-fold higher CA activity than southern genotypes, independent of small differences in LMA. Commensurate with their higher g_m, the northern genotypes also showed greater absolute (but not relative) reductions in g_m in the presence of a CA inhibitor.

In addition to more-or-less static structural and/or potentially dynamic biochemical controls, subcellular "behavior" may also affect g_m. Mesophyll cells are capable of relocating their chloroplasts to optimize photosynthetic performance under low and/or inconsistent light energy, or to protect them from photodamage caused by excess light energy (Schurr et al. 2006; Takamatsu & Takagi 2011). Chloroplast movement in reaction to light supply is a blue light photoresponse, the amount of blue light functioning as a representative indicator of total PPFD (Haupt & Wagner 1984; Gorton et al. 1999). In most plant species the blue and near UV light receptors, phototropins and sometimes cryptochromes, directly perceive blue light (Goh 2009; Banaś et al. 2012). The ratio of blue to red light can thus be used to manipulate chloroplast positioning while keeping the total supply of photosynthetically active radiation (PAR) constant. Note that the proportion of blue light in global PAR during midday in the summer varies little with latitude; for example, on the solstice, the ratio of blue (470 nm) over red (630 nm) is only 1.2% greater at the northern range limit of *P. trichocarpa* (62° N) than at the southern range limit (31° N) (Bird & Riordan 1986; solar spectrum calculator available at https://www2.pvlighthouse.com.au).

Chloroplast positioning is expected to affect g_m by changing the chloroplast surface area exposed to the intercellular air space (Evans & von Caemmerer 1996; Evans & Loreto 2000). High versus low fluxes of blue light trigger different chloroplast responses (Banaś et al. 2012). Actin filaments and microtubules are two types of cytoskeletal proteins known to control redistribution of chloroplasts via a blue light transduction pathway (Takagi 2003; Verchot-Lubicz & Goldstein 2010; Banaś et al. 2012). Cytochalasins (i.e., form D), as potent inhibitors of actin-based chloroplast motility (Collings et al. 1996; Malec et al. 1996; Foissner et al. 2007), have been used to test the role of chloroplast repositioning as it relates to g_m (Tholen et al. 2008; Loreto et al. 2009).

To explore what role chloroplast positioning might have in relation to latitudinal variation in mesophyll conductance (g_m) of black cottonwood, I examined photosynthetic response to different blue light treatments in six representative genotypes (three northern and three southern). In a first experiment, the effect of increasing blue to red light ratio (in a constant total photosynthetic photon flux density) on gas exchange and g_m was tested. It was expected that a higher proportion of blue to red light would negatively affect g_m and, consequently, A_n. I hypothesized that northern genotypes would be more sensitive to blue light, consistent with their greater g_m and A_n. In a second experiment, I assessed the effects of blue light on chloroplast positioning as inferred from changes in the relationship between leaf greenness (i.e., the chlorophyll content index) and actual chlorophyll content. I predicted that chloroplast repositioning would parallel changes in g_m and thus be more profoundly obvious in northern genotypes. In a third experiment, I used petiolar-feeding with cytochalasin D to block chloroplast repositioning. I hypothesized that by blocking chloroplast movements, cytochalasin D would also prevent any blue light-induced reduction in g_m. Because this hypothesis was ultimately rejected, a fourth and final experiment tested for an effect of blue light on carbonic anhydrase activity as a possible alternative explanation for blue light related reductions in g_m.

3.2 Material and methods

3.2.1 Plant material

To study the effects of blue light on gas exchange (Experiment 1), cuttings of three northern and three southern *P. trichocarpa* genotypes (Table 2.1) were taken in late January to early February from the Totem Field common garden, University of British Columbia. Bagged cuttings were kept in a dark cold room at 4°C until they were rooted and planted. Cuttings were grown with supplemental lighting in a greenhouse (minimum PPFD = 500 µmol m^{-2} s^{-1}) under a 20 hour

photoperiod, maximum temperature of 25°C during day and 20°C during night, in 3.78 L pots containing a 70% peat moss and 30% perlite mixture. Measurements began after 6 weeks growth and, by processing one plant per day, lasted for approximately 5 weeks. The experiment had a completely randomized design with four biological replicates per genotype.

3.2.2 Light treatments and photosynthesis measurements

On each plant, the youngest fully expanded leaf was chosen to measure photosynthetic variables using a 6400-40 chlorophyll fluorescence chamber (LI-COR Biosciences, Lincoln, LE, USA). Eight blue light-emitting diodes (470 nm), identical to the three already present within the LI-COR 6400 XT chamber head, were added to the light source to increase the maximum amount of blue light (BL) and maintain a total PPFD of 1200 µmol m^{-2} s^{-1}. The output of the additional LEDs was controlled manually using an external power source. Red light (RL) (630 nm) was provided by the original LI-COR 6400 XT light source (Figure 3.1).

All measurements were conducted in the greenhouse between 09:30 h and 13:30 h. Leaves were dark-adapted for 25 min prior to any gas exchange measurements to obtain the maximum quantum yield of photosystem II. Leaves were then light-adapted for 25 min under each of five BL:RL supply ratios; 0:100, 10:90, 20:80, 40:60, and 60:40. The 10:90 treatment (i.e., 10% BL) represented the control condition. The sample CO_2 concentration inside the chamber was 400 µmol mol^{-1}, leaf temperature was 25°C, (VPD) was controlled between 1.4-1.6 kPa, and flow rate was 300 µmol air s^{-1}. The quantum yield of photosystem II (Φ_{PSII}) under actinic light was obtained by application of saturating flashes (>7000 µmol m^{-2} s^{-1}) as per Genty et al. (1989). Disc punches were taken from leaves and dried at 70°C for 72 hours to calculate leaf mass per area (LMA, mg mm^{-2}).

Figure 3.1 Photosynthetic traits were measured under five different blue light to red light ratios (0:100, 10:90, 20:80, 40:60, 60:40) at a constant total PPFD (1200 µmol m^{-2} s^{-1}).

3.2.3 Calculation of g_m

The "constant *J* method" was used to estimate g_m based on measurements of chlorophyll fluorescence. I have previously shown in black cottonwood that the results of this method and estimation of g_m by stable carbon isotope discrimination are well correlated and of comparable magnitude (Chapter 2; Momayyezi & Guy 2017). The electron transport rate (J_{flu}) was calculated according to Genty et al. (1989):

$$J_{flu} = \Phi_{PSII} \times PPFD \times \alpha \times \beta \quad (1)$$

where the fraction of absorbed quanta reaching photosystem II (β) was estimated to equal 0.5 and 0.4 under 10 and 60% BL, respectively (see Appendix A, Figure A.3), by extrapolating to Φ_{CO_2} = 0 the linear relationship between Φ_{PSII} and the corresponding quantum yield for net assimilation rate (Φ_{CO_2}) under non-photorespiratory conditions (2% O_2) over a range of PPFD from 50 to 1200 µmol m^{-2} s^{-1} (Valentini et al. 1995). The leaf absorptance (α) was measured for five replications and averaged under 10% BL (0.858 ± 1.03) and 60% BL (0.811 ± 1.49), using a CI-710 leaf spectrometer (CID BioScience Inc. Camas, WA, USA). g_m was then calculated under 10 and 60% BL according to Harley et al. (1992):

$$g_m = A_n / \left[C_i - \left(\frac{\Gamma^*(J_{flu}+8(A_n+R_d))}{J_{flu}-4(A_n+R_d)}\right)\right] \quad (2)$$

where A_n is the net assimilation rate, C_i is the CO_2 concentration in the intercellular air space, R_d is the non-photorespiratory respiration rate in the light, and Γ^* is the chloroplast CO_2 photocompensation point (assumed here to equal the intercellular CO_2 photocompensation point, C_i^*) (Gilbert et al. 2012). As per Momayyezi & Guy (2017), Γ^* and R_d were taken to be 1.12 ± 0.37 µmol mol^{-1} and 43.41 ± 1.25 µmol m^{-2} s^{-1}, respectively.

The ratio of g_s/g_m was calculated as a measure of the limitation of g_m on photosynthesis relative to g_s (i.e., values greater than 1 indicate a greater limitation due to g_m than to g_s). From g_m under 10 and 60% BL, the CO_2 concentration at sites of carboxylation (C_c) was estimated according to equation 3 (Harley et al. 1992):

$$C_c = C_i - \frac{A_n}{g_m} \qquad (3)$$

3.2.4 Light response curves

To confirm that a PPFD of 1200 µmol m^{-2} s^{-1} was saturating irrespective of the light treatment, A_n and g_m were estimated as above but over a range of PPFD from 50 to 1300 µmol m^{-2} s^{-1} under 10 and 60% BL (Figure 3.2). The genotype showing the largest differences in A_n under control and 60% BL was used for this purpose (i.e., SKNP-4).

3.2.5 CCI measurement and chlorophyll extraction

In Experiment 2, Chlorophyll content index (CCI) was measured for all genotypes immediately after 10, 40, and 60% BL treatments (25 min) using a CCM 200 plus (Opti-Science, Inc, Hudson, NH, USA) chlorophyll content meter. Additionally, the most northerly genotype with the largest changes in CCI (TATB-4) was used in a test to confirm that high blue light treatment (60% BL) did not affect the actual leaf chlorophyll content (ACC). Three leaf discs (0.27 cm^2 each) were punched from the lamina immediately after irradiation with 10% and 60% BL. Discs were transferred to 10 mL vials containing 6 mL of N,N-dimethylformamide (DMF) as an extractant. Vials were wrapped in aluminum foil to prevent photooxidation and were stored at 4°C until the tissue was bleached (24 hours). Total chlorophyll was determined spectrophotometrically as per Porra et al. (1989). I express CCI relative to ACC as an index of relative chloroplast positioning, lower numbers presumably being associated with more self-shading among chloroplasts.

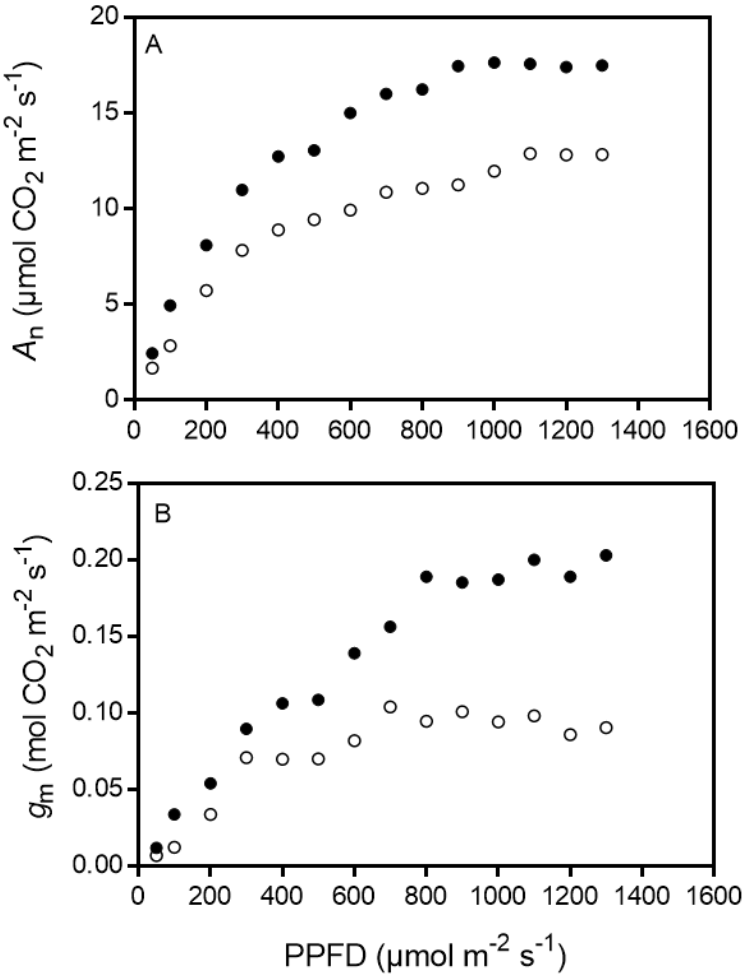

Figure 3.2 Light response curves for net assimilation rate (A_n, µmol CO_2 m^{-2} s^{-1}) and mesophyll conductance (g_m, mol CO_2 m^{-2} s^{-1}) of the SKNP-4 genotype under 10% (●) or 60% BL (○). Photosynthetic photon flux density (PPFD) was varied from 50 to 1300 µmol m^{-2} s^{-1} while CO_2 concentration was held constant at 400 µmol mol^{-1}.

3.2.6 Inhibition of chloroplast movements

The three youngest fully developed leaves from ramets of TATB-4 were used in five replications to compare the effect of low (10%) and high (60%) blue light on g_m with and without cytochalasin D (Experiment 3). A 3 µM cytochalasin D solution in 10 mM dimethyl sulfoxide (DMSO) was prepared by dissolving the actin depolymerizing agent in DMSO and diluting with distilled water. Distilled water alone, and 10 mM DMSO in distilled water, were the two control treatments. Petioles were cut under water and leaves were immediately transferred to 2 mL vials containing either cytochalasin D solution or one of the two controls (Figure 3.3). After one hour under natural lighting in the greenhouse, leaves were light adapted under 10 and 60% BL prior to gas exchange measurements as detailed above. CCI and ACC were measured after each blue light treatment.

3.2.7 Carbonic anhydrase activity

The two youngest fully developed leaves in four replications from two genotypes, one chosen randomly from the northern group (TATB-4) and one chosen randomly from the southern group (LONG-1), were used to test the effect of high blue light on CA activity (Experiment 4). Only two genotypes were used because of technical limitations. From each plant, two petioles were cut under water and placed in 5 mL vials containing distilled water. After 90 min under greenhouse light, one leaf was light adapted under 10% and the other one under 60% BL for 25 min. Gas exchange measurements were obtained as described above. Immediately after measurements, CCI was measured for leaves. Leaf discs from the other side of the mid-rib, adjacent to the area of measurement, were collected using a paper punch to calculate LMA.

Remaining tissue was immediately frozen on dry ice for determination of CA activity as described

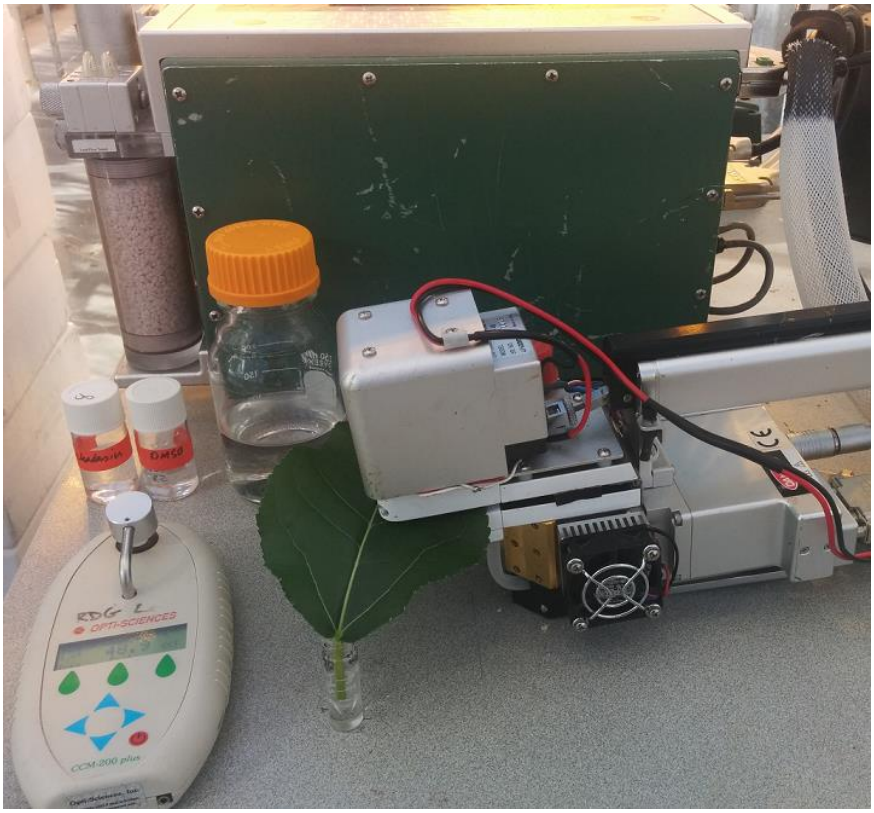

Figure 3.3 Cytochalasin D dissolved in DMSO was fed through leaf petioles to inhibit chloroplast movement. Photosynthetic traits were measured at low and high BL under distilled water, DMSO, and cytochalasin D in DMSO.

by Wilbur & Anderson (1948). For this purpose, 1.77 cm^2 leaf discs (~36 mg fresh weight) were cut with a cork borer from the area used for gas exchange measurements, and ground at liquid nitrogen temperature (-196°C) using disposable polypropylene pestles (length, 8.5 cm) in 1.5 mL polypropylene microcentrifuge tubes. All subsequent steps were at 4°C. After thawing, 70 µL of 40 mM potassium phosphate buffer (pH= 8.3) was added and the homogenate was centrifuged for 15 min at 4500×*g*. A 10 µL aliquot of supernatant was added to a further 0.5 mL of the buffer solution containing 20 ppm bromothymol blue as a pH indicator. The time required for the pH of the buffer solution to change from 8.3 to 6.3 for control (T_{Control}) and enzyme-containing (T_{Enzyme}) solutions was recorded visually upon the further addition of 0.5 mL of CO_2-saturated water. The CO_2-saturated water was prepared by bubbling CO_2 through distilled water for two hours (also at 4ºC). As a control, 10 µL of buffer solution was used in place of the supernatant. There were four technical replicates per assay. Enzyme activity was calculated as follows:

$$\text{Units CA / mL of supernatant} = \frac{(T_{\text{Control}} - T_{\text{Enzyme}}) \times df}{(T_{\text{Enzyme}}) \times V} \qquad (4)$$

where *df* is the dilution factor and *V* is the volume of enzyme extract used. Activities were expressed on a leaf area basis.

3.2.8 Statistics

All statistical tests used completely randomized designs. Data were transformed where needed to meet assumptions of normality and equal variance. In Experiment 1, mixed linear models in SAS 9.4 (SAS Institute Inc. NC, USA 2013) were used to compare effects of all five light treatments on A_n, g_s and C_i for the six genotypes independently, without considering latitude as a factor (adjusted *P* value for number of paired comparisons = 0.005). Then, mixed linear models were

used to compare the 60% blue light treatment effects on A_n, g_m, g_s, g_s/g_m and C_c, compared with 10% BL controls, for northern vs. southern genotypes. Both light treatment (T) and latitude (L) were considered fixed factors and genotypes were nested within latitude; because treatments were paired, replicates (plants) were nested within genotypes. Pairwise mean comparisons were used to test treatment effects within and between northern and southern latitudes (adjusted *P* value for number of paired comparisons according to Bonferroni correction was 0.008). A *t*-test was used to compare LMA in northern vs. southern genotypes.

For Experiment 2, a similar mixed linear model to Experiment 1 was used to compare CCI under 10, 40 and 60% BL within and between northern and southern latitudes. Pairwise mean comparisons were used to test treatment effects in northern vs. southern latitudes (adjusted *P* value for number of paired comparisons according to Bonferroni correction was 0.003). A two-way ANOVA ($P < 0.05$) was used to compare means for CCI, ACC and CCI/ACC ratio in TATB-4 using GraphPad Prism 6 software (GraphPad Software, Inc. CA, USA).

For Experiment 3, the effects of cytochalasin D on A_n, g_m, g_s, C_i, C_c, CCI, ACC, and CCI/ACC were analyzed using mixed linear models with two fixed effects (solution type [S], and light treatment [T]) in three and two levels, respectively (adjusted *P* value for number of paired comparisons = 0.003). For Experiment 4, a *t*-test with data paired by plant was used to analyze the effect of high blue light on CA activity, A_n, g_m, g_s, C_i, C_c and CCI ($P < 0.05$).

3.3 Results

3.3.1 Blue light effect on g_m

Photosynthetic rates were generally higher in the northern genotypes than in the southern

genotypes (Figure 3.4A). For example, under control (10% BL) conditions, A_n was 21% higher in the northern genotypes ($P < 0.008$) (Table 3.1). In contrast, LMA was not significantly different (0.042 ± 0.001 mg mm^{-2} vs. 0.037 ± 0.001 mg mm^{-2} in northern versus southern genotypes, respectively). Latitudinal differences in A_n were less pronounced at higher relative fluxes of blue light because northern genotypes were relatively more sensitive than southern genotypes (T × L, $P < 0.001$) (Table 3.1). Like A_n, g_s was significantly higher in the northern genotypes than in the southern genotypes at 10% BL ($P < 0.008$), but not at 60% BL (Table 3.1).

Across all genotypes combined, A_n was 8.9% higher under 10% BL relative to 0% BL ($P < 0.001$), and 16.9% higher relative to 60% BL ($P < 0.001$). Statistical power was insufficient to detect these differences in all pairwise comparisons within individual genotypes (Figure 3.4A), but as the proportion of blue light was increased, A_n went down such that at 60% BL, four out of the six genotypes had significantly lower A_n. Similarly, across all genotypes combined, g_s was 16.4% higher under 10% BL relative to 0% BL ($P < 0.001$), and 15.3% higher relative to 60% BL ($P < 0.001$), but significantly so at the genotypic level only in the northern genotypes SKNP-4 and TAKA-2 (Figure 3.4B). Intercellular air space CO_2 concentration was very consistent among genotypes and between light treatments, the only significant difference being between low (0 and 10%) and high (60%) blue light in TAKA-2 (Figure 3.4C).

Because β was affected by light quality but was not estimated for 0, 20 and 40% BL, g_m could only be properly calculated for the control (10%) and high (60%) blue light treatments. On average, the northern genotypes had consistently higher g_m than the southern genotypes under 10% BL ($P < 0.008$) (Table 3.1). Northern genotypes were both absolutely and relatively more sensitive than southern genotypes to higher supply ratios of blue light. Mesophyll conductance in both northern

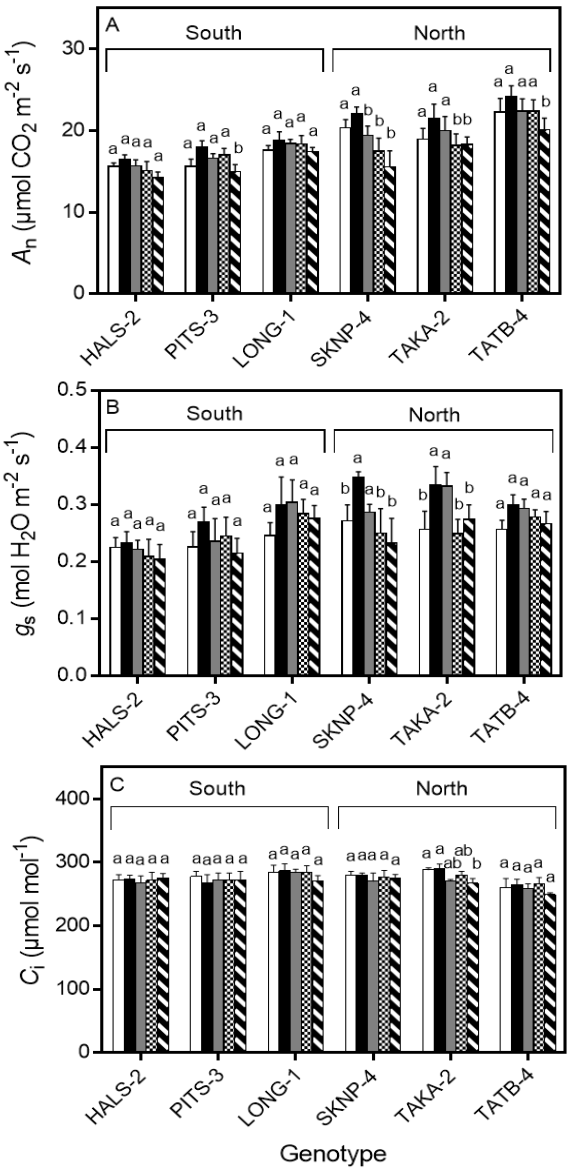

Figure 3.4 Mean values (± SE, n = 4) for A, net assimilation rate (A_n, μmol CO_2 m^{-2} s^{-1}); B, stomatal conductance (g_s, mol H_2O m^{-2} s^{-1}); C, intercellular air space CO_2 concentration (C_i, μmol mol^{-1}) of six *Populus trichocarpa* genotypes under five blue:red light supply ratios. For each genotype, from left (white bar) to right (striped bar), the proportion of blue light is 0, 10, 20, 40 and 60% BL. Different letters show significant differences between control (10% BL) and other treatments for each genotype at $P < 0.005$.

Table 3.1 Physiological traits for northern vs. southern genotypes under two different blue light treatments (10 and 60% BL). Different letters show significant differences within and between latitudes ($P < 0.008$) within a column (± SE, $n = 4$).

	% blue	A_n	g_m	g_s	g_s/g_m	C_c
north	10	22.58 ± 0.80 ^{a}	0.244 ± 0.027 ^{a}	0.33 ± 0.013 ^{a}	1.49 ± 0.13 ^{a}	176.37 ± 6.52 ^{a}
	60	18.41 ± 0.73 ^{bc}	0.153 ± 0.016 ^{bc}	0.26 ± 0.017 ^{b}	1.82 ± 0.11 ^{b}	146.45 ± 5.80 ^{bc}
south	10	17.76 ± 0.52 ^{b}	0.135 ± 0.005 ^{b}	0.27 ± 0.020 ^{b}	2.00 ± 0.14 ^{ab}	144.54 ± 5.43 ^{b}
	60	15.53 ± 0.55 ^{c}	0.107 ± 0.006 ^{c}	0.23 ± 0.016 ^{b}	2.26 ± 0.21 ^{ab}	130.87 ± 5.70 ^{c}

A_n, net assimilation rate (μmol CO_2 m^{-2} s^{-1}); g_m, mesophyll conductance (mol CO_2 m^{-2} s^{-1}); g_s, stomatal conductance (mol H_2O m^{-2} s^{-1}); g_s/g_m (stomatal conductance over mesophyll conductance ratio); C_c, CO_2 concentration at sites of carboxylation (μmol mol^{-1}).

and southern genotypes was decreased under 60% BL compared to the 10% BL control ($P < 0.008$) (Table 3.1). The percent reduction in g_m from control levels was significantly greater ($P < 0.05$) for the northern genotypes than for the southern genotypes (37.3% vs. 20.7%, respectively). In every situation the g_s/g_m ratio was always greater than 1, indicating that g_m presented the greater limitation on photosynthesis. The effects of blue light on g_m were larger than they were on g_s in all genotypes. However, g_s/g_m was significantly increased under high blue light only for northern genotypes ($P = 0.003$) (Table 3.1), to the point where differences in relative limitation between northern and southern genotypes disappeared at the highest blue light supply ratio. High blue light significantly decreased C_c in both northern and southern genotypes by 16.9% and 9.4%, respectively, compared to the control ($P < 0.008$) (Table 3.1), but there was no latitude by treatment interaction effect in this regard ($P = 0.167$).

3.3.2 Blue light effect on chloroplast positioning

In Experiment 2, and reflecting their higher photosynthetic capacity, the northern genotypes had two-fold greater CCI compared to southern ones ($P < 0.003$) (Table 3.2). Exposure to 60% BL significantly reduced CCI across ($P = 0.0013$) and within ($P < 0.008$) all genotypes, but most particularly in the three northern accessions (by up to 31%). The 40% BL treatment significantly reduced CCI only across genotypes ($P = 0.015$). I noticed that CCI recovered fully within 30 min of exposure to high blue light (not presented). In contrast to CCI, ACC was unaffected during exposure to 60% BL (Table 3.3), as measured in a genotype chosen for its large transient changes in CCI (TATB-4). Consequently, the relationship between CCI and chlorophyll content (CCI/ACC) was found to be blue-light dependent ($P < 0.05$).

Table 3.2 Effects of blue light treatment on chlorophyll content index (CCI) for northern vs. southern *Populus trichocarpa* genotypes. Different letters show significant differences ($P < 0.003$) for mean values (± SE, $n = 4$).

	10% BL	40% BL	60% BL
north	43.18 ± 2.83 [a]	35.49 ± 2.03 [ab]	29.70 ± 1.89 [b]
south	21.15 ± 0.56 [c]	18.47 ± 0.69 [cd]	17.56 ± 0.58 [d]

Table 3.3 Test for lack of effect of the blue light:red light supply ratio on chlorophyll content using leaves of the TATB-4 genotype. Actual chlorophyll content (ACC), chlorophyll content index (CCI), and CCI/ACC ratio immediately after 25 min exposure to 10% and 60% BL are presented. Different letters show significant differences between light treatments for mean values (± SE, n = 4) ($P < 0.05$).

% BL	ACC (µg/cm^2)	CCI	CCI/ACC
10	61.30 ± 1.03 [a]	54.03 ± 1.42 [a]	0.88 ± 0.02 [a]
60	64.56 ± 0.93 [a]	43.92 ± 0.95 [b]	0.68 ± 0.01 [b]

3.3.3 Effect of cytochalasin D on chloroplast repositioning and changes in g_m

In Experiment 3, there were no differences between distilled water and DMSO controls (Table 3.4). Furthermore, plant response to high blue light was consistent with Experiments 1 and 2 in all measured variables. Pretreatment with cytochalasin D, however, significantly decreased A_n, g_m and C_c in 10% BL controls ($P < 0.003$). There were some interaction effects between cytochalasin D and light treatment. Subsequent exposure to 60% BL had no further impact on A_n but did cause a further reduction in g_m to levels that were similar to distilled water and DMSO controls (S × T, $P < 0.0001$). Exposure to 60% BL reduced C_c to a similar value in all leaves ($P < 0.0001$) and without interaction (S × T, $P = 0.837$). Leaves treated with cytochalasin D had reduced CCI relative to DMSO controls but not distilled water controls at 10% BL, and not at 60% BL (S × T, $P = 0.002$). Actual chlorophyll content was also reduced by cytochalasin D relative to distilled water and DMSO controls, but significantly so only at 60% BL ($P = 0.0009$). There was no net effect of cytochalasin D on CCI/ACC under 10% BL, and, in sharp contrast to distilled water and DMSO controls, there was no change in CCI/ACC upon exposure to high blue light (S × B, $P = 0.547$).

3.3.4 Blue light effect on CA activity

In Experiment 4 (Table 3.5), high blue light significantly reduced CA activity by 19.8% (0.24 units $cm^{-2} \pm 0.05$ SE) compared to the control treatment ($P = 0.003$). Effects on A_n, g_m, C_c, CCI and C_i were all consistent with previous experiments.

3.4 Discussion

After entering the leaf through stomatal pores, ambient CO_2 molecules transiting to the site of carboxylation need to overcome a series of resistances in both gas and liquid phases. Structural

Table 3.4 Effect of cytochalasin D on A_n, g_m, g_s, C_i, C_c, CCI, ACC, and CCI/ACC in the TATB-4 genotype tested under 10 and 60% BL in distilled water, DMSO, and DMSO + cytochalasin D. Different letters show significant differences between mean values within each row (± SE, n = 5) ($P < 0.003$).

	distilled water		DMSO		cytochalasin D + DMSO	
	10% BL	60% BL	10% BL	60% BL	10% BL	60% BL
A_n	16.94 ± 0.25 ^{a}	14.71 ± 0.79 ^{ab}	17.00 ± 0.54 ^{a}	14.26 ± 0.43 ^{b}	12.95 ± 0.58 ^{b}	13.05 ± 0.71 ^{b}
g_m	0.298 ± 0.037 ^{a}	0.184 ± 0.047 ^{bc}	0.303 ± 0.046 ^{a}	0.165 ± 0.046 ^{bc}	0.137 ± 0.010 ^{b}	0.106 ± 0.008 ^{c}
g_s	0.25 ± 0.01 ^{a}	0.24 ± 0.02 ^{a}	0.22 ± 0.02 ^{a}	0.22 ± 0.02 ^{a}	0.20 ± 0.02 ^{a}	0.20 ± 0.02 ^{a}
C_i	279.00 ± 6.79 ^{a}	285.68 ± 8.76 ^{a}	263.00 ± 10.41 ^{a}	279.01 ± 10.53 ^{a}	279.85 ± 11.06 ^{a}	276.37 ± 11.02 ^{a}
C_c	219.29 ± 12.02 ^{a}	189.74 ± 11.68 ^{bc}	202.97 ± 11.34 ^{ad}	175.10 ± 9.26 ^{bc}	183.11 ± 11.76 ^{bd}	151.68 ± 8.53 ^{c}
CCI	37.91 ± 0.31 ^{ac}	28.54 ± 0.16 ^{b}	39.57 ± 0.33 ^{a}	28.89 ± 0.65 ^{b}	32.37 ± 0.39 ^{bc}	31.25 ± 0.89 ^{b}
ACC	49.13 ± 1.77 ^{ab}	49.71 ± 2.40 ^{a}	49.46 ± 0.79 ^{a}	50.05 ± 1.02 ^{a}	44.09 ± 2.43 ^{ab}	41.05 ± 2.05 ^{b}
CCI/ACC	0.77 ± 0.08 ^{a}	0.58 ± 0.07 ^{b}	0.80 ± 0.06 ^{a}	0.58 ± 0.11 ^{b}	0.74 ± 0.09 ^{a}	0.76 ± 0.09 ^{a}

A_n, net assimilation rate (μmol CO_2 m^{-2} s^{-1}); g_m, mesophyll conductance (mol CO_2 m^{-2} s^{-1}); g_s, stomatal conductance (mol H_2O m^{-2} s^{-1}); C_i, intercellular air space CO_2 concentration (μmol mol^{-1}); C_c, CO_2 concentration at sites of carboxylation (μmol mol^{-1}); CCI, chlorophyll content index; ACC, actual chlorophyll content (μg/cm^2); CCI/ACC, chlorophyll content index, actual chlorophyll content ratio.

Table 3.5 Effect of 60% BL on CA activity, A_n, g_m, g_s, C_i, C_c and CCI in. Different letters show significant differences between mean values (± SE, n = 4) within each row ($P < 0.05$). Genotype was not a factor in this experiment, so data presented here are means across both TATB-4 and LONG-1 combined.

	distilled water	
	10% BL	60% BL
CA activity	1.16 ± 0.20 [a]	0.93 ± 0.13 [b]
A_n	17.54 ± 0.84 [a]	15.93 ± 0.69 [b]
g_m	0.202 ± 0.027 [a]	0.145 ± 0.018 [b]
g_s	0.298 ± 0.012 [a]	0.283 ± 0.013 [a]
C_i	292.30 ± 3.50 [a]	294.52 ± 5.21 [a]
C_c	197.97 ± 7.21 [a]	175.66 ± 7.94 [b]
CCI	34.11 ± 2.96 [a]	26.52 ± 1.33 [b]

CA activity, carbonic anhydrase activity (units cm^{-2}); A_n, net assimilation rate (µmol CO_2 m^{-2} s^{-1}); g_m, mesophyll conductance (mol CO_2 m^{-2} s^{-1}); g_s, stomatal conductance (mol H_2O m^{-2} s^{-1}); C_i, intercellular air space CO_2 concentration (µmol mol^{-1}); C_c, CO_2 concentration at sites of carboxylation (µmol mol^{-1}); CCI, chlorophyll content index.

and biochemical components of mesophyll cells and their interaction regulate CO_2 conductance. Consistent with results presented by Momayyezi & Guy (2017), northern *P. trichocarpa* genotypes showed higher A_n, g_m and g_s in this study. In Momayyezi & Guy (2017), genotypic variation in g_m was shown to be associated with carbonic anhydrase activity. Chloroplast movement in response to light quality can also affect g_m and limit photosynthesis (Flexas et al. 2008; Flexas et al. 2012). In the present chapter (Table 3.1), increasing the blue to red light ratio from 10:90 to 60:40 negatively impacted A_n, g_m and C_c in both northern and southern genotypes of black cottonwood, and, bearing out the first hypothesis, more so in the northern genotypes. In addition, g_s was significantly reduced in the northern genotypes but not the southern genotypes. Consistent with other reports (Mansfield & Meidner 1966; Suetsugu et al. 2014) there was also a general tendency towards increased g_s from 0 to 10% BL, significant here in two northern genotypes. Low amounts of blue light are known to induce stomatal opening by exciting photoreceptors located in chloroplast membranes of guard cells (Sharkey & Raschke 1981; Zeiger & Field 1982).

Given their intrinsically higher g_m, it was not surprising to detect a greater absolute reduction in g_m in northern genotypes, but there was also a greater per cent reduction in northern genotypes (37%) relative to southern genotypes (21%). Similarly (Table 3.2), the higher blue light treatments (40 and 60% BL), resulted in significantly higher percent reductions in CCI (18 and 31%, respectively) in northern genotypes than in southern genotypes (13 and 17%). These reversible changes in chlorophyll content index occurred without any change in actual chlorophyll content (Table 3.3), consistent with changes in chloroplast positioning. The implication is that high blue light reduced the CCI by reducing the effectiveness of green light reflection. Measurements of leaf transmittance show that more visible light passes through black cottonwood leaves under these

conditions (not presented). In contrast, Higa & Wada (2016) observed little or no change in chloroplast repositioning under either 3 µmol m^{-2} s^{-1} or 20-50 µmol m^{-2} s^{-1} blue light in climbing plants, but these flux densities were very low. More consistent with the present study, Nauš et al. (2010) also found remarkable and reversible decreases in CCI when tobacco leaves were exposed to high blue light (340 µmol m^{-2} s^{-1}), particularly in younger leaves (35% decrease in CCI). Blue light perception by phototropins stimulates directional chloroplast rearrangement via the cytoskeletal network (Banaś et al. 2012). At low irradiance, chloroplasts move more towards the periclinal (face) position to absorb the maximum amount of light, whereas under high irradiance they escape to the anticlinal (profile) position as a photoprotective response to excess light energy (Kagawa & Wada 1999; Kasahara et al. 2002).

Tholen et al. (2008) demonstrated that short term exposure of *Arabidopsis* leaves to 1200 µmol m^{-2} s^{-1} of white light, in contrast to blue-filtered light, significantly reduced the chloroplast surface area exposed to intercellular air space by changing the chloroplast position from face to profile. This change in positioning was accompanied by a decrease in A_n and g_m, the latter estimated by two methods (isotope discrimination and A-C_i curve fitting). Using the variable J chlorophyll fluorescence method, Loreto et al. (2009) observed a reduction in A_n and g_m in *N. tabacum* and *Platanus orientalis* within 3 min of exposure to 80% BL in a total PPFD of 300 µmol m^{-2} s^{-1}. Paradoxically, however, they found no effect on C_c and C_i and so concluded that the reduction in photosynthesis was related to photochemical limitations and not CO_2 conductance. In contrast, in *Populus* × *canadensis*, PPFD-saturated A_n, g_s and g_m (by the variable J chlorophyll fluorescence method) decreased by 30, 46, and 25% under pure blue light compared to white light, and C_i began to increase at PPFD > 1200 µmol m^{-2} s^{-1} (Pallozzi et al. 2013). In the present study, high blue light

(i.e., three times higher than Loreto et al. [2009], but not as extreme as the higher levels used by Pallozzi et al. [2013]) resulted in reductions in g_m that reduced C_c by 17 and 9% in northern and southern genotypes, respectively (Table 3.1). However, blue light had no significant effect on C_i (Figure 3.4C). Because chloroplast movements normally take longer than a few minutes, Loreto et al. (2009) concluded that the rapid reduction in g_m they observed was unrelated to repositioning. Furthermore, when treated with cytochalasin D to inhibit movement (not directly shown in that study), there was still a rapid effect of blue light on g_m. Although time courses for blue light effects on CCI/ACC and g_m were not constructed in the present study, these two responses were similarly separable when black cottonwood leaves were treated with cytochalasin D. These data support the Loreto et al. (2009) proposition that g_m reduction under blue light is unlikely to result from chloroplast movements alone.

In this study under 10% BL, cytochalasin D decreased A_n and g_m compared to both controls, and C_c relative to the distilled water control only (Table 3.4). These effects may relate to the disruption of chloroplast movements. The risk of photodamage increases under high blue light if chloroplast movements are stopped (Kasahara et al. 2002). Loreto et al. (2009) showed that treatment with cytochalasin D promotes photoinhibition (as indicated by reductions in quantum efficiency) in the presence of high blue light (2200 µmol m^{-2} s^{-1}). Tholen et al. (2008) reported a significant increase in g_m and the exposure of chloroplast surface area to adjacent intercellular air space under white light (not filtered for blue light) when *Arabidopsis* chloroplasts were fixed by cytochalasin D in the face position. Besides inhibition of chloroplast movements, it is not evident if cytochalasin D has any direct effect on photosynthesis, but cytochalasin E is thought to possibly have some impact on light harvesting by causing a decay in the fluorescence emission spectrum over time (Kshirsagar

et al. 2001). Cytochalasin D also has negative effects on other actin-based movements (e.g., other organelles; Williamson 1993) that might ultimately influence photosynthesis.

If blue light has effects on g_m independent from chloroplast movements, then it may act through changes in either aquaporin regulation or carbonic anhydrase activity. The effect of high blue light on aquaporins is not known but, as shown in Table 3.5, exposure to 60% BL elicited a significant reduction in CA activity by ~20%. According to the model of Tholen & Zhu (2011), a reduction in stromal CA activity of this magnitude should have little or no effect on g_m and A_n. However, as shown by Momayyezi & Guy (2017), carbonic anhydrase activity in these same black cottonwood genotypes is strongly correlated with g_m under both natural and inhibitor-induced treatments. Inhibition of CA activity by 43% reduced g_m and A_n by 48% and 27%, respectively (Momayyezi & Guy 2017). Therefore, the localization of specific CA activities and/or interaction with aquaporins might also account for some portion of the blue light effect on g_m.

Irrespective of the mechanism of the blue light effect on g_m, the present work uncovers differences in g_m in response to blue light as a function of latitude of origin in black cottonwood. There are similar but less pronounced patterns in g_s. Momayyezi & Guy (2017) reported that g_s and g_m were more-or-less equally limiting to photosynthesis in this species. In the present study, g_m was more limiting than g_s under all conditions, but, as indicated by g_s/g_m (Table 3.1), it became significantly more limiting under high blue light only in northern genotypes, presumably because they had much higher g_m in the first place.

3.5 Conclusion

The greater reduction in g_m in response to high blue light in northern compared to southern *P. trichocarpa* genotypes is commensurate with a greater reduction in CCI (and in CCI/ACC). This

suggests that chloroplast movements can directly affect g_m by changing how chloroplasts access cell wall perimeter positions adjacent to intercellular air space. Treatment with cytochalasin D, however, fully disabled all changes in CCI/ACC but did not eliminate the effects of high blue light on g_m. Therefore, as suggested by Loreto et al. (2009), blue light effects on g_m would seem to be at least partially independent of chloroplast repositioning. As shown here, the modulation of g_m by blue light may be associated with changes in CA activity.

Chapter 4: Effect of mercuric chloride on mesophyll conductance in diverse *Populus trichocarpa* Torr. & Gray genotypes

4.1 Introduction

Populus trichocarpa (black cottonwood) covers a wide coastal area from southern California (31° latitude) to the southeast of Alaska (62° latitude) and inland in British Columbia to the west side of the Rocky Mountains in western Alberta. At the provenance level, net assimilation rate and stomatal conductance are reported to be positively intercorrelated with latitude in black cottonwood (Gornall & Guy 2007; McKown 2014a). In black cottonwood, mesophyll conductance, the inverse of resistance, to CO_2 diffusion increases with latitude (Chapter 2 and 3; Momayyezi & Guy 2017).

To reach active sites of carboxylation at rubisco, CO_2 diffusion must overcome a series of gas- and liquid-phase resistances from the atmosphere to the stromal space inside chloroplasts (Flexas et al. 2008). To mediate g_m rapidly, diffusion through the liquid phase, which includes cell wall, membrane and cytoplasmic components, etc., may be differentially affected by carbonic anhydrase activity, chloroplast positioning, and the transport capacity of aquaporins (Flexas et al. 2008; Evans et al. 2009; Flexas et al. 2012). In Chapter 2, it was shown that northern black cottonwood genotypes have significantly greater g_m, which is in turn associated with a greater CA activity (Momayyezi & Guy 2017). The relationship between CA activity and g_m was the same whether variation was natural (i.e., genotypic) or induced by titrating CA with the inhibitor acetazolamide. Commensurate with their higher g_m, the same northern genotypes show a greater down-regulation of g_m in response to high blue light, in parallel with changes in their chlorophyll content index (Chapter 3). Although an effect on g_m via chloroplast repositioning was implicated, g_m was still

down-regulated by blue light even when such movements were blocked by treatment with cytochalasin D. It was shown, however, that CA activity was reduced ~20% by high blue light, thus providing a possible alternative mechanism for the blue light effect on g_m. In this chapter I use another inhibitor, mercuric chloride, to investigate the possibility that genotypic variation in g_m may also be related to differences in aquaporins (AQPs).

Aquaporins are integral proteins that provide channels for the movement of water molecules and sometimes neutral solutes (i.e., silicic acid) and gases (CO_2, NH_3) (Maurel et al. 2008) across biomembranes. They occur in five main subfamilies in eudicot plants (Anderberg et al. 2012). The plasma membrane intrinsic proteins (PIPs) constitute one subfamily and are known to promote CO_2 diffusion, in addition to water movement (Uehlein et al. 2003). The PIP subfamily consists of 15 members in cottonwood, which is more than Arabidopsis (13), rice (11), barley (10), and maize (13) (Chaumont et al. 2001; Johanson et al. 2001; Sakurai et al. 2005; Katsuhara & Hanba 2008; Gupta & Sankararamakrishnan 2009; Almeida-Rodriguez et al. 2010). Cottonwood also has more overall major intrinsic proteins (MIPs) (55 genes, aquaporins and aquaglyceroporins) with an additional subfamily (XIPs, functionally uncharacterized and found in a few eudicot genera; e.g., *Populus*) compared to many other studied species (Tuskan et al. 2006; Gupta & Sankararamakrishnan 2009; Cohen et al. 2013). Water balance and redistribution under drought in *P. balsamifera* and *P. simonii* × *balsamifera* (Almeida-Rodriguez et al. 2010), and hydraulic conductance recovery in *P. trichocarpa* (Laur & Hacke 2014), are reported to be linked with the expression level of AQPs, in particular, the PIPs.

The importance of AQPs in regulating g_m is clear from studies of transgenic *N. tabacum* over- or under-expressing plasma membrane aquaporin 1 (NtAQP1) (Uehlein et al. 2003; Flexas et al. 2006;

Uehlein et al. 2008). Transgenic lines of *P. tremula* × *alba*, lacking PIP1 showed greater mesophyll resistance compared with wild-type plants (Secchi & Zwieniecki 2014). Although reduced PIP1 expression decreases g_m it has no major impact on photosynthesis and g_s (Secchi & Zwieniecki 2014). In addition to work on genetically modified plants, the roles of AQPs in vivo have been studied in experiments with inhibitors to block their functioning. Mercuric chloride II ($HgCl_2$) selectively binds cysteine domains in aquaporin proteins (Murata et al. 2000; Savage & Stroud 2007) and interrupts the transfer of water through the channel pores (Barone et al. 1997; Tazawa et al. 1997). Similarly, as shown by the pioneering work of Terashima & Ono (2002), $HgCl_2$ also disrupts CO_2 transfer through AQPs and thereby reduces g_m. Mercuric chloride is, however, not without other biochemical effects. Indeed, mercury compounds may also directly impact CO_2 diffusion by blocking the active site (histidine) of carbonic anhydrase (Blundell & Jenkins 1977). An inhibitory effect of $HgCl_2$ on CA in mammalian cells has been reported (Yang et al. 2000; Blank & Ehmke 2003).

I conducted three experiments with $HgCl_2$ to explore the potential involvement of AQPs in determining variation in g_m in black cottonwood. In the first experiment, I attempted to block AQPs with $HgCl_2$ in six representative genotypes (three northern and three southern). It was hypothesized that photosynthesis in northern genotypes with intrinsically higher g_m would be more susceptible to $HgCl_2$ treatment than in southern genotypes with lower g_m. In a second experiment limited to just two genotypes, I used $HgCl_2$ to rule out or confirm concurrent effects on CA activity. Finally, in the last experiment, I tested the combined effects of blue light and $HgCl_2$ on g_m because these two agents may or may not affect different components of the CO_2 diffusion pathway (i.e., chloroplast repositioning versus AQP and/or CA activity, respectively). I expected the effects of blue light and $HgCl_2$ to be fully additive if their targets are completely independent.

4.2 Material and methods

4.2.1 Plant material

Branch cuttings of six representative *P. trichocarpa* genotypes, three northern (SKNP-4, TAKA-2 and TATB-4) and three southern (HALS-2, PITS-3 and LONG-1) (Table 2.1), were taken in late January to early February from the Totem Field common garden at the University of British Columbia (UBC). Bagged cuttings were kept in a dark cold room at 4°C until they were recut into ~10 cm lengths with two lateral buds for rooting and planting (Pointeau & Guy 2014). Cuttings were grown with supplemental lighting in a greenhouse (minimum PPFD = 500 µmol m^{-2} s^{-1}) under a 20 hour photoperiod, maximum temperature of 25°C during day and 20°C during night, in 3.78 L pots containing a 70% peat moss and 30% perlite mixture.

4.2.2 Treatments and photosynthesis measurements

The two youngest fully expanded leaves per plant were used to measure A_n, g_s and the intercellular C_i using a LI-COR 6400 XT gas exchange system fitted with a 6400-40 chlorophyll fluorescence chamber. In Experiment 1, one leaf was treated with aqueous mercuric chloride II ($HgCl_2$) to inhibit AQPs, and the other used as a control. Control and $HgCl_2$ treatments, and order of measurement, were randomly assigned to the leaves to eliminate effects of any possible age or time dependent errors. Each leaf was cut at the petiole base under distilled water and placed in a 5 mL vial filled with either distilled water (control) or 1.5 mM aqueous $HgCl_2$ solution. After 90 minutes, leaves were placed inside the LI-COR 6400 XT cuvette to equilibrate to chamber conditions under light for 25 minutes prior to gas exchange measurements. All routine measurements were done in triplicate under 10% blue to 90% red light proportion at a total photosynthetic photon flux density (PPFD) of 1200 µmol m^{-2} s^{-1}, flow rate of 300 µmol air s^{-1} and

vapour pressure deficit between 1.4-1.6 kPa. Leaf temperature was maintained at 25°C and the ambient chamber CO_2 concentration was set to 400 µmol mol^{-1}. The control leaf was dark adapted for 20 minutes prior to all other measurements to obtain the maximum quantum yield of photosystem II. Later, during gas exchange measurements, the (Φ_{PSII}) under actinic light was obtained by application of saturating flashes (>7000 µmol m^{-2} s^{-1}) as per Genty et al. (1989).

Chlorophyll content index (unit-less) was measured for all genotypes immediately after gas exchange measurements using a CCM 200 plus (Opti-Science, Inc, Hudson, NH, USA) chlorophyll content meter.

4.2.4 Carbonic anhydrase activity

In Experiment 2, the two youngest fully developed leaves, in four replications from each of two genotypes, were randomly assigned to treatments designed to test the effect of $HgCl_2$ on CA activity. Only two genotypes were used because of technical limitations; namely TATB-4 and LONG-1 (to be consistent with Chapter 3). Petioles were cut under water and placed in 5 mL vials containing either distilled water (control) or 1.5 mM $HgCl_2$. After 90 minutes under greenhouse light, both leaves were light adapted under 10% blue light for 25 minutes. The distilled water treatment was used as the control for both high blue light and $HgCl_2$ effects on CA activity. Gas exchange data and CCI were obtained as described above. Leaf discs from the other side of the mid-rib, adjacent to the area of measurement, were collected using a paper puncher and dried at 70°C for 72 hours to determine leaf mass per area (LMA, mg mm^{-2}).

Remaining tissue was immediately frozen on dry ice for determination of CA activity as described by Wilbur & Anderson (1948). For this purpose, 1.77 cm^2 leaf discs (~36 mg fresh weight) were cut with a cork borer from the area used for gas exchange measurements, and ground at liquid

nitrogen temperature (-196°C) using disposable polypropylene pestles (length, 8.5 cm) in 1.5 mL polypropylene microcentrifuge tubes. All subsequent steps were at 4°C. After thawing, 70 µL of 40 mM potassium phosphate buffer (pH = 8.3) was added and the homogenate was centrifuged for 15 min at 4500×*g*. A 10 µL aliquot of supernatant was added to a further 0.5 mL of the buffer solution containing 20 ppm bromothymol blue as a pH indicator. The time required for the pH of the buffer solution to change from 8.3 to 6.3 for control (T_{Control}) and enzyme-containing (T_{Enzyme}) solutions was recorded visually upon the further addition of 0.5 mL of CO_2-saturated water. The CO_2-saturated water was prepared by bubbling CO_2 through distilled water for two hours (also at 4ºC). As a control, 10 µL of buffer solution was used in place of the supernatant. There were four technical replicates per assay. Enzyme activity was calculated as follows:

$$\text{Units CA / mL of supernatant} = \frac{(T_{\text{Control}} - T_{\text{Enzyme}}) \times df}{(T_{\text{Enzyme}}) \times V} \qquad (1)$$

where *df* is the dilution factor and *V* is the volume of enzyme extract used. Activities were expressed on a leaf area basis.

4.2.5 Combined high blue light and mercuric chloride treatment

In Experiment 3, the four youngest fully developed leaves from TATB-4 and LONG-1 were used in four replications to test the combined effects of $HgCl_2$ and high blue light in a factorial experiment. Petioles were cut under water and placed in 5 mL vials containing either distilled water or 1.5 mM $HgCl_2$. After 90 min under natural light in the greenhouse, leaves were adapted to their respective light treatments, 10% or 60% BL in a total PPFD of 1200 µmol m^{-2} s^{-1} for 25 min prior to gas exchange measurements as detailed above.

4.2.6 Calculation of g_m

The "constant *J* method" was used to estimate g_m based on measurements of chlorophyll fluorescence. I have previously shown in black cottonwood that the results of this method and estimation of g_m by stable carbon isotope discrimination are well correlated and of comparable magnitude (Momayyezi & Guy 2017). The electron transport rate (J_{flu}) was calculated according to Genty et al. (1989):

$$J_{flu} = \Phi_{PSII} \times PPFD \times \alpha \times \beta \qquad (2)$$

where the fraction of absorbed quanta reaching photosystem II (β) was estimated to equal 0.5 under 10% BL. The leaf absorptance, α, was taken to be 0.827 based on the average value (± 0.03) as determined by Momayyezi & Guy (2017). In Experiment 3 only, β and α, both were previously measured for black cottonwood genotypes under 10% BL (β = 0.5; α = 0.858 ± 1.03) and 60% BL (β = 0.4; α = 0.811 ± 1.49) as determined in Chapter 3. g_m was then calculated according to Harley et al. (1992):

$$g_m = A_n / \left[C_i - \left(\frac{\Gamma^*(J_{flu}+8(A_n+R_d))}{J_{flu}-4(A_n+R_d)}\right)\right] \qquad (3)$$

where A_n, and C_i are net assimilation rate and CO_2 concentration in the intercellular air space, R_d is the non-photorespiratory respiration rate in the light, and Γ^* is the chloroplast CO_2 photocompensation point (assumed here to equal the intercellular CO_2 photocompensation point). As determined in Chapter 2 (Momayyezi & Guy 2017), Γ^* and R_d were taken to be 1.12 ± 0.37 μmol mol^{-1} and 43.41 ± 1.25 μmol m^{-2} s^{-1}, respectively.

The ratio g_s/g_m was calculated as a measure of the limitation of g_m on photosynthesis relative to g_s (i.e., values greater than 1 indicate a greater limitation due to g_m than to g_s). From g_m, the CO_2

concentration at sites of carboxylation (C_c) was estimated according to equation 3 (Harley et al. 1992):

$$C_c = C_i - \frac{A_n}{g_m} \quad (4)$$

4.2.7 Statistics

For Experiment 1, mixed linear models in SAS 9.4 (SAS Institute Inc. NC, USA 2013) were used to compare the effect of $HgCl_2$ treatment on A_n, g_s, g_m and C_c for the six genotypes independently, without considering latitude as a factor (adjusted *P* value for number of paired comparisons = 0.05). Then, mixed linear models were used to compare the $HgCl_2$ treatment effect on A_n, g_m, g_s, g_s/g_m, C_i and C_c, compared with distilled water controls, for northern and southern genotypes within each latitude and for northern vs. southern genotypes. Both solution treatment (T) and latitude (L) were considered fixed factors and genotypes were nested within latitude. Because treatments were paired, replicates (plants) were nested within genotypes. Pairwise mean comparisons were used to test treatment effects within and between northern and southern latitudes (the adjusted *P* value for number of paired comparisons according to the Bonferroni correction was 0.008).

Similar mixed linear models were used to compare absolute and percentage reductions in A_n, g_m, g_s and C_c under $HgCl_2$ relative to the control (*P* value = 0.05). A *t*-test was used to compare LMA in northern vs. southern genotypes. For Experiment 2, *t*-tests with data paired by plant were used to analyze the effect of $HgCl_2$ on CA activity, A_n, g_m, g_s, g_s/g_m, C_i, C_c and CCI ($P < 0.05$). For Experiment 3, the combined effects of $HgCl_2$ and blue light, both as fixed effects in two levels with data blocked by plant (random effect), on A_n, g_m, g_s, g_s/g_m, C_i and C_c, were analyzed using mixed models (adjusted *P* value for number of paired comparisons = 0.008).

Logarithm, square root, or squared transformations were performed to meet normality and equal variance assumptions where needed.

4.3 Results

4.3.1 Mercuric chloride effect on g_m

In Experiment 1, and in contrast to Chapters 2 and 3, there was a small (14.4%) but significant difference in LMA between northern (0.0438 mg mm^{-2} ± 0.0009) and southern (0.0375 mg mm^{-2} ± 0.0008) genotypes ($P = 0.0005$). There was a greater (24.9%) difference in A_n between northern and southern genotypes, but only under the control (distilled water) condition ($P < 0.008$). Across all genotypes combined, the $HgCl_2$ treatment reduced A_n by 26.3% relative to the control ($P < 0.0001$). The differences in pairwise comparisons were significant within each genotype ($P < 0.05$) (Figure 4.1). However, northern genotypes were more sensitive to $HgCl_2$ (T × L, $P < 0.0001$) (Table 4.1) with greater absolute and relative reductions in A_n compared to southern genotypes ($P < 0.05$) (Table 4.2). Consequently, there was no latitudinal difference in A_n when plants were treated with $HgCl_2$ (Table 4.1).

Mercuric chloride significantly decreased g_m and g_s by 51.7% and 21.1%, respectively, across all genotypes combined ($P < 0.0001$). Considered separately, mercuric chloride significantly ($P < 0.05$) decreased g_m in all individual genotypes (Figure 4.2), and g_s in all genotypes except the PITS-3 genotype (Figure 4.3). Similar to A_n, g_m and g_s were significantly greater in northern genotypes (48.4 and 15.2%, respectively) than southern genotypes ($P < 0.008$) (Table 4.1), but the differences were not significant under $HgCl_2$. Both absolute and relative reductions in g_m and g_s were significantly greater in northern genotypes than southern genotypes (T × L, $P < 0.0001$) (Table 4.2).

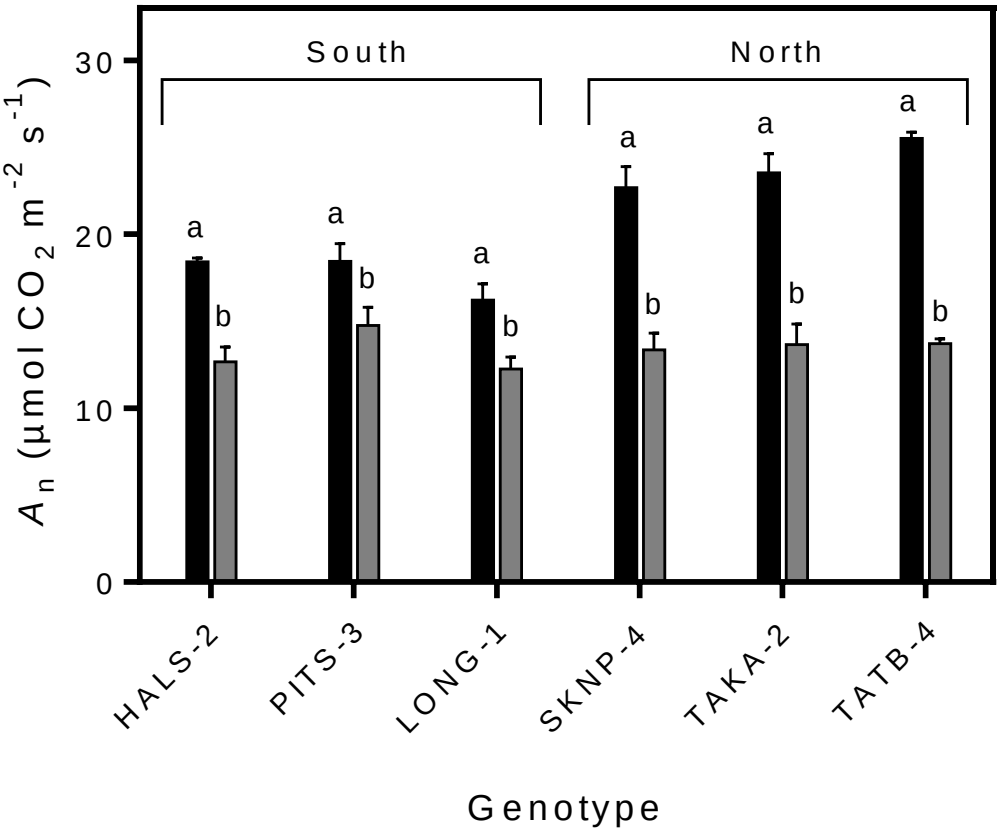

Figure 4.1 Mean values (± SE) for net assimilation rate (A_n, µmol CO_2 m^{-2} s^{-1}) of six *Populus trichocarpa* genotypes under two treatments (distilled water in black, and $HgCl_2$ in grey). Different letters show significant differences between distilled water (control), and $HgCl_2$ treatments for each genotype at $P < 0.05$.

Table 4.1 A_n, g_m, g_s, g_s/g_m, C_i and C_c in northern vs. southern genotypes under control and $HgCl_2$ treatments. For each column, different letters show significant differences for mean values ± SE at $P < 0.008$.

	treatment	A_n	g_m	g_s	g_s/g_m	C_i	C_c
north	distilled water	23.90 ± 0.62 ^{a}	0.31 ± 0.03 ^{a}	0.33 ± 0.01 ^{a}	1.17 ± 0.11 ^{a}	267.66 ± 4.08 ^{a}	183.82 ± 5.22 ^{a}
	$HgCl_2$	13.57 ± 0.47 ^{bd}	0.13 ± 0.01 ^{bc}	0.23 ± 0.01 ^{bc}	1.98 ± 0.22 ^{bc}	281.46 ± 5.32 ^{bc}	168.38 ± 5.24 ^{bc}
south	distilled water	17.70 ± 0.52 ^{c}	0.16 ± 0.01 ^{b}	0.28 ± 0.01 ^{b}	1.82 ± 0.19 ^{ab}	285.16 ± 6.46 ^{ab}	172.10 ± 5.89 ^{ab}
	$HgCl_2$	13.22 ± 0.56 ^{d}	0.10 ± 0.01 ^{c}	0.25 ± 0.01 ^{c}	2.93 ± 0.38 ^{c}	298.09 ± 7.40 ^{c}	150.56 ± 9.27 ^{c}

A_n, net assimilation rate (µmol CO_2 m^{-2} s^{-1}); g_m, mesophyll conductance (mol CO_2 m^{-2} s^{-1}); g_s, stomatal conductance (mol H_2O m^{-2} s^{-1}); g_s/g_m (stomatal conductance over mesophyll conductance ratio); C_i, intercellular air space CO_2 concentration (µmol mol^{-1}); C_c, CO_2 concentration at sites of carboxylation (µmol mol^{-1}).

Table 4.2 Percentage and absolute reductions in A_n, g_m g_s and C_c under $HgCl_2$ treatment from control for the northern vs. the southern genotypes. Different letters show significant differences for mean values ± SE at $P < 0.05$.

		north	south
A_n	absolute	10.33 ± 0.57 [a]	4.47 ± 0.42 [b]
	percentage	43.06 ± 1.84 [a]	25.23 ± 2.23 [b]
g_m	absolute	0.176 ± 0.023 [a]	0.067 ± 0.006 [b]
	percentage	56.21 ± 3.80 [a]	41.79 ± 3.13 [b]
g_s	absolute	0.097 ± 0.009 [a]	0.031 ± 0.006 [b]
	percentage	29.57 ± 2.85 [a]	11.00 ± 2.41 [b]
C_c	absolute	15.51 ± 3.07 [a]	21.51 ± 8.96 [a]
	percentage	8.42 ± 1.62 [a]	12.51 ± 4.98 [a]

A_n, net assimilation rate (µmol CO_2 m^{-2} s^{-1}); g_m, mesophyll conductance (mol CO_2 m^{-2} s^{-1}); g_s, stomatal conductance (mol H_2O m^{-2} s^{-1}); C_c, CO_2 concentration at sites of carboxylation (µmol mol^{-1}).

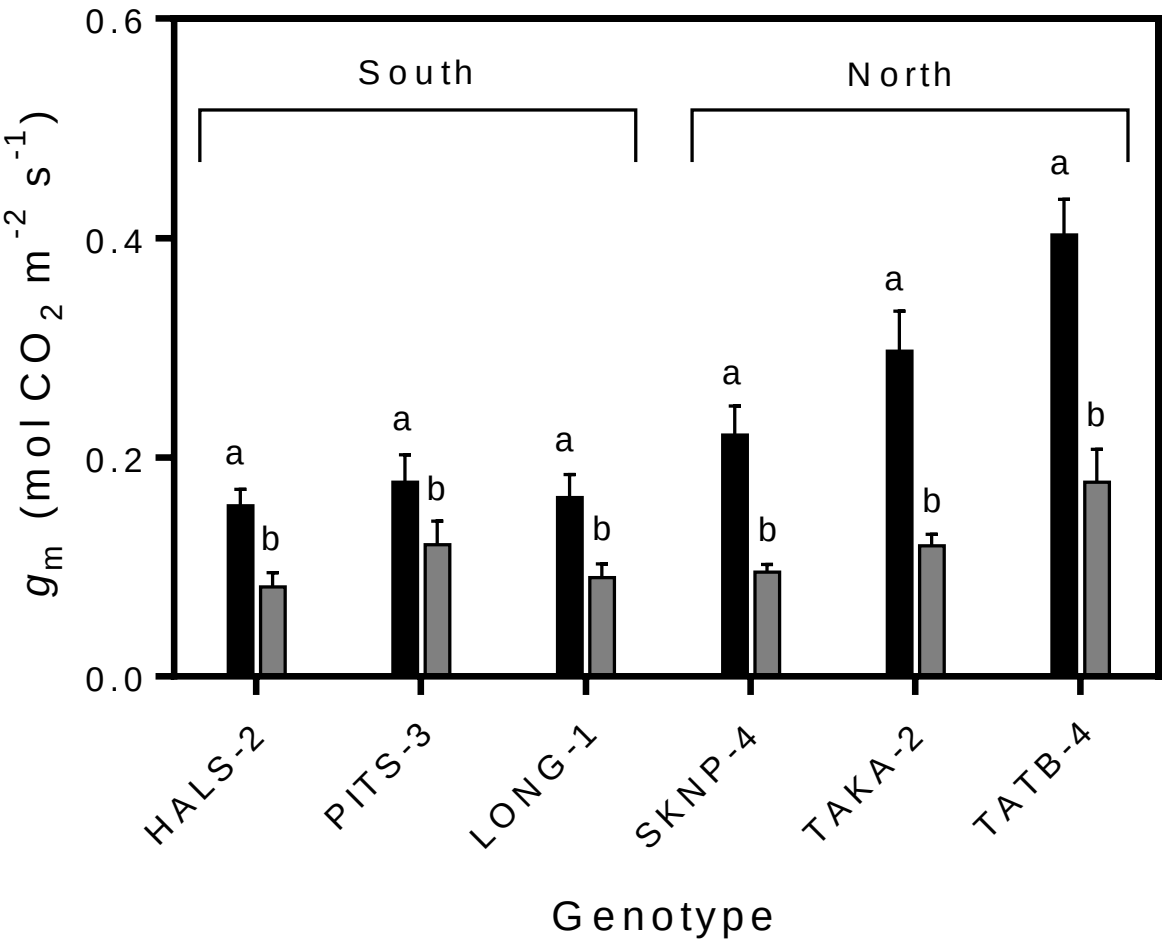

Figure 4.2 Mean values (± SE) for mesophyll conductance (g_m, mol CO_2 m^{-2} s^{-1}) of six *Populus trichocarpa* genotypes under two treatments (distilled water in black, and $HgCl_2$ in grey). Different letters show significant differences between distilled water (control), and $HgCl_2$ treatments for each genotype at $P < 0.05$.

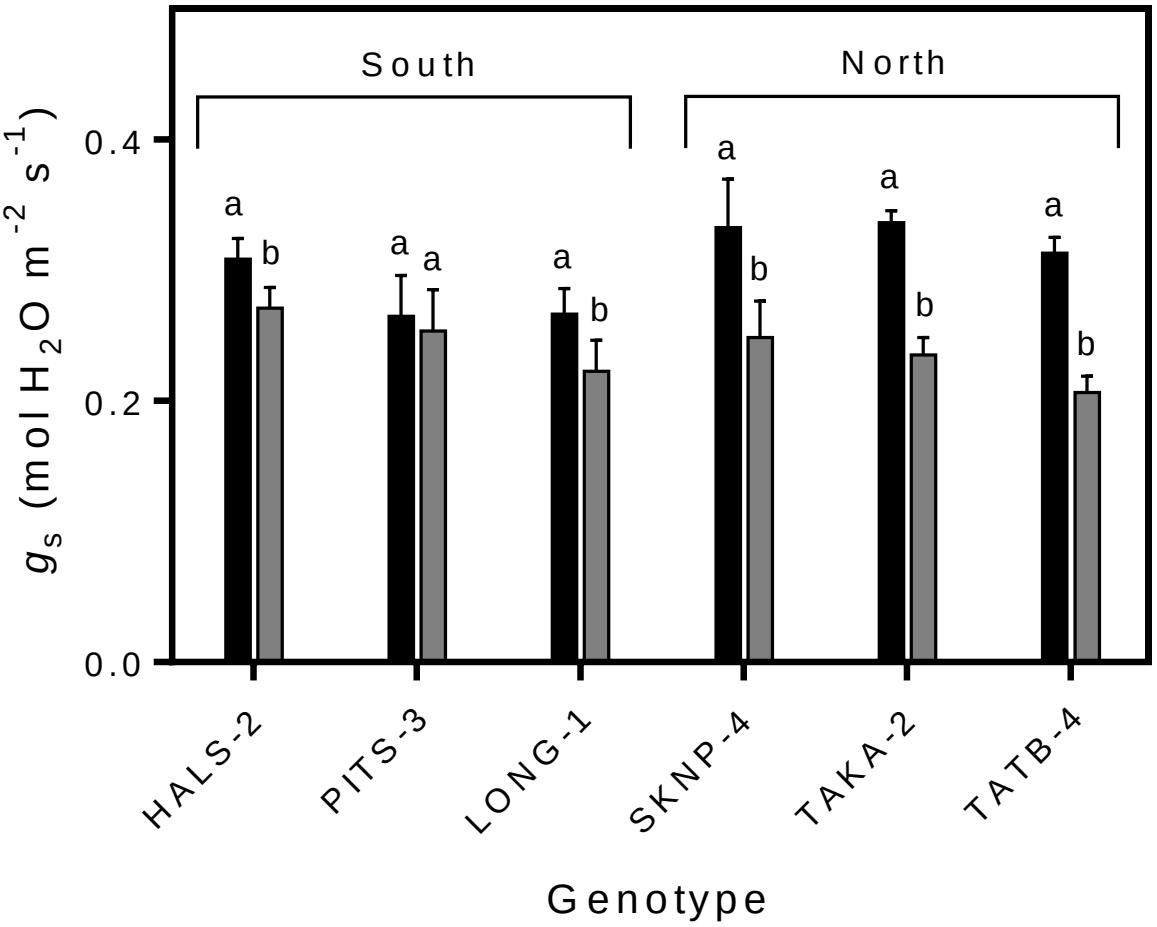

Figure 4.3 Mean values (± SE) for stomatal conductance (g_s, mol H_2O m^{-2} s^{-1}) of six *Populus trichocarpa* genotypes under two treatments (distilled water in black, and $HgCl_2$ in grey). Different letters show significant differences between distilled water (control), and $HgCl_2$ treatments for each genotype at $P < 0.05$.

There was no significant difference between northern and southern genotypes in C_c (Table 4.1). Mercuric chloride significantly decreased C_c by 10.4% (P = 0.0005). There was no latitude by treatment interaction (P = 0.177) and absolute and relative reductions in C_c were equal in both northern and southern genotypes (Table 4.2). Considered separately, $HgCl_2$ chloride decreased C_c in just three genotypes ($P < 0.05$) (Figure 4.4). Similar to C_c, C_i and g_s/g_m did not differ between northern and southern genotypes under either control or treatment conditions (Table 4.1). Mercuric chloride significantly increased C_i (P = 0.0005) and g_s/g_m ($P < 0.0001$) across all genotypes (Table 4.1). The latitude by treatment interaction was not significant for either g_s/g_m (P = 0.297) or C_i (P = 0.085) and absolute and relative increases were not statistically different in both northern and southern genotypes (Table 4.2). The effects of $HgCl_2$ on A_n, g_m, g_s, g_s/g_m, C_i, C_c and CCI observed in Experiment 1 were almost fully reproducible in Experiments 2 and 3, and if not in degree or level of significance, then certainly in direction.

4.3.2 Mercuric chloride effect on CA activity

In Experiment 2, CA activity decreased by 31.9% (0.37 unit cm^{-2} ± 0.08 SE) under $HgCl_2$ treatment compared to the control (distilled water) (Table 4.3).

4.3.3 Combined blue light and mercuric chloride effect and changes in g_m

In Experiment 3 (and in full concurrence with Chapter 3), 60% BL decreased g_m and C_c significantly compared to 10% BL (Table 4.4). However, the reduction in A_n was not significant under 60% BL due to insufficient statistical power. In the 10% BL control light treatment, pretreatment with $HgCl_2$ reduced A_n by 18.4% and g_s by 19.5% ($P < 0.008$), while C_i was marginally but not significantly increased. There was a much larger effect on g_m and, consequently, C_c (reduced by 41.7% and 19.6%, respectively) (Table 4.4). High blue light in combination with

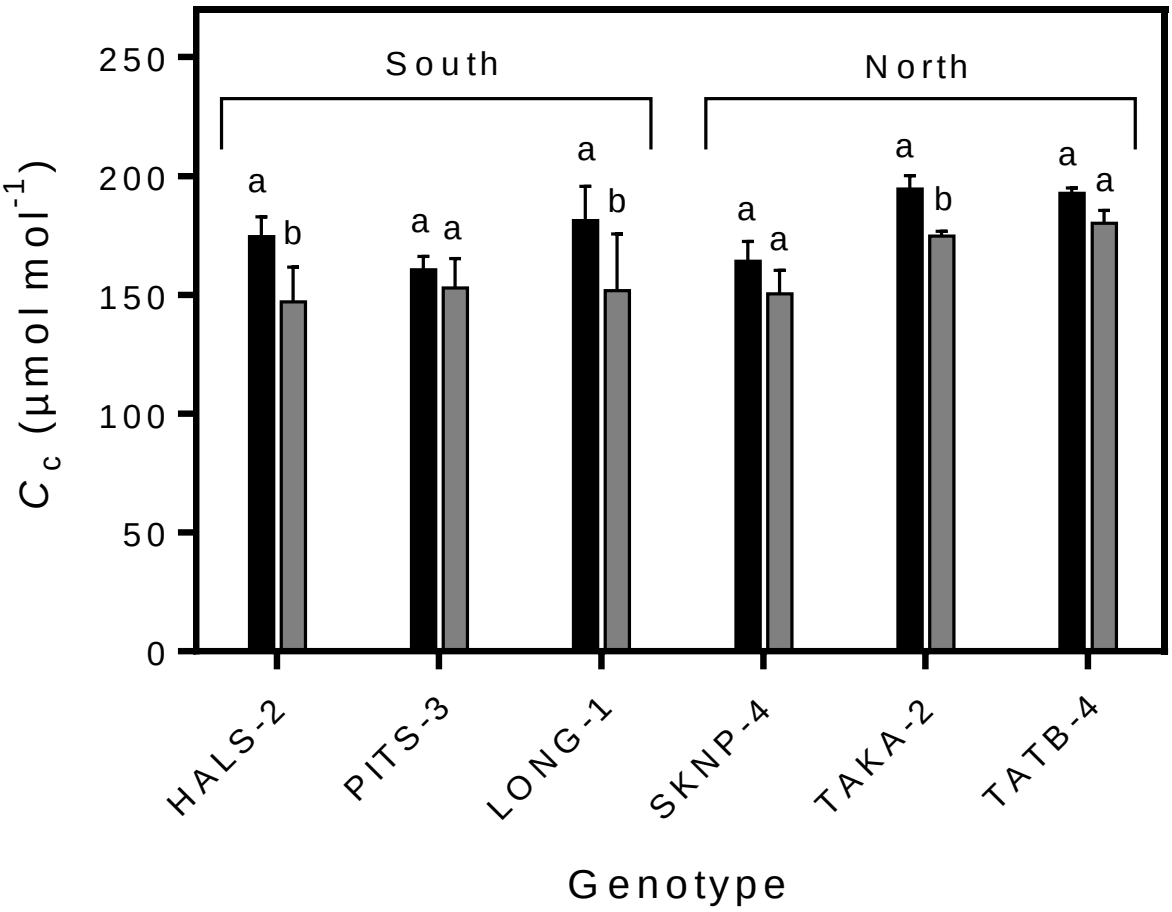

Figure 4.4 Mean values (± SE) for CO_2 concentration at sites of carboxylation (C_c, µmol mol^{-1}) of six *Populus trichocarpa* genotypes under two treatments (distilled water in black, and $HgCl_2$ in grey). Different letters show significant differences between distilled water (control), and $HgCl_2$ treatments for each genotype at $P < 0.05$.

Table 4.3 Effect of 1.5 mM aqueous $HgCl_2$ on CA activity, A_n, g_m, g_s, g_s/g_m, C_i, C_c and CCI. Different letters show significant differences between mean values (± SE, $n = 4$) within each row ($P < 0.05$). Genotype was not a factor in this experiment, so data presented here are means across both TATB-4 and LONG-1 combined. Data for distilled water controls are the same here as in Chapter 3, Table 3.5. Slight differences in g_m and C_c between the two tables are due to minor differences in the assumed value of α.

	distilled water	1.5 mM aqueous $HgCl_2$
CA activity	1.16 ± 0.20 [a]	0.79 ± 0.11 [b]
A_n	17.54 ± 0.84 [a]	15.02 ± 0.97 [b]
g_m	0.203 ± 0.030 [a]	0.115 ± 0.010 [b]
g_s	0.298 ± 0.012 [a]	0.264 ± 0.013 [b]
g_s/g_m	1.62 ± 0.16 [a]	2.36 ± 0.16 [b]
C_i	292.30 ± 3.50 [a]	296.34 ± 5.44 [a]
C_c	198.02 ± 8.18 [a]	163.09 ± 11.56 [b]
CCI	34.11 ± 2.96 [a]	35.41 ± 2.71 [a]

CA activity, carbonic anhydrase activity (units cm^{-2}); A_n, net assimilation rate (μmol CO_2 m^{-2} s^{-1}); g_m, mesophyll conductance (mol CO_2 m^{-2} s^{-1}); g_s, stomatal conductance (mol H_2O m^{-2} s^{-1}); g_s/g_m (stomatal conductance over mesophyll conductance ratio); C_i, intercellular air space CO_2 concentration (μmol mol^{-1}); C_c, CO_2 concentration at sites of carboxylation (μmol mol^{-1}); CCI, chlorophyll content index.

Table 4.4 Effect of high blue light and 1.5 mM aqueous $HgCl_2$ on A_n, g_m, g_s, C_i and C_c under 10 and 60% BL. Different letters show significant differences between mean values (± SE, n = 4) within each row ($P < 0.008$). Genotype was not a factor in this experiment, so data presented here are means across both TATB-4 and LONG-1 combined.

	distilled water		1.5 mM aqueous $HgCl_2$	
	10% BL	60% BL	10% BL	60% BL
A_n	13.57 ± 0.80 [a]	11.93 ± 0.64 [ac]	11.00 ± 0.33 [c]	9.73 ± 0.29 [b]
g_m	0.187 ± 0.026 [a]	0.117 ± 0.008 [b]	0.109 ± 0.020 [b]	0.070 ± 0.009 [c]
g_s	0.169 ± 0.013 [a]	0.150 ± 0.012 [ab]	0.136 ± 0.007 [b]	0.136 ± 0.009 [b]
g_s/g_m	1.00 ± 0.11 [a]	1.29 ± 0.07 [b]	1.47 ± 0.20 [b]	2.15 ± 0.28 [c]
C_i	258.89 ± 6.73 [a]	259.05 ± 5.27 [a]	259.37 ± 5.89 [a]	272.09 ± 6.98 [a]
C_c	178.2 ± 10.0 [a]	154.99 ± 9.53 [b]	143.26 ± 9.00 [b]	120.42 ± 9.04 [c]

A_n, net assimilation rate (μmol CO_2 m^{-2} s^{-1}); g_m, mesophyll conductance (mol CO_2 m^{-2} s^{-1}); g_s, stomatal conductance (mol H_2O m^{-2} s^{-1}); g_s/g_m (stomatal conductance over mesophyll conductance ratio); C_i, intercellular air space CO_2 concentration (μmol mol^{-1}); C_c, CO_2 concentration at sites of carboxylation (μmol mol^{-1}).

$HgCl_2$ resulted in further significant reductions in g_m, C_c and A_n (reduced in total by 62.6%, 32.4% and 28.3%, respectively), but not g_s; hence, C_i was increased, but not significantly so after Bonferroni correction ($P = 0.023$). Treatment with either $HgCl_2$ (as in Experiment 2) or 60% BL increased g_s/g_m, and their combined effect was additive (Table 4.4).

4.4 Discussion

As per my expectation, the $HgCl_2$ treatment reduced A_n compared to controls in every circumstance (Figure 4.1, Tables 4.1, 4.3, 4.4). Although g_s was also reduced in every case, stomatal limitation of photosynthesis was lower (experiment 1) or unchanged (experiments 2 and 3) in the presence of $HgCl_2$, as evidenced by a significant increase (experiment 1) or no change (experiments 2 and 3) in C_i. Mercuric chloride reduced g_m to a much greater degree than g_s, causing an increase in g_s/g_m and a greater relative limitation of photosynthesis (e.g., Table 4.1, 4.3, 4.4). Hence, in contrast to C_i, C_c was reduced under the $HgCl_2$ treatment in all three experiments. The results are in agreement with earlier experimental evidence determining the negative effect of low AQP activity on CO_2 diffusion and photosynthesis by chemical inhibition or under-expression in transgenic plants. As described by Terashima & Ono (2002), 1.2 mM $HgCl_2$ reduced g_m (by 72%), A_n and C_c in *V. faba*, and 2 mM $HgCl_2$ significantly decreased A_n and J_{flu} in *P. vulgaris*. Also, consistent with the current study, Terashima & Ono (2002) observed reductions in g_s in *P. vulgaris*. Concurrent effects of $HgCl_2$ on g_s may be indirect or direct. Stomatal conductance and g_m are often observed to co-vary with A_n (Flexas et al. 2008). By various mechanisms (Assmann & Jegla 2016), guard cells may sense and respond to the increase in C_i caused by a decrease in g_m. Alternatively, $HgCl_2$ may block AQPs in guard cells and affect water movement and g_s directly (Sarda et al. 1997; Kaldenhoff et al. 2008).

Although the effect of AQP inhibition on g_m in cottonwoods has not been previously studied, Secchi et al. (2009) showed that $HgCl_2$ inhibits the water transport capacity of most members of the cottonwood PIP2 subfamily by 30-50% when the genes are expressed in *Xenopus* oocytes. Also in cottonwoods, 0.2 mM $HgCl_2$ was shown to suppress recovery of leaf hydraulic conductance in dehydrated leaves and was suggested to be associated with blocked AQPs (Laur & Hacke 2014).

Only a few studies have focused on CO_2 transport activity of AQPs. As an example, the g_m of transgenic *P. tremula* × *alba* lines with down-regulated PIP1 is decreased relative to wild-type plants (Secchi & Zwieniescki 2013). Despite a positive relationship between g_m and PIP1 expression, g_m reduction does not seem to affect A_n and g_s in these transgenic plants when not stressed for water. Whereas under conditions of water stress, greater reductions in g_s and xylem hydraulic conductance in transgenic lines, relative to wildtype plants, reflected their reduced PIP1 expression (Secchi & Zwieniescki 2014). In contrast to poplars, over- and down-regulation of NtAQP1 (a PIP) in *N. tabacum* changed A_n and g_s in transgenic plants in parallel with g_m (by 20%) compared to wild-type plants (Flexas et al. 2006; Uehlein et al. 2008).

Consistent with both Chapters 2 and 3, the northern genotypes had significantly higher A_n (by 21-33% across all three studies), g_s (10-18%) and, most particularly, g_m (45-59%) than the southern genotypes. Similar to data presented in Chapter 2, northern genotypes also had a significantly greater LMA (14%), but this is not sufficient, in and of itself, to account for the observed differences in photosynthetic traits. Furthermore, it cannot possibly account for the over two-fold greater sensitivity of northern genotypes to $HgCl_2$ in absolute terms (Table 4.2). Even in relative terms, A_n, g_s and g_m were all significantly more sensitive to $HgCl_2$ in the northern genotypes, as

hypothesized in the introduction. Per cent reductions were 43 vs. 25% for A_n, 30 vs. 11% for g_s, and 56 vs. 43% for g_m, in northern vs. southern genotypes, respectively.

The differences in the susceptibility of conductance (either g_m or g_s or both) to $HgCl_2$ may reflect differences in AQP activity, function (water and/or CO_2 transport), or AQP-specific inhibition constants. Not all AQPs are equally affected by $HgCl_2$ (Heinen et al. 2009). Water transport through NtAQP1 and a TIP in Arabidopsis, for example, is reported to be insensitive to mercury (Daniels et al. 1994; Biela et al. 1999). Differences in location of cysteine residues (caused by mutations), as mercury receptors, are known to influence the sensitivity of AQPs to mercurial compounds (Savage & Stroud 2007; To & Torres 2015). Subcellular location of particular AQPs can also influence their functioning. Under low NtAQP1 expression, the plasma membrane NtAQP1 (with five times higher permeability to CO_2) is less limiting to internal conductance than NtAQP1 in the chloroplast membrane (Uehlein et al. 2008).

Although $HgCl_2$ was expected to mainly target AQPs, it may have affected photosynthesis or, more specifically, g_m, by additional means. There are reports that CA activity and AQP1 function in mammalian cells are simultaneously inhibited by 65-300 μM $HgCl_2$ (Yang et al. 2000; Blank & Ehmke 2003). Indeed, treatment with $HgCl_2$ decreased CA activity by ~32% relative to controls in Experiment 2 (Table 4.3). Therefore, the greater reduction in g_m in northern genotypes under $HgCl_2$ could also be related to their intrinsically greater CA activity and the notable dependence of g_m, and consequently A_n, on CA activity (Chapter 2; Momayyezi & Guy 2017). It is possible that CA and AQP interact or are functionally related. There are reports (e.g., Wang et al. 2016) that physical interaction between CA (βCA4) and AQP (PIP2;1) affects stomatal opening through the CO_2-signalling pathway in guard cells of Arabidopsis.

In Chapter 3, it was shown that blue light effects on g_m must be at least partially independent of chloroplast movements. In the present chapter, blue light and $HgCl_2$ had totally additive effects on g_m (Table 4.4). High blue light reduced g_m by 36-37% in both the presence and absence of $HgCl_2$. Likewise, $HgCl_2$ reduced g_m by 40-42% irrespective of the amount of blue light. This suggests that their mechanisms of action may be independent, but not necessarily so. Because high blue light caused a reduction in CA activity in Chapter 3, it would be interesting to know if $HgCl_2$ and blue light have additive effects on CA, but this was not tested.

4.5 Conclusion

Northern *P. trichocarpa* genotypes with greater A_n, g_s and g_m were shown to be more sensitive to $HgCl_2$ treatment, in both absolute and percentage terms, compared to southern genotypes. This observation is consistent with a greater role for AQPs in determining g_m in northern genotypes. However, it was also shown that CA activity, previously shown to be higher in northern genotypes, was significantly reduced under $HgCl_2$ treatment. Both the effects of blue light and $HgCl_2$ on g_m may be partly related to reductions in CA activity.

Chapter 5: General discussion

5.1 Conductance and photosynthesis

The production of food and biofuel from crop species is ultimately dependent on their photosynthetic capacity. In many natural and agricultural ecosystems, photosynthesis and plant productivity are limited by the availability of resources, often water and/or nitrogen (Webb et al. 1983; Vitousek et al. 1991; Reich et al. 1997; Huxman et al. 2004). For decades there has been a huge global effort focused on improving resource-use efficiencies to increase photosynthesis and yield, and to improve stress resistance. Water and nitrogen use efficiencies have been extensively studied in relation to stomatal and mesophyll conductance to increase photosynthetic performance (Buckley & Warren 2014). However, given the realization (Warren 2008) that g_m may account for up to 40% of the total diffusion limitation on photosynthesis, exploration of component constraints on g_m is imperative to a comprehensive approach to plant improvement. For the same reason, an understanding of the extent, pattern and basis of natural variation in g_m is crucial to a comprehensive view of plant adaptation.

It is known that A_n increases with latitude in *P. trichocarpa* genotypes and that this variation is paralleled by latitudinal variation in g_s (Gornall & Guy 2007; McKown et al. 2014a). As a consequence, C_i is relatively static with latitude. Therefore, and given the cline in photosynthetic rates, maintenance of C_c with latitude should demand an increase in g_m of similar magnitude to g_s. Indeed, as shown in Chapter 2 using two methods, there was an almost two-fold difference in g_m between northern and southern *P. trichocarpa* genotypes, which considerably exceeds the difference in g_s. Mesophyll conductance was strongly correlated with A_n. It appears that higher A_n in northern genotypes, which may be an adaptation to shorter growing seasons (Benowicz et al.

2000; Gornall & Guy 2007), is even better supported by enhanced g_m than it is by g_s. Given that in *P. trichocarpa* there is no strong latitudinal cline in LMA (as an indicator of anatomical effects on g_m [Milla-Moreno et al. 2016]), the physiological basis of g_m was explored by studying responses to inhibition of carbonic anhydrase activity (Chapter 2), blue light effects on chloroplast repositioning (Chapter 3), and blocking of aquaporin functioning (Chapter 4).

5.2 Response of g_m to various treatments across genotypes

The chief significance of Chapter 2, in the broader field of plant physiology, is that it represents the first published evidence of an important and central role for carbonic anhydrase in determining g_m and, ultimately, C_3 photosynthesis. That CA should function in this capacity was, of course, expected, but not borne out by experimentation until now.

I found g_m to be strongly related to CA activity in black cottonwood genotypes in the natural state and, importantly, in similar fashion and degree when partially inhibited by acetazolamide (Chapter 2; Momayyezi & Guy 2017). Northern *P. trichocarpa* genotypes have roughly twice as much CA activity as southern genotypes on either a leaf mass or area basis. Although the absolute reduction in g_m under acetazolamide was higher in northern genotypes, the per cent reduction was similar to the southern genotypes, as was the percent reduction in A_n in both northern and southern genotypes (Table 5.1). I suggest that the higher CA activity of northern genotypes is key to their greater g_m (~ 2 fold) and, in part, their higher A_n (~ 1.5 fold). Nonetheless, given the published theoretical limits on the impact of CA on g_m (Tholen & Zhu 2011), but also the results of my further experiments, it is very likely that variation in CA activity is not wholly responsible for variation in g_m in *P. trichocarpa*.

As shown in Chapter 3, exposure to high blue light reduced g_m and A_n in both northern and

Table 5.1 Percentage reduction (± SE) in mesophyll conductance from the corresponding control under 1 mM acetazolamide, 60% BL, and 1.5 mM $HgCl_2$. Different letters show significant differences between mean values within each row as determined in previous chapters ($P < 0.05$).

treatment	g_m percent reduction		A_n percent reduction	
	north	south	north	south
acetazolamide	47.8 ± 5.4 [a]	44.2 ± 7.3 [a]	24.7 ± 1.7 [a]	26.7 ± 3.7 [a]
blue light	36.3 ± 2.8 [a]	21.0 ± 2.2 [b]	18.5 ± 3.4 [a]	12.6 ± 1.9 [b]
mercuric chloride	56.2 ± 3.8 [a]	41.8 ± 3.1 [b]	43.1 ± 1.8 [a]	25.2 ± 2.2 [b]

southern genotypes, but the effect was significantly greater in northern genotypes in both absolute and per cent terms (Table 5.1). In all genotypes there was a reversible decrease in CCI under high blue light, whereas ACC remained unchanged. Again, this behavior, indicative of chloroplast repositioning, was more pronounced in the northern genotypes; i.e., northern genotypes with greater CCI showed higher reductions in CCI. Concurrence between chloroplast repositioning and changes in g_m suggests that the two are related, as previously reported by Tholen et al. (2008) and Loreto et al. (2009). However, the further reduction (23%) in g_m with high blue light under cytochalasin D (a chloroplast movement inhibitor) may relate to an independent effect of blue light on a different target. Interestingly, CA activity was reduced by ~20% under high blue light. These results suggest that high blue light may mediate CO_2 diffusion by having effects on both chloroplast repositioning and CA activity. It is possible that the greater blue light sensitivity of g_m in northern genotypes is related not only to their outwardly more pronounced light avoidance movements but also to their higher CA activity.

In Chapter 4, and similar to the independent effects of acetazolamide and blue light, g_m and A_n in northern genotypes were reduced more by $HgCl_2$ in northern genotypes than in southern genotypes. As with blue light treatment, northern genotypes were also relatively more sensitive to $HgCl_2$ than southern genotypes (Table 5.1). The greater susceptibility of northern genotypes to $HgCl_2$ may relate to higher AQP activity. Again, however, reductions in g_m were accompanied by reductions in CA activity (by ~32%), which may therefore partly account for the greater sensitivity to $HgCl_2$ of northern genotypes. Another explanation could be related to physical interactions between CA and AQP in the CO_2 diffusion pathway (Borisova et al. 2012; Wang et al. 2016). Mercuric chloride may disrupt their combined function by interfering with either moiety. The same may be true of acetazolamide.

My central hypothesis that in *P. trichocarpa*, variation in g_m would correlate with latitude, is accepted. I can also conclude that this variation reflects differences in CA activity, but the relative roles of AQP functioning and/or chloroplast positioning remain uncertain and, in the research presented here, not separable from CA activity.

5.3 Limitations of research

A main limitation to the current study is the application of "selective" chemical inhibitors which may in fact have multiple targets. As noted in Chapter 2, acetazolamide can interrupt AQP function in mammalian cells (untested in plants). Similarly, mercuric chloride is known to impair CA activity, consistent with the changes in CA activity presented in Chapter 4. Both agents may have further targets that directly and/or indirectly affect photosynthesis. Further work with transgenic plants may provide more reliable and specific evidence if based on expression of different or redundant CA isozymes or AQPs.

Another limitation of the present work is the relatively low number of genotypes (six) and latitudes ("north" vs "south") studied in most experiments. The number of accessions used was limited by technical considerations (time and equipment). I did an initial screening of g_m in 12 genotypes to partially compensate for these low numbers, but it would have been better to have still more in order to be certain of the clinal patterns observed. The high reproducibility between experiments in terms of genotypic differences is, however, reassuring. In principle, given more time, I could have used more genotypes in every experiment, but this would not necessarily improve the overall quality of the data. The slow process of measurement for leaf gas exchange variables increases the overall length of experimental measurements for a larger sampling population as a significant source of error.

In this thesis, the combined effects of acetazolamide and blue light, and the combined effects of acetazolamide, mercuric chloride and high blue light, were not tested. The interpretation of the latter would have been difficult due to the complexity of possible interactions between different components of g_m and the non-selective impacts of chemicals on them. The former treatment combination, however, may have been interesting given what was observed in Chapter 4, where mercuric chloride and high blue light in combination reduced g_m additively.

Another possible limitation to my work was that the inhibitor concentrations used were based on the available literature and there was no attempt on my part to establish optimal system-specific concentrations (although I did check the maximum viable concentration for mercuric chloride that did not cause wilting). Even so, because of transport effects, dilution and/or foliar accumulation (because of transpiration), it is not possible to know the precise concentration of any chemical agent once it is delivered to the blade through the petiole. I did optimize the length of my feeding experiments by checking the delivery of red food dye to the laminal veins (not presented).

A final limitation relates to the lack of direct microscopic evidence of chloroplast movements under high blue light to verify observations in Chapter 3. It's highly unlikely, however, that readily reversible changes in CCI unaccompanied by any effect on ACC are due to anything else.

5.4 Future directions

Overall, the results of this thesis point to an important role for carbonic anhydrase in g_m and, presumably, the local adaptation of photosynthesis. I did not anticipate this, and it's important that these findings be extended to other species, including crop plants. Since *P. trichocarpa* and *P. balsamifera* overlap in nature and both show similar clinal patterns in A_n and g_m, investigation of CA activity in natural *P. balsamifera* genotypes and the impact on g_m variation could be very

interesting. Because clinal variation in LMA seems to be more pronounced in *P. balsamifera* (Soolanayakanahally et al. 2009, 2015) than it is in *P. trichocarpa*, it's possible that in this species anatomy has played a more important role than biochemistry in the local adaptation of photosynthetic rate. We might predict, for example, that CA activity per unit leaf area in *P. balsamifera* should vary as a function latitude simply because LMA does, whereas the activity per unit mass should be more consistent. These studies could be extended to other north-temperate trees sympatric with the cottonwoods, such as red alder and paper birch, to further understand biogeographic trends in g_m, CA activity and related photosynthetic traits. Because of similarities in range, and perhaps then selective pressures, it might be expected that *B. papyrifera* would show patterns similar to *P. balsamifera*, whereas *A. rubra* might more closely resemble *P. trichocarpa*. This kind of information may reveal a general pattern of adaptation, or it may show that although different species achieve similar variation in photosynthesis, they do so in different ways. Some of this work has been completed but was not included in this thesis, as the decision was taken to focus on the *P. trichocarpa* story.

Given the relative ease and speed of assay, it would also be valuable to measure CA activity across a much large number of genotypes from the BCMoFNR *P. trichocarpa* and the AgCanBaP *P. balsamifera* collections for purposes of genome-wide association study (GWAS). Full genome sequences for almost all of these accessions are available (Suarez-Gonzalez et al. 2016). This approach might indicate which genes are controlling expression and/or regulation of CA activity in response to natural selection. A similar approach based on the sensitivity of different genotypes to blue light may also be illuminating.

Data in Chapter 3 show that high blue light causes a reduction in CA activity as well as chloroplast repositioning, both of which may or may not impact g_m by independent mechanisms. One possible

noninvasive way to tease this apart would be to conduct an experiment to establish the time course of CA inhibition/down-regulation vs. chloroplast movements (i.e., by blue light), relative to changes in g_m. Parallel study of CA transcript levels and/or actual protein levels would also be illuminating (i.e., in a time course, but also between treatments and among genotypes).

Despite model predictions, there is limited molecular genetic evidence of a role for CA in g_m. Future transgenic studies should target different and multiple CAs to help clarify the situation and, if successful, pin-point the cellular location of the associated limitation (e.g., stromal vs membrane-bound, etc.). The possibility of cooperativity between CA and AQP proteins in relation to the facilitation of CO_2 diffusion also needs further testing. A first step in that regard would be to check for physical interaction between these proteins in photosynthetic cells other than stomata (Wang et al. 2016).

Bibliography

Aitken S. N. & Whitlock M. C. (2013) Assisted gene flow to facilitate local adaptation to climate change. *Annual Review of Ecology Evolution and Systematics* **44,** 367-388.

Aitken S.N., Yeaman S., Holliday J.A., Wang T. & Curtis-McLane S. (2008) Adaptation, migration or expiration: climate change outcomes for tree populations. *Evolutionary Applications* **1,** 95-111.

Almeida-Rodriguez A.M., Cooke J.E.K., Yeh F. & Zwiazek J.J. (2010) Functional characterization of drought-responsive aquaporins in *Populus balsamifera* and *Populus simonii* × *balsamifera* clones with different drought resistance strategies. *Physiologia Plantarum* **140,** 321-333.

Alonso-Cantabrana H. & von Caemmerer S. (2015) Carbon isotope discrimination as a diagnostic tool for C_4 photosynthesis in C_3-C_4 intermediate species. *Journal of Experimental Botany* **67,** 3109-3121.

Anderberg H.I., Kjellbom P. & Johanson U. (2012) Annotation of *Selaginella moellendorffi* major intrinsic proteins and the evolution of the protein family in terrestrial plants. *Frontiers in plant Science* **20:33** doi:10.3389/fpls.2012.00033.

Assmann S.M. & Jegla T. (2016) Guard cell sensory systems: recent insights on stomatal responses to light, abscisic acid, and CO_2. *Current Opinion in Plant Biology* **33,** 157-167.

Badger M.R. & Price G.D. (1994) The role of carbonic anhydrase in photosynthesis. *Annual Review of Plant Physiology and Plant Molecular Biology* **45,** 369-392.

Banaś A.K., Aggarwal C., Labuz J., Sztatelman O. & Gabryś H. (2012) Blue light in chloroplast movements. *Journal of Experimental Botany* **63,** 1559-1574.

Barone L.M., Shih C. & Wasserman B.P. (1997) Mercury-induced conformational changes and identification of conserved surface loops in plasma membrane aquaporins from higher plants. *The Journal of Biological Chemistry* **272,** 30672-30677.

Benomar L., Lamhamedi M.S., Rainville A., Beaulieu J., Bousquet J. & Margolis H.A. (2016) Genetic adaptation vs. ecophysiological plasticity of photosynthetic-related traits in young *Picea glauca* trees along a regional climatic gradient. *Frontiers in Plant Science* **7:48** doi: 10.3389/fpls.2016.00048.

Benowicz A., Guy R.D. & El-Kassaby Y.A. (2000) Geographic pattern of genetic variation in photosynthetic capacity and growth in two hardwood species from British Columbia. *Oecologia* **123,** 168- 174.

Bernacchi C.J., Portis A.R., Nakano H., von Caemmerer S. & Long S.P. (2002) Temperature response of mesophyll conductance; implications for the determination of rubisco enzyme kinetics and for limitations to photosynthesis *in vivo*. *Plant Physiology* **130,** 1992-1998.

Biela A., Grote K., Otto B., Hoth S., Hedrich R. & Kaldenhoff R. (1999) The *Nicotiana tabacum* plasma membrane aquaporin NtAQP1 is mercury-insensitive and permeable for glycerol. *The Plant Journal* **18,** 565-570.

Bird R.E. & Riordan C. (1986) Simple solar spectral model for direct and diffuse irradiance on horizontal and titled planes at the Earth's surface for cloudless atmospheres. *Journal of Climate and Applied Meteorology* **25,** 87-97.

Blank M.E. & Ehmke H. (2003) Aquaporin-1 and $HCO3^-$-Cl^- transporter-mediated transport of CO_2 across the human erythrocyte membrane. *Journal of Physiology* **550.2,** 419-429.

Blundell T.L. & Jenkins J.A. (1977) The binding of heavy metals to proteins. *Chemical Society Reviews* **6,** 139-171.

Borisova M.M., Kozuleva M.A., Rudenko N.N., Naydov I.A., Klenina I.B. & Ivanov B.N. (2012) Photosynthetic electron flow to oxygen and diffusion of hydrogen peroxide through the chloroplast envelope via aquaporins. *Biochimica et Biophysica Acta* **1817,** 1314-1321.

Bradfield J.R.G. (1947) Plant carbonic anhydrase. *Nature* **159,** 467-468.

Brinkman R. (1933) The occurrence of carbonic anhydrase in lower marine animals. *The Journal of Physiology* **80,** 171-173.

Bronson D.R., Gower S.T., Tanner M. & van Herk I. (2009) Effects of ecosystem warming on boreal black spruce bud burst and shoot growth. *Global Change Biology* **15,** 1534-1543.

Buckley T.N. & Warren C.R. (2014) The role of mesophyll conductance in the economics of nitrogen and water use in photosynthesis. *Photosynthesis Research* **119,** 77-88.

Chaumont F., Barrieu F., Wojcik E., Chrispeels M.J. & Jung R. (2001) Aquaporins constitute a large and highly divergent protein family in maize. *Plant Physiology* **125,** 1206-1215.

Cohen D., Bogeat-Triboulot M., Vialet-Chabrand S., Merret R., Courty P., Moretti S., Bizet F., …, Hummel I. (2013) Developmental and environmental regulation of aquaporin gene expression across *Populus* species: divergence or redundancy? *PLOS one* **8,** 1-12.

Coleman J.E. (1975) Chemical reactions of sulfonamides with carbonic anhydrase. *Annual Review of Pharmacology* **15,** 221-242.

Collings D.A., Wasteneys G.O. & Williamson R.E. (1996) Actin-microtubule interactions in the alga *Nitella*: analysis of the mechanism by which microtubule depolymerization potentiates cytochalasin's effects on streaming. *Protoplasma* **191,** 178-190.

Daniels M.J., Mirkov T.E. & Chrispeels M.J. (1994) The plasma membrane of *Arabidopsis thaliana* contains a mercury-insensitive aquaporin that is a homolog of the tonoplast water channel protein TIP. *Plant Physiology* **106,** 1325-1333.

Dang Q.L., Xie C.Y., Ying C. & Guy R.D. (1994) Genetic variation of ecophysiological traits in red alder (*Alnus rubra* Bong.). *Canadian Journal of Forest Research* **24,** 2150- 2156.

DeBell D.S. (1990) Black cottonwood. P. 570-576 in silvics of North America. Volume 2, Hardwoods. R.M. Burns and B.H. Honkala, coords. USDA Forest Service, Washington D.C. Agriculture Handbook 654.

Dickmann D.I. (2001) An overview of the genus *Populus*. In *Poplar Culture in North America* (eds D.I. Dickman, J.G. Isebrands, J.E. Eckenwalder & J. Richardson), pp. 1-42, Part A. NRC Research Press, Ottawa, Canada.

Dillen S.Y., Rood S.B. & Ceulemans R. (2010) Growth and physiology. In *Genetics and Genomics of Populus, Plant Genetics and Genomics: Crops and Models* (eds S. Jansson, R. Bhalerao & A. Groover) 8, 39- 63. Springer Science. New York, NY, USA.

DiMario R.J., Quebedeaux J.C., Longstreth D.J., Dassanayake M., Hartman M.M. & Moroney J.V. (2016) The cytoplasmic carbonic anhydrases βCA2 and βCA4 are required for optimal plant growth at low CO_2. *Plant Physiology* **171,** 280-293.

Dimou M., Paunescu A., Aivalakis G., Flemetakis E. & Katinakis P. (2009) Co-localization of carbonic anhydrase and phosphoenol-pyruvate carboxylase and localization of pyruvate

kinase in roots and hypocotyls of etiolated *Glycine max* seedlings. *International Journal of Molecular Sciences* **10,** 2896-2910.

Eckenwalder J.E. (1996) Systematics and evolution of *Populus*. In *Biology of Populus and its Implications for Management and Conservation* (eds R.F. Stettler, H.D. Bradshaw, P.E. Heilman & T.M. Hinckley), pp. 7-32, NRC Research Press, Ottawa, Canada.

Ellis B., Jansson S., Strauss S.H. & Tuskan G.A. (2010) Why and how *Populus* became a "model tree". In *Genetics and Genomics of Populus, Plant Genetics and Genomics: Crops and Models* (eds S. Jansson, R. Bhalerao & A. Groover) 8, 3-14. Springer Science. New York, NY, USA.

Evans J.R. (1983) Nitrogen and photosynthesis in the flag leaf of wheat (*Triticum aestivum* L.) *Plant Physiology* **72,** 297-302.

Evans J.R. & Loreto F. (2000) Acquisition and diffusion of CO_2 in higher plant leaves. In *Photosynthesis: physiology and metabolism* (eds R.C. Leegood, T.D. Sharkey & S. von Caemmerer), pp. 321-351. Kluwer Academic Publishers, New York, USA.

Evans J.R. & Terashima I. (1988) Photosynthetic characteristics of spinach leaves grown with different nitrogen treatments. *Plant, and Cell Physiology* **29,** 157-165.

Evans J.R. & von Caemmerer S. (1996) Carbon dioxide diffusion inside leaves. *Plant Physiology* **110,** 339-346.

Evans J.R., Kaldenhoff R., Genty B. & Terashima I. (2009) Resistances along the CO_2 diffusion pathway inside leaves. *Journal of Experimental Botany* **60,** 2235-2248.

Evans J.R., Sharkey T.D., Berry J.A. & Farquhar G.D. (1986) Carbon isotope discrimination measured with gas exchange to investigate CO_2 diffusion in leaves of higher plants. *Australian Journal of Plant Physiology* **13,** 281-292.

Fabre N., Reiter I.M., Becuwe-Linka N., Genty B. & Rumeau D. (2007) Characterization and expression analysis of genes encoding α and β carbonic anhydrases in *Arabidopsis*. *Plant, Cell and Environment* **30,** 617-629.

Farquhar G.D. & Cernusak L.A. (2012) Ternary effects on the gas exchange of isotopologues of carbon dioxide. *Plant, Cell and Environment* **35,** 1221-1231.

Farquhar G.D. & Sharkey T.D. (1982) Stomatal conductance and photosynthesis. *Annual Review of Plant Physiology and Plant Molecular Biology* **33,** 317-345.

Farquhar G.D., von Caemmerer S. & Berry J.A. (1980) A biochemical model of photosynthetic CO_2 assimilation in leaves of C_3 species. *Planta* **149,** 78-90.

Fedorchuk T., Rudenko N., Ignatova L. & Ivanov B. (2014) The presence of soluble carbonic anhydrase in the thylakoid lumen of chloroplasts from *Arabidopsis* leaves. *Journal of Plant Physiology* **171,** 903-906.

Ferreira F.J., Guo C. & Coleman J.R. (2008) Reduction of plastid-localized carbonic anhydrase activity results in reduced Arabidopsis seedling survivorship. *Plant Physiology* **147,** 585-594.

Fett J.P. & Coleman J.R. (1994) Characterization and expression of two cDNAs encoding carbonic anhydrase in *Arabidopsis thaliana*. *Plant Physiology* **105,** 707-713.

Flexas J., Barbour M.M., Brendel O., Cabrera H.M., Carriquí M., Díaz-Espejo A., …, Warren C.R. (2012) Mesophyll diffusion conductance to CO_2: an unappreciated central player in photosynthesis. *Plant Science* **193-194,** 70-84.

Flexas J., Ribas-Carbó M., Diaz-Espejo A., Galmés J. & Medrano H. (2008) Mesophyll conductance to CO_2: current knowledge and future prospects. *Plant, Cell and Environment* **31,** 602-621.

Flexas J., Ribas-Carbó M., Hanson D.T., Bota J., Otto B., Cifre J., McDowell N., …, Kaldenhoff R. (2006) Tobacco aquaporin NtAQP1 is involved in mesophyll conductance to CO_2 *in vivo*. *The Plant Journal* **48,** 427-439.

Flexas J., Scoffoni C., Gago J. & Sack L. (2013) Leaf mesophyll conductance and leaf hydraulic conductance: an introduction to their measurement and coordination. *Journal of Experimental Botany* **64,** 3965-3981.

Foissner I. & Wasteneys G.O. (2007) Wide-ranging effects of eight cytochalasins and latrunculin A and B on intracellular motility and actin filament reorganization in Characean internodal cells. *Plant and Cell Physiology* **48,** 585-597.

Gaastra P. (1959) Photosynthesis of crop plants as influenced by light, carbon dioxide, temperature, and stomatal diffusion resistance. *Mededelingen van de Landbouwhogeschool te Wageningen, Nederland* **13,** 1- 68.

Genty B., Briantais J.M. & Baker N.R. (1989) The relationship between the quantum yield of photosynthetic electron transport and quenching of chlorophyll fluorescence. *Biochimica et Biophysica Acta* **990,** 87-92.

Gilbert M.E., Pou A., Zwieniecki M.A. & Holbrook N.M. (2012) On measuring the response of mesophyll conductance to carbon dioxide with the variable *J* method. *Journal of Experimental Botany* **63,** 413-425.

Gillon J.S. & Yakir D. (2000) Internal conductance to CO_2 diffusion and $C^{18}OO$ discrimination in C_3 leaves. *Plant Physiology* **123,** 201-213.

Gillon J.S. & Yakir D. (2001) Influence of carbonic anhydrase activity in terrestrial vegetation on the ^{18}O content of atmospheric CO_2. *Science* **291,** 2584-2587.

Goh C.H. (2009) Phototropins and chloroplast activity in plant blue light signaling. *Plant Signaling & Behavior* **4,** 693-695.

Gornall J.L. & Guy R.D. (2007) Geographic variation in ecophysiological traits of black cottonwood (*Populus trichocarpa*). *Canadian Journal of Botany* **85,** 1202-1213.

Gorton H.L., Williams W.E. & Vogelmann T.C. (1999) Chloroplast movement in *Alocasia macrorrhiza*. *Physiologia Plantarum* **106,** 421-428.

Gupta A.B. & Sankararamakrishnan (2009) Genome-wide analysis of major intrinsic proteins in the tree plant *Populus trichocarpa*: characterization of XIP subfamily of aquaporins from evolutionary perspective. *BMC Plant Biology* **9:134,** doi: 10.1186/1471-2229-9-134.

Guy R.D., Fogel M.L. & Berry J.A. (1993) Photosynthetic fractionation of the stable isotopes of oxygen and carbon. *Plant Physiology* **101,** 37-47.

Hachez C., Zelazny E. & Chaumont F. (2006) Modulating the expression of aquaporin genes *in planta*: a key understand their physiological functions? *Biochimica et Biophysica Acta* **1758,** 1142- 1156.

Harley P.C., Loreto F., Di Marco G. & Sharkey T.D. (1992) Theoretical considerations when estimating the mesophyll conductance to CO_2 flux by analysis of the response of photosynthesis to CO_2. *Plant Physiology* **98,** 1429-1436.

Hassiotou F., Ludwig M., Renton M., Veneklaas E.J. & Evans J.R. (2009) Influence of leaf dry mass per area, CO_2, and irradiance on mesophyll conductance in sclerophylls. *Journal of Experimental Botany* **60,** 2303-2314.

Haupt W. & Wagner G. (1984) Chloroplast movement. In *Membranes and sensory transduction* (eds G. Colombetti & F. Lenci), pp 331-375. Plenum Press. New York. NY. USA.

Heckwolf M., Pater D., Hanson D.T. & Kaldenhoff R. (2011) The *Arabidopsis thaliana* aquaporin AtPIP1;2 is a physiologically relevant CO_2 transport facilitator. *The Plant Journal* **67,** 795-804.

Heinen R.B., Ye Q. & Chaumont F. (2009) Role of aquaporins in leaf physiology. *Journal of Experimental Botany* **60,** 2971-2985.

Hewett-Emmett D. & Tashian R.E. (1996) Functional diversity, conservation, and convergence in the evolution of the α-, β-, and γ-carbonic anhydrase gene families. *Molecular Phylogenetics and Evolution* **5,** 50-77.

Higa T. & Wada M. (2016) Chloroplast avoidance movement in not functional in plants grown under strong sunlight. *Plant, Cell and Environment* **39,** 871-882.

Hoffmann A.A. & Sgró C.M. (2011) Climate change and evolutionary adaptation. *Nature* **470,** 479-485.

Huang S., Hainzl T., Grundström C., Forsman C., Samuelsson G. & Sauer-Eriksson E. (2011) Structural studies of β-carbonic anhydrase from the green alga *Coccomyxa*: inhibitor complexes with anions and acetazolamide. *PLoS One* **6,** e28458.

Huxman T.E., Smith M.D., Fay P.A., Knapp A.K., Shaw M.R., Loik M.E., …, Williams D.G. (2004) Convergence across biomes to a common rain-use efficiency. *Nature* **429,** 651-654.

Ignatova L.K., Rudenko N.N., Mudrik V.A. & Fedorchuk T.P. (2011) Carbonic anhydrase activity in *Arabidopsis thaliana* thylakoid membrane and fragments enriched with PSI or PSII. *Photosynthesis Research* **110,** 89-98.

Jacobson B.S., Fong F. & Heath R.L. (1975) Carbonic anhydrase of spinach. *Plant Physiology* **55,** 468-474.

Johanson U., Karlsson M., Johansson I., Gustavsson S., Sjövall S., Fraysse L., ..., Kjellbom P. (2001) The complete set of genes encoding major intrinsic proteins in Arabidopsis provides a framework for a new nomenclature for major intrinsic proteins in plants. *Plant Physiology* **126,** 1358-1369.

Jones H.G. & Slatyer R.O. (1972) Estimation of the transport and carboxylation components of the intracellular limitation to leaf photosynthesis. *Plant Physiology* **50,** 283-288.

Kagawa T. & Wada M. (1999) Chloroplast-avoidance response induced by high-fluence blue light in prothallial cells of the fern *Adiantum capillusveneris* as analyzed by microbeam irradiation. *Plant Physiology* **119,** 917-923.

Kaldenhoff R. & Fischer M. (2006) Aquaporins in plants. *Acta Physiologica* **187,** 169-176.

Kaldenhoff R., Ribas-Carbo M., Flexas Sans J., Lovisolo C., Heckwolf M. & Uehlein N. (2008) Aquaporins and plant water balance. *Plant, Cell and Environment* **31,** 658-666.

Kaluthota S., Pearce D.W., Evans L.M., Letts M.G., Whitham T.G. & Rood S.B. (2015) Higher photosynthetic capacity from higher latitude: foliar characteristics and gas exchange of southern, central and northern populations of *Populus angustifolia*. *Tree Physiology* **35,** 936-948.

Kamegawa A., Hiroaki Y., Tani K. & Fujiyoshi Y. (2016) Two-dimensional crystal structure of aquaporin-4 bound to the inhibitor acetazolamide. *Microscopy* **65,** 177-184.

Kasahara M., Kagawa T., Oikawa K., Suetsugu N., Miyao M. & Wada M. (2002) Chloroplast avoidance movement reduces photodamage in plants. *Nature* **420,** 829-832.

Katsuhara M. & Hanba Y.T. (2008) Barley plasma membrane intrinsic proteins (PIP aquaporins) as water and CO_2 transporters. *European Journal of Physiology* **456,** 687-691.

Keller S.R., Levsen N., Olson M.S. & Tiffin P. (2012) Local adaptation in the flowering-time gene network of balsam poplar, *Populus balsamifera* L. *Molecular Biology and Evolution.* **29,** 3143-3152.

Keller S.R., Soolanayakanahally R.Y., Guy R.D., Slim S.N., Olson M.S. & Tiffin P. (2011) Climate-driven local adaptation of ecophysiology and phenology in balsam poplar, *Populus balsamifera* L. (*Salicaceae*). *American Journal of Botany* **98**, 99-108.

Kshirsagar A., Reid A.J., McColl S.M., Saunders V.A., Whalley A.J.S. & Evans E.H. (2001) The effect of fungal metabolites on leaves as detected by chlorophyll fluorescence. *New Phytologist* **151,** 451-457.

Lanigan G.J., Betson N., Griffiths H. & Seibt U. (2008) Carbon isotope fractionation during photorespiration and carboxylation in *Senecio*. *Plant Physiology* **148,** 2013-2020.

Laur J. & Hacke U.G. (2014) The role of water channel proteins in facilitating recovery of leaf hydraulic conductance from water stress in *Populus trichocarpa*. *PLOS one* **9,** 1-10.

Lonergan T.A. & Sargent M.L. (1978) Effects of acetazolamide (diamox), ethoxzolamide and high levels of CO_2 on carbonic anhydrase, photosystem activity, and oxygen evolution in *Euglena gracilis*. *Physiologia Plantarum* **43,** 55-61.

Loreto F., Tsonev T. & Centritto M. (2009) The impact of blue light on leaf mesophyll conductance. *Journal of Experimental Botany* **60,** 2283-2290.

Maini J. S. & Cayford J. H. (1968) Growth and utilization of poplars in Canada. Canadian Department of Forestry and Rural Development, Forestry Branch, Department Publication 1205. Ottawa, ON. 257 p.

Makino A., Sakashita H., Hidema J., Mae T., Ojima K. & Osmond B. (1992) Distinctive responses of ribulose-1,5-bisphosphate carboxylase and carbonic anhydrase in wheat leaves to nitrogen nutrition and their possible relationships to CO_2-transfer resistance. *Plant Physiology* **100,** 1737-1743.

Malec P., Rinaldi R.A. & Gabryś H. (1996) Light-induced chloroplast movements in *Lemna trisulca.* Identification of the motile system. *Plant Science* **120,** 127-137.

Mansfield T.A. & Meidner H. (1966) Stomatal opening in light of different wavelengths: effects of blue light independent of carbon dioxide concentration. *Journal of Experimental Botany* **17,** 510-521.

Marchin R.M., Sage E.L. & Ward J.K. (2008) Population-level variation of *Fraxinus americana* (white ash) is influenced by precipitation differences across the native range. *Tree Physiology* **28,** 151-159.

Maurel C., Verdoucq L., Luu D. & Santoni V. (2008) Plant aquaporins: membrane channels with multiple integrated functions. *The Annual Review of Plant Biology* **59,** 595-624.

McKown A.D., Guy R.D., Klápště J., Geraldes A., Friedmann M., Cronk Q.C.B., …, Douglas C.J. (2014a) Geographical and environmental gradients shape phenotypic trait variation and genetic structure in *Populus trichocarpa. New Phytologist* **201,** 1263-1276.

McKown A.D., Guy R.D., Quamme L.A., Klápště J., La Mantia J., Constabel C.P., …, Azam M.S. (2014b) Association genetics, geography and ecophysiology link stomatal patterning in *Populus trichocarpa* with carbon gain and disease resistance trade-offs. *Molecular Ecology* **23,** 5771-5790.

Milla-Moreno E.A., McKown A.D., Guy R.D. & Soolanayakanahally R.Y. (2016) Leaf mass area predicts palisade structural properties linked to mesophyll conductance in balsam poplar (*Populus balsamifera* L.) *Botany* **94,** 225-239.

Momayyezi M. & Guy R.D. (2017) Substantial role for carbonic anhydrase in latitudinal variation in mesophyll conductance of *Populus trichocarpa* Torr. & Gray. *Plant, Cell and Environment* **40,** 138-149.

Moroney J.V., Bartlett S.G. & Samuelsson G. (2001) Carbonic anhydrases in plants and algae. *Plant, Cell and Environment* **24,** 141-153.

Murata K., Mitsuoka K., Hirai T., Walz T., Agre P., Heymann J.B., Engel A. & Fujiyoshi Y. (2000) Structural determinants of water permeation through aquaporin-1. *Nature* **407,** 599-605.

Nauš J., Prokopová J., Řebíček J. & Špundová M. (2010) SPAD chlorophyll meter reading can be pronouncedly affected by chloroplast movement. *Photosynthesis Research* **105,** 265-271.

Niemiec S.S., Ahrens G.R., Willits S. & Hibbs D.E. (1995) Hardwoods of the Pacific Northwest. Research Contribution 8. Forestry Publications Office, Oregon State University, Forest Research Laboratory, Corvallis, Oregon, USA. pp. 24-32.

Pallozzi E., Tsonev T., Marino G., Copolovici L., Niinemets Ü., Loreto F. & Centritto M. (2013) Isoprenoid emissions, photosynthesis and mesophyll diffusion conductance in response to blue light. *Environmental and Experimental Botany* **95,** 50-58.

Parkhurst D.F. (1994) Diffusion of CO2 and other gases inside leaves. *New Phytologist* **126,** 449-479.

Parmesan C. (2006) Ecological and evolutionary responses to recent climate change. *Annual Review of Ecology, Evolution, and Systematics* **37,** 637-669.

Peguero-Pina J.J., Flexas J., Galmés J., Niinemets Ü., Sancho-Knapik D., Barredo G., …, Gil-Pelegrín, E. (2012) Leaf anatomical properties in relation to differences in mesophyll conductance to CO_2 and photosynthesis in two related Mediterranean *Abies* species. *Plant, Cell and Environment* **35,** 2121-2129.

Perez-Martin A., Michelazzo C., Torres-Ruiz J.M., Flexas J., Fernández J.E., Sebastiani L. & Diaz-Espejo A. (2014) Regulation of photosynthesis and stomatal and mesophyll conductance under water stress and recovery in olive trees: correlation with gene expression of carbonic anhydrase and aquaporins. *Journal of Experimental Botany* **65,** 3143-3156.

Pointeau V.M. & Guy R.D. (2014) Comparative resource-use efficiencies and growth of *Populus trichocarpa* and *Populus balsamif*era under glasshouse conditions. *Botany* **92,** 443-451.

Pons T.L., Flexas J., von Caemmerer S., Evans J.R., Genty B., Ribas-Carbo M. & Brugnoli E. (2009) Estimating mesophyll conductance to CO_2: methodology, potential errors, and recommendations. *Journal of Experimental Botany* **60,** 2217-2234.

Porra R.J., Thompson W.A. & Kriedemann P.E. (1989) Determination of accurate extinction coefficients and simultaneous equations for assaying chlorophylls a and b extracted with four different solvents: verification of the concentration of chlorophyll standards by atomic absorption spectroscopy. *Biochimica et Biophysica Acta* **975,** 384-394.

Price G.D., von Caemmerer S., Evans J.R., Yu J.W., Lloyd J., Oja V., …, Badger M.R. (1994) Specific reduction of chloroplast carbonic anhydrase activity by antisense RNA in transgenic tobacco plants has a minor effect on photosynthetic CO_2 assimilation. *Planta* **193,** 331-340.

Reich P.B., Grigal D.F., Aber J.D. & Gower S.T. (1997) Nitrogen mineralization and productivity in 50 hardwood and conifer stands on diverse soils. *Ecology* **78,** 335-347.

Ribas-Carbo M., Still C. & Berry J. (2002) Automated system for simultaneous analysis of $\delta^{13}C$, $\delta^{18}O$ and CO_2 concentrations in small air samples. *Rapid Communications in Mass Spectrometry*. **16,** 339-345.

Rudenko N.N., Ignatova L.K. & Ivanov B.N. (2007) Multiple sources of carbonic anhydrase activity in pea thylakoids: soluble and membrane-bound forms. *Photosynthesis Research* **91,** 81-89.

Ryan N.M. (2015) Growth and ecophysiology of wide intraspecific balsam poplar (*Populus balsamifera* L.) hybrids. University of British Columbia. Retrieved from https://open.library.ubc.ca/cIRcle/collections/24/items/1.0166758.

Saarela J.M., Gillespie L.J., Consaul L.L. & Bull R.D. (2011) Balsam poplar (*Populus balsamifera*; Salicaceae) beyond the tree line in the western Canadian mainland arctic (northwest territories). *Arctic* **65,** 1- 12.

Sakurai J., Ishikawa F., Yamaguchi T., Uemura M. & Maeshima M. (2005) Identification of 33 rice aquaporin genes and analysis of their expression and function. *Plant and Cell Physiology* **46,** 1568-1577.

Sarda X., Tousch D., Ferrare K., Legrand E., Dupuis J.M., Casse-Delbart F. & Lamaze T. (1997) Two TIP-like genes encoding aquaporins are expressed in sunflower guard cells. *The Plant Journal* **12,** 1103-1111.

Savage D.F. & Stroud R.M. (2007) Structural basis of aquaporin inhibition by mercury. *Journal of Molecular Biology* **368,** 607-617.

Savolainen O., Lascoux M. & Merilä J. (2013) Ecological genomics of local adaptation. *Nature Reviews Genetics* **14,** 807-820.

Schurr U., Walter A. & Rascher, U. (2006) Functional dynamics of plant growth and photosynthesis- from steady-state to dynamics– from homogeneity to heterogeneity. *Plant, Cell and Environment* **29,** 340-352.

Scozzafava A., Briganti F., Ilies M.A & Supuran C.T. (2000) Carbonic anhydrase inhibitors: synthesis of membrane-impermeant low molecular weight sulfonamide possessing *in vivo* selectively for the membrane-bound versus cytosolic isozymes. *Journal of Medical Chemistry* **43,** 292-300.

Secchi F., Maciver B., Zeidel M.L. & Zwieniecki M.A. (2009) Functional analysis of putative genes encoding the PIP2 water channel subfamily in *Populus trichocarpa*. *Tree Physiology* **29,** 1467-1477.

Secchi F. & Zwieniecki M.A. (2013) The physiological response of *Populus tremula* × *alba* leaves to the down-regulation of PIP1 aquaporin gene expression under no water stress. *Frontiers in Plant Science* **4,** 1-9.

Secchi F. & Zwieniecki M.A. (2014) Down-regulation of plasma intrinsic protein1 aquaporin in poplar trees is detrimental to recovery from embolism. *Plant Physiology* **164,** 1789-1799.

Semmens C., Ketler R., Schwendenmann L., Nesic Z. & Christen A. (2014) Isotopic composition of CO_2 in gasoline, diesel and natural gas combustion exhaust in Vancouver, BC, Canada. http://hdl.handle.net/2429/50324

Sharkey T.D. (2016) What gas exchange data can tell us about photosynthesis. *Plant, Cell and Environment* **39,** 1161-1163.

Sharkey T.D. & Raschke K. (1981) Effect of Light Quality on Stomatal Opening in Leaves of *Xanthium strumarium* L. *Plant Physiology* **68,** 1170-1174.

Shingles R., Moroney J.V. & McCarty R.E. (1997) Carbonic anhydrase-mediated movement of carbon dioxide across chloroplast inner envelope vesicles. *Plant Physiology* **114**(S), 198.

Soolanayakanahally R.Y., Guy R.D., Slim S.N., Drewes E.C. & Schroeder W.R. (2009) Enhanced assimilation rate and water use efficiency with latitude through increased photosynthetic capacity and internal conductance in balsam poplar (*Populus balsamifera* L.). *Plant, Cell and Environment* **32,** 1821-1823.

Soolanayakanahally R.Y., Guy R.D., Street N.R., Robinson K.M., Silim S.N., Albrectsen B.R. & Jansson S. (2015) Comparative physiology of allopatric *Populus* species: geographic clines in photosynthesis, height growth, and carbon isotope discrimination in common gardens. *Frontiers in Plant Science* **6,** 1-11.

Stemler A. (1986) Carbonic anhydrase associated with thylakoids and photosystem II particles from maize. *Biochimica et Biophysica Acta* **850,** 97-107.

Stemler A. & Jursinic P. (1983) The effect of carbonic anhydrase inhibitors formate, bicarbonate, acetazolamide, and imidazole on photosystem II in maize chloroplasts. *Archives of Biochemistry and Biophysics* **221,** 227-237.

Suarez-Gonzalez A., Hefer C.A., Christe C., Corea O., Lexer C., Cronk Q.C.B. & Douglas C.J. (2016) Genomic and functional approaches reveal a case of adaptive introgression from *Populus balsamifera* (balsam poplar) in *P. trichocarpa* (black cottonwood). *Molecular Ecology* **25,** 2427–2442

Suetsugu N., Takami T., Ebisu Y., Watanabe H., Iiboshi C., Doi M. & Shimazaki K. (2014) Guard cell chloroplasts are essential for blue light-dependent stomatal opening in Arabidopsis. *PLOS ONE* **9,** 1-7.

Swader J.A. & Jacobson B.S. (1972) Acetazolamide inhibition of photosystem II in isolated spinach chloroplasts. *Phytochemistry* **11,** 65-70.

Takagi S. (2003) Actin-based photo-orientation movement of chloroplasts in plant cells. *The Journal of Experimental Biology* **206,** 1963-1969.

Takagi S., Takamatsu H. & Sakurai-Ozato N. (2009) Chloroplast anchoring: its implications for the regulation of intracellular chloroplast distribution. *Journal of Experimental Botany* **60,** 3301-3310.

Takamatsu H. & Takagi S. (2011) Actin-dependent chloroplast anchoring is regulated by Ca^{2+} – calmodulin in spinach mesophyll cells. *Plant & Cell Physiology* **52,** 1973-1982.

Tanimura Y., Hiroaki Y. & Fujiyoshi Y. (2009) Acetazolamide reversibly inhibits water conduction by aquaporin-4. *Journal of Structural Biology* **166,** 16-21.

Tazawa M., Ohkuma E., Shibasaka M. & Nakashima S. (1997) Mercurial-sensitive water transport in barley roots. *Journal of Plant Research* **110,** 435-442.

Terashima I. & Ono K. (2002) Effects of $HgCl_2$ on CO_2 dependence of leaf photosynthesis: evidence indicating involvement of aquaporins in CO_2 diffusion across the plasma membrane. *Plant and Cell Physiology* **43,** 70-78.

Tholen D. & Zhu X.G. (2011) The mechanistic basis of internal conductance: a theoretical analysis of mesophyll cell photosynthesis and CO_2 diffusion. *Plant Physiology* **156,** 90-105.

Tholen D., Boom C., Noguchi K., Ueda S., Katase T. & Terashima I. (2008) The chloroplast avoidance response decreases internal conductance to CO_2 diffusion in *Arabidopsis thaliana* leaves. *Plant, Cell and Environment* **31,** 1688- 1700.

To J. & Torres J. (2015) Can stabilization and inhibition of aquaporins contribute to future development of biomimetic membranes? *Membranes* **5,** 352-368.

Tomás M., Flexas J., Copolovici L., Galmés J., Hallik L., Medrano H., …, Niinemets Ü. (2013) Importance of leaf anatomy in determining mesophyll diffusion conductance to CO_2 across

species: quantitative limitations and scaling up by models. *Journal of Experimental Botany* **64,** 2269-2281.

Tosens T., Niinemets Ü., Westoby M. & Wright I.J. (2012) Anatomical basis of variation in mesophyll resistance in eastern Australian sclerophylls: news of a long and winding path. *Journal of Experimental Botany* **63,** 5105-5119.

Tsuzuki M., Miyachi S. & Edwards G.E. (1985) Localization of carbonic anhydrase in mesophyll cells of terrestrial C_3 plants in relation to CO_2 assimilation. *Plant, Cell and Environment* **26,** 881-891.

Tuskan G.A., Difazio S., Jansson S., Bohlmann J., Grigoriev I., Hellsten U., …, Rokhsar D. (2006) The genome of black cottonwood, *Populus trichocarpa* (Torr. & Gray). Science **313,** 1596-1604.

Tuskan G.A., DiFazio S.P. & Teichmann T. (2003) Poplar genomics is getting popular: the impact of the poplar genome project on tree research. *Plant Biology* **5,** 1- 3.

Uehlein N., Lovisolo C., Siefritz F. & Kaldenhoff R. (2003) The tobacco aquaporin NtAQP1 is a membrane CO_2 pore with physiological functions. *Nature* **425,** 734-736.

Uehlein N., Otto B., Hanson D.T., Fischer M., McDowell N. & Kaldenhoff R. (2008) Function of *Nicotiana tabacum* aquaporins as chloroplast gas pores challenges the concept of membrane CO_2 permeability. *The Plant Cell* **20,** 648-657.

Utsunomiya E. & Muto S. (1993) Carbonic anhydrase in the plasma membranes from leaves of C_3 and C_4 plants. *Physiologia Plantarum* **88,** 413-419.

Valentini R., Epron D., De Angelis P., Matteucci G. & Dreyer E. (1995) *In situ* estimation of net CO_2 assimilation, photosynthetic electron flow and photorespiration in Turkey oak (*Q.*

cerris L.) leaves: diurnal cycles under different levels of water supply. *Plant, Cell & Environment* **18,** 631-640.

Valladares F., Matesanz S., Guilhaumon F., Araújo M.B., Balaguer L., Benito-Garzón M., …, Zavala M.A. (2014) The effects of phenotypic plasticity and local adaptation on forecasts of species range shifts under climate change. *Ecology Letters* **17,** 1351-1364.

Verchot-Lubicz J. & Goldstein R.E. (2010) Cytoplasmic streaming enables the distribution of molecules and vesicles in large plant cells. *Protoplasma* **240,** 99-107.

Viereck L.A. & Little Jr. E.L. (1974) Guide to Alaska trees. United States Department of Agriculture Forest Service. Agricultural Handbook No. 472, pp 1-19. Washington, D.C. USA.

Vilas G., Krishnan D., Loganathan S.K., Malhotra D., Liu L., Beggs M.R., …, Alexander R.T. (2015) Increased water flux induced by an aquaporin-1/carbonic anhydrase II interaction. *Molecular Biology of the Cell* **26,** 1106-1118.

Vitousek P.M. & Howarth R.W. (1991) Nitrogen limitation on land and in the sea: how can it occur? *Biogeochemistry* **13,** 87-115.

Wang C., Hu H., Qin X., Zeise B., Xu D., Rappel W., …, Schroeder J.I. (2016) Reconstitution of CO_2 regulation of SLAC1 anion channel and function of CO_2-permebale PIP2;1 aquaporin as carbonic anhydrase4 interactor. *The Plant Cell* **28,** 568-582.

Warren C.R. (2008) Stand aside stomata, another actor deserves centre stage: the forgotten role of the internal conductance to CO_2 transfer. *Journal of Experimental Botany* **59,** 1475-1487.

Way D.A. & Oren R. (2010) Differential responses to changes in growth temperature between trees from different functional groups and biomes: a review and synthesis of data. *Tree Physiology* **30,** 669-688.

Webb W.L., Lauenroth W.K., Szarek S.R. & Kinerson R.S. (1983) Primary production and abiotic controls in forests, grasslands, and desert ecosystems in the United States. *Ecology* **64,** 134-151.

Weise S.E., Carr D.J., Bourke A.M., Hanson D.T. Swarthout D. & Sharkey T.D. (2015) The *arc* mutants of *Arabidopsis* with fewer large chloroplasts have a lower mesophyll conductance. *Photosynthesis Research* **124,** 117-126.

Werdan K. & Heldt H.W. (1972) Accumulation of bicarbonate in intact chloroplasts following a pH gradient. *BBA Bioenergetics* **283,** 430-441.

Wertin T.M., McGuire M.A. & Teskey R.O. (2012) Effects of predicted future and current atmospheric temperature and [CO_2] and high and low soil moisture on gas exchange and growth of *Pinus taeda* seedlings at cool and warm sites in the species range. *Tree Physiology* **32,** 847-858.

Wilbur K.M. & Anderson N.G. (1948) Electrometric and colorimetric determination of carbonic anhydrase. *Journal of Biological Chemistry* **176,** 147-154.

Williams T.G., Flanagan L.B. & Coleman J.R. (1996) Photosynthetic gas exchange and discrimination against $^{13}CO_2$ and $C^{18}O^{16}O$ in tobacco plants modified by an antisense construct to have low chloroplastic carbonic anhydrase. *Plant Physiology* **112,** 319-326.

Williamson R.E. (1993) Organelle movements. *Annual Review of Plant Physiology and Plant Molecular Biology* **44,** 181-202.

Wingate L., Seibt U., Moncrieff J.B., Jarvis P.G. & Lloyd J. (2007) Variations in ^{13}C discrimination during CO_2 exchange by *Picea sitchensis* branches in the field. *Plant, Cell and Environment* **30,** 600-616.

Wu Q., Pierce J.R. & Delamere N.A. (1998) Cytoplasm pH responses to carbonic anhydrase inhibitors in cultures rabbit nonpigmented ciliary epithelium. *Journal of Membrane Biology* **162,** 31-31.

Yang B., Fekuda N., van Hoek A., Matthay M.A., Ma T. & Verkman A.S. (2000) Carbon dioxide permeability of aquaporin-1 measured in erythrocytes and lung of aquaporin-1 null mice and in reconstituted proteoliposomes. *The Journal of Biological Chemistry* **275,** 2686-2692.

Zeiger E. & Field C. (1982) Photocontrol of the functional coupling between photosynthesis and stomatal conductance in the intact leaf. *Plant Physiology* **70,** 370-375.

Appendix A- Supporting information

Table A.1 A_n, g_s and g_m mean values (± SE) over five replications in attached and detached leaves. Data were introduced to PROC GLM in SAS 9.4 for analysis of variances. There were no significant differences between attached and detached leaves.

	attached leaves	detached leaves
A_n	15.36 ± 1.21	15.02 ± 1.01
g_s	0.221 ± 0.007	0.222 ± 0.006
g_m	0.169 ± 0.020	0.180 ± 0.020

A_n, net assimilation rate (μmol CO_2 m^{-2} s^{-1}); g_s, stomatal conductance (mol H_2O m^{-2} s^{-1}); g_m, mesophyll conductance (mol CO_2 m^{-2} s^{-1}).

Table A.2 Leaf absorptance mean values (± SD) over five replications in six *Populus trichocarpa* genotypes. Data were introduced to PROC GLM in SAS 9.4 for analysis of variances. There were no significant differences in leaf absorptance between genotypes.

	HALS-2	PITS-3	LONG-1	SKNP-4	TAKA-2	TATB-4
leaf absorptance	0.847 ± 0.017	0.832 ± 0.045	0.802 ± 0.022	0.812 ± 0.022	0.835 ± 0.026	0.831 ± 0.017

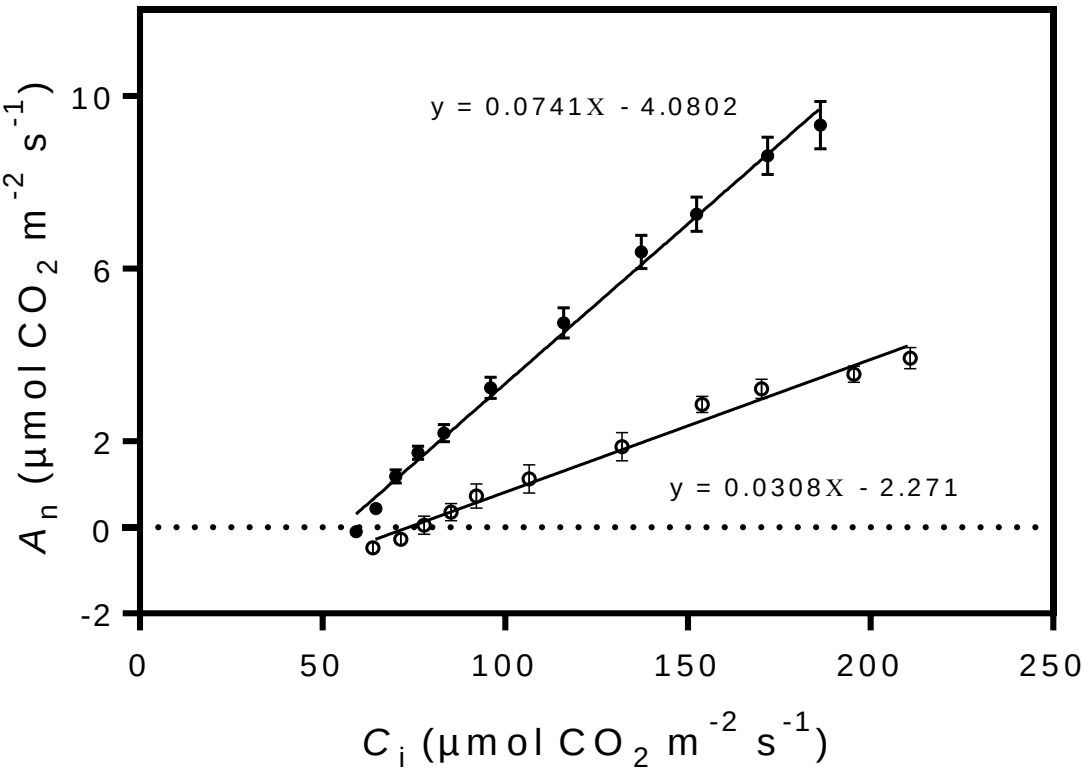

Figure A.1 Estimation of CO_2 compensation point (C_i*, µmol mol^{-1}) and dark respiration rate (R_d, µmol m^{-2} s^{-1}) using the Laisk method (Gilbert et al. 2012, see Materials and Methods for details). Each point represents the mean of six plants (± SE). *A*-C_i curves were built under two irradiances of 125 (○) and 500 (●) µmol m^{-2} s^{-1}.

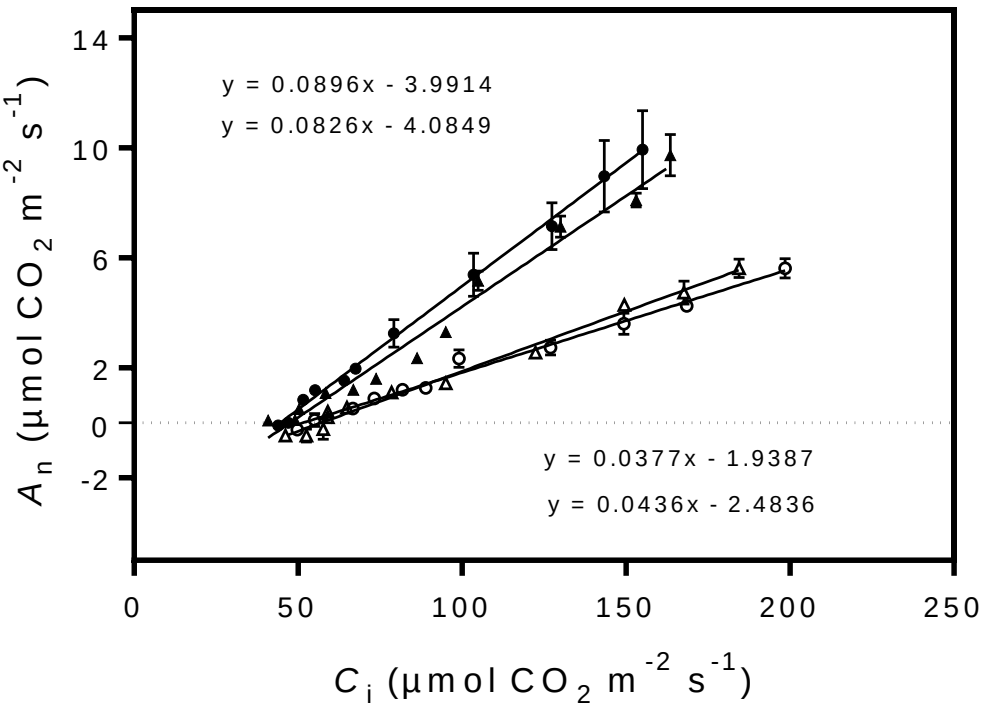

Figure A.2 Estimation of CO_2 compensation point (C_i*, µmol mol^{-1}) and dark respiration rate (R_d, µmol m^{-2} s^{-1}) using the Laisk method (Gilbert et al. 2012, see Materials and Methods for details) under control (distilled water) (●, ○) and 1 mM acetazolamide (▲, △) treatments. Each point represents the mean of two plants (± SE). *A*-C_i curves were built under two irradiances of 125 (hollow) and 500 (solid) µmol m^{-2} s^{-1}.

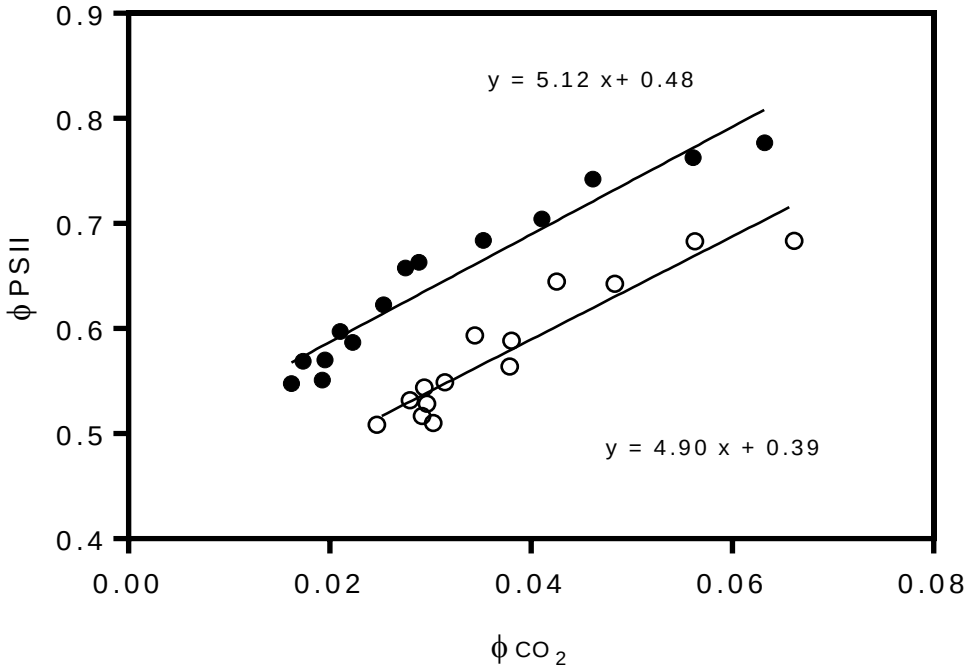

Figure A.3 Relationship between quantum yield of photosystem II (Φ_{PSII}) and quantum yield for net assimilation rate (Φ_{CO_2}) under non-photorespiratory conditions (2% O_2). Measurements were on the SKNP-4 genotype over a range of PPFD from 50 to 1200 µmol m^{-2} s^{-1} under either 10% (●) or 60% BL (○).